Hierarchical neural control of human postural balance and bipedal walking in sagittal plane

by

Sungho Jo

B.S., Seoul National University (1999)
S.M., Massachusetts Institute of Technology (2001)

Submitted to the Department of Electrical Engineering and Computer Science
in partial fulfillment of the requirements for the degree of

Doctor of Philosophy

at the

MASSACHUSETTS INSTITUTE OF TECHNOLOGY

May 2006

Author .....
Department of Electrical Engineering and Computer Science
May 18, 2006

Certified by .....
Steve G. Massaquoi
Assistant Professor of Electrical Engineering and Computer Science /
Harvard-MIT Health Sciences and Technology
Thesis Supervisor

Accepted by .....
Arthur C. Smith
Chairman, Department Committee on Graduate Students

Hierarchical neural control of human postural balance and bipedal walking in sagittal plane

by

Sungho Jo

Submitted to the Department of Electrical Engineering and Computer Science
on May 18, 2006, in partial fulfillment of the
requirements for the degree of
Doctor of Philosophy

Abstract

The cerebrocerebellar system has been known to be a central part in human motion control and execution. However, engineering descriptions of the system, especially in relation to lower body motion, have been very limited. This thesis proposes an integrated hierarchical neural model of sagittal planar human postural balance and biped walking to 1) investigate an explicit mechanism of the cerebrocerebellar and other related neural systems, 2) explain the principles of human postural balancing and biped walking control in terms of the central nervous systems, and 3) provide a biologically inspired framework for the design of humanoid or other biomorphic robot locomotion. The modeling was designed to confirm neurophysiological plausibility and achieve practical simplicity as well.

The combination of scheduled long-loop proprioceptive and force feedback represents the cerebrocerebellar system to implement postural balance strategies despite the presence of signal transmission delays and phase lags. The model demonstrates that the postural control can be substantially linear within regions of the kinematic state-space with switching driven by sensed variables. A improved and simplified version of the cerebrocerebellar system is combined with the spinal pattern generation to account for human nominal walking and various robustness tasks. The synergy organization of the spinal pattern generation simplifies control of joint actuation. The substantial decoupling of the various neural circuits facilitates generation of modulated behaviors. This thesis suggests that kinematic control with no explicit internal model of body dynamics may be sufficient for those lower body motion tasks and play a common role in postural balance and walking. All simulated performances are evaluated with respect to actual observations of kinematics, electromyogram, etc.

Thesis Supervisor: Steve G. Massaquoi
Title: Assistant Professor of Electrical Engineering and Computer Science / Harvard-MIT Health Sciences and Technology

Dedicated to my loving parents,
Chuja Oh, and Sinhaeng Jo.

In life as a human being, nothing is secure. Just follow your heart.

Acknowledgments

My life as a MIT graduate student has finally come to an end. The last seven years have given me both good and bad memories, some of each which I can no longer remember. However, the remaining will forever now be recalled as good... as a part of my youth. It is always lovely to achieve something.

I appreciate the research supervision of professor Steve Massaquoi. Steve had the most influence upon me at MIT. And my appreciation goes to my committee professors, Rodney Brooks and Hugh Herr. Professor Gregory Wornell also should be mentioned. Thankfully he was a good academic supervisor. The huge fruit at MIT is that I met many good friends such as Iahn Cajigas-Gonzalez, Takazuka Takahashi, Zhi-Hong Mao, Andreas Hofmann and others as my labmates. Allen Atamer, my first foreign friend, can never be missed. Susan Kim, who was willing(?) to be my younger sister, was a good English teacher. John Perry was always generous to be a good conservation partner. Megatonic thanks to all of you!! My wonderful Korean friends at MIT are hard to be named one by one because there are too many. They would know how thankful I am.

Most of all, special appreciation falls to my lovely parents and younger brother, Sungkyung. Though we were apart, their support never ceased to inspire and encourage me.

Contents

List of Figures

List of Tables

Chapter 1

Introduction

1.1 Motivation

Human postural balancing and walking control are worthwhile targets for research because they would advance the understanding of important human behaviors and will likely provide some fresh ideas on the efficient and robust motion generations of humanoid robotic systems. Humans routinely coordinate many degrees of freedom smoothly and effortlessly to achieve complex motion tasks, and learn new motion executions effectively. Most current robots and artificial systems are not based on human motor control system, and suffer many difficulties with the behaviors that are quite natural to humans. The research on human postural balancing and walking is expected to be advantageous to understand and reproduce such human natural, but highly complex nonlinear dynamic behaviors. For example, human walking is actuated by uni- and bi-articular muscle groups around joints. Biped walking robots developed up to now have no such muscle coordination of walking. The muscle coordination, even though complex, may be one of the key factors for human efficient and robust walking generation.

The cerebrum, cerebellum, and spinal cord interact to support balance and walking, but relatively little is known about how. Studies of human balancing and walking physiology are incomplete. Central remaining questions include whether complex con-

trol systems are not necessary to compel human balancing and walking even though they are complex nonlinear dynamic behaviors, and whether actual human motor systems may function in a simple way. Some progress has been made in understanding how these structures interact in arm reaching tasks (Massaquoi 1999). Therefore, there is the possibility that some of these principles could be extended to postural balance and locomotion. The possibility is proposed in the sense that neural network structures are uniformly identical regardless of behaviors they are concerned about. Specifically modeling and analysis may be able to show how uniform structures contribute to different movement or postural tasks. If this can be achieved, then the principles are likely to be useful to design advanced robotic control systems.

1.2 Problem Statement

The thesis is to propose an overall biological model to explain human postural balance and walking. The goal is attacked first by investigating whether an existing model of cerebrocerebellar control of arm motion can be applied and if necessary extended or otherwise modified to describe human control of 1) undisturbed upright balance and biped walking and 2) simple disturbances during standing and walking. To design the human behaviors, explicit models of neural systems as well as musculoskeletal dynamic systems subject to biological constraints, are rigorously investigated. Preliminary findings (Jo 2002) suggest that stabilized long-loop feedback with scheduling of linear gains may afford realistic balance control in the absence of explicit internal dynamics models and the cerebrocerebellar system may contribute to balance control by such a mechanism. In addition, simple rhythmic activation patterns could provide basic biped walking motions even though the body dynamics is multi-jointed, highly nonlinear and complicated. However, the simple activations were unable to stabilize consistent walking patterns therefore, long-loop feedback is required for stabilization of biped walking. This thesis intends to focus on investigating the cerebrocerebellar control to explain postural balance, and its improvement to be continuously applied to stabilization of biped walking, and inducing a synthetic principle of the mecha-

nisms of postural balance and walking. The proposed biological mechanism will be evaluated and analyzed in terms of biomechanics and neurophysiology. In addition, some suggestions of robotic design based on the biological system will be presented.

Chapter 2

BACKGROUND

2.1 The biomechanics of balance and walking

2.1.1 Biomechanics for upright postural balance

Upright postural balance describes the dynamics of body posture to prevent falling over a relatively small base of support under gravitational field. As for postural balance without stepping, the stable balancing condition can be analyzed using the following equation under assumption that a one link inverted pendulum describes human sway motions.

$$F_y \cdot x_{cop} - Mg \cdot x_{com} = I\ddot{\theta}_a \tag{2.1}$$

where F_y is vertical reaction force, Mg is human total weight; x_{cop} is the center of pressure (COP). x_{com} is the horizontal component of the center of mass (COM) (e.g., the center of gravity (COG)); I is the moment of inertia of the total body about the ankle joint; θ_a is the ankle joint angle.

If $F_y \cdot x_{cop} > Mg \cdot x_{com}$, the body tends to sway backwards. Then, x_{cop} needs to decrease until it locates posterior to x_{com} . If $F_y \cdot x_{cop} < Mg \cdot x_{com}$, the body experience forward sway, therefore, x_{cop} needs to increase until it locates anterior to x_{com}. Ideally when $F_y \cdot x_{cop} = Mg \cdot x_{com}$, the body remains with static posture. Increasing x_{cop} is done by increasing plantarflexion activation and decreasing it by

decreasing plantarflexion activation (Gatev et al 1999).

2.1.2 Biomechanics for bipedal locomotion

Two basic models for biped locomotion are walking and running. A gait of walking consists of stance and swing phases and a gait of running consists of stance and flight phases. Stance phase describes the period when a foot remains on the ground, and either swing or flight describes the period when a foot does not touch on the ground. Basic walking model is analogous to an inverted pendulum at stance phase. At midstance, the COM is at its highest point and gravitational potential energy is at maximal and kinetic energy at minimal. The exchange between kinetic and gravitational potential energies is cyclical over gaits. On the other hands, a running leg acts as a spring, therefore, a simple running model is a mass-spring system. At the braking phase during stance, the spring gets compressed and energies are stored as elastic energy. At midstance, the COM reaches its lowest point. The stored elastic energy recoils the spring at propulsive phase during stance to produce kinetic and gravitational potential energies. Both models principally exchange and store energies repeatedly to produce forward thrust, and stability. In addition, some of observation (Vaughan et al 2003) verifies that the ground reaction forces pass close to the joint centers so as to minimize the required energies to support a body.

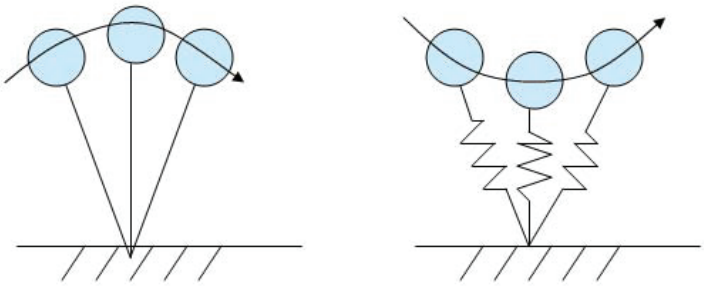

Figure 2-1: Simple walking (left) and running (right) models.

2.2 State of the art in bipedal robotic balance and locomotion

2.2.1 Robotic postural balance

For a successful planar bipedal walking robot design, some conditions are important (Pratt and Pratt 1998): height, pitch, and speed have to be stabilized; the swing leg has to move to an appropriate location; transition between phases has to be at appropriate times. Indicators of postural stability during stance phase to satisfy the above condition have been investigated. A popular technique to deal with dynamic stable walking is to manipulate the zero moment point (ZMP) (Vukobratovic et al 1990; Hemami and Farnsworth 1977). In fact, ZMP is defined to be a point on the foot where the net ground reaction force acts actually. It is equivalent to COP when the foot is at rest, e.g., during stance phase with no slip. This measure can be used as constraint to design a controller. Some studies also suggested that foot rotation is an indicator of postural instability (Goswami 1999; Hofmann 2006). The foot rotation indicator (FRI) is where the net ground reaction force would have to act to keep the foot stationary. Real walking robots such as Honda ASIMO, and Sony QRIO control relative relations between ZMP and COM to achieve stable walking posture (Hirai et al 1998; www.sony.net/SonyInfo/QRIO/). Principally, maintaining posture requires the ankle torque to compensate for torque caused by position of COM relative to COP (or ZMP) in order to keep COM within stable support area.

2.2.2 Robotic locomotion

Most recent approaches to design a biped walking model can be categorized as follows.

1. Preprogrammed / Pattern generator

   A desired trajectory for each joint motion is provided. Many optimal or adaptive control schemes are applied to make actual trajectory follow the desired one to produce walking motions (Tzafestas et al 1997; van der Kooji et al 2003; Yang

1993; Fujimoto et al 1998). For example, sliding controller or model-based controller is designed for robust walking. The optimal expenditure energy can also be an objective for a control design to generate muscular effort for locomotion (Anderson and Pandy 2001; Vaughan 2003). It is necessary to verify the neural structure in order for the preprogrammed scheme to be biological plausible. Active walking motions have been generated in the manner of preprogramming. Honda ASIMO and Sonny QRIO are famous biped walking robots with the strategy (Hirai et al 1998). Both robots follow desired walking patterns detecting ZMP for postural stability constraint.

Recently, the neural pattern generator (NPG) is popularly applied for walking robots. Limit cycle oscillators such as Rayleigh (Pina et al 2005) or Van der Pol (Dutra 2003) could be used to generate movement patterns, however, biologically inspired pattern generators are more popular (Miyakoshi et al 1998; Endo 2002; Taga 1995). The NPGs are inspired from animal locomotion, and are comprised of several interconnected subnetworks which produce stable oscillations. Kinematic pattern generators provide oscillating desired trajectories and simple proportional derivative (PD) feedback controllers manipulate motion trajectories sometimes even with reinforcement learning algorithm for real time adjustment (Morimoto et al 2004; Nakanish et al 2004). The kinematic pattern generator is called movement primitive. In viewpoint of reinforcement learning, the movement primitives are simplified control policies which are optimal to a certain cost criterion. An appropriate combination of a small number of movement primitives provides control vector without concerning the complexity of high dimensional motor learning. Studies demonstrate that such scheme achieves natural human-like locomotion, but the structure seems to be less biological. The NPGs in animals seem to regulate muscle activation signals not desired kinematics. The muscle activation signals may partially contain the characteristic of desired kinematic information, but the muscle activation waveforms are not clearly consistent with desired kinematics.

2. Passive walking

This walking strategy is mechanical system-concentrated. Pure passive walkers can not walk on flat ground, and therefore, small energy sources are inevitably required to sustain walking. Walking cycle adapts by phasic muscle activation that only works when they need to, not depend on gravity. Thus, the energy supply is either gravity or a constant joint torque. The walking gait is sustained simply by interaction of gravity and inertia with minimal joint torque for modulation, starting and stopping, and is represented as a natural limit cycle (McGeer 1993). Passive walking models usually recruit ballistic motions with no bending knee. Without energy, the gait oscillation will decay eventually. Energy is mainly applied at push-off phase of stance leg to produce forward thrust (Collins et al 2001; van der Linde 1999). The feature is biologically human-like (Zajac 2003). Passive walking is efficient in viewpoint of energy (Collins et al 2001).

Preprogramming strategy is good at nominal execution, but problematic unless unexpected disturbance is quickly responded to. Moreover, most of systems by this strategy are model-based so that they are not appropriate for real time control due to intensive computation for detailed motions. Generating motion pathways based on estimated models is computationally demanding. For robust execution, this strategy generally requires highly active (high gain) control. On the other hand, passive walking strategy requires less effort and is energetically efficient, but less robust. The strategy also needs an intelligent real time control for flexible motion generations. Humans execute natural and flexible, but highly complex nonlinear dynamic behaviors with suitable efficiency and robustness.

2.3 Physiology of balance and locomotion

2.3.1 Postural balance control

Upright postural balancing describes the dynamics of body posture to prevent falling over a relatively small base of support under gravitational field. Several experimental methods have been employed to study human balance control, and a major method (Nashner and McCollum 1985; Horak and Nashner 1986; Henry et al 1998 was to investigate human postural response to backward platform translations. Humans have been noted to exhibit characteristically different balancing kinematics that emphasizes either ankle or hip motion depending upon the magnitude and speed of the platform translation. The postural "strategy" being implemented can be characterized by assessing the determinants of body's COM control.

1. Ankle strategy

   Slow disturbances result in comparable peak excursions at the ankle and hip. In this case, because the COM is much farther from the ankle than the hip, the ankle motion has dominant control over the COM positioning, and therefore over balance. This type of motion is considered "ankle strategy" (Nashner and McCollum 1985). For low disturbance velocities, there is extremely little activation of ventral musculature while the dorsal muscles are activated in ascending sequence, despite the shorter long-loop reflex times of the knee and hip musculature. This is a recognized pattern in ankle strategy motions (Horak and Nashner 1986).

2. Mixed (ankle and hip) strategy

   On the other hand, rapid disturbances yield progressively greater hip motion until both joints contribute more equally to balance, especially later within the recovery motion. This pattern may be termed "mixed ankle and hip strategy". It enables the body to remain within the feasible balance configuration region by limiting ankle movement, and restricting ankle torque to levels consistent with maintaining heel contact with the platform. The flexion at the hip and

extension at the ankle that promote COM recovery are aided by the abrupt deceleration of the platform at all translational velocities, as was described by Runge et al (1999). At higher velocities, there is early activation of ventral muscles at the knee and hip, and late activation of the dorsal muscles at these joints. This is the characteristic muscle activation pattern associated with the mixed ankle-hip strategy (Horak and Nashner 1986).

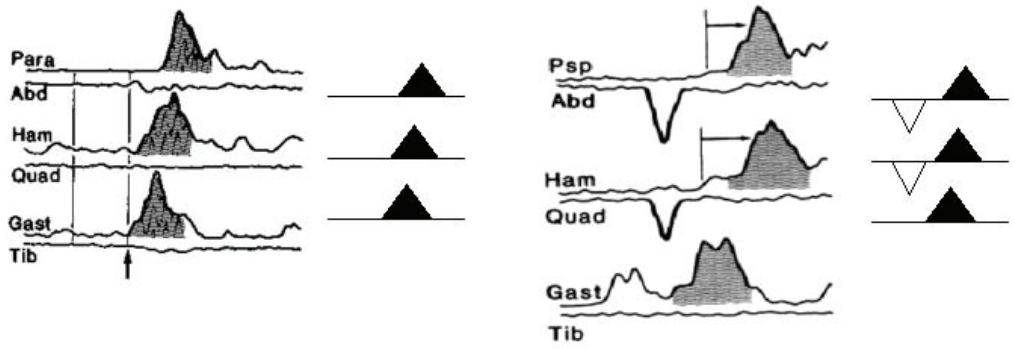

Figure 2-2: Human postural EMG responses to backward platform translation: ankle strategy EMG patterns (left), mixed ankle and hip strategy EMG patterns (right) (adapted from Horak and Nashner 1986), dorsal muscles: Para (Psp): Paraspinals, Ham: Hamstrings, Gast: Gastrocnemius; ventral muscles: Abd: Rectus abdominis, Quad: Rectus femoris, Tib: Tibialis anterior.

Human erect posture in reality is maintained a bit forward tilt from the vertical (Gatev et al 1999). This helps keep the center of mass closer to the center of the stable support area is located at front of body. Therefore, ankle flexor activities are rare and ankle extensors are considerably activated. Ankle extensors contribute the most toward control of the ankle joint torque and therefore the body posture during quiet stance. Activity of gastrocnemius lateralis is closely correlated with postural micro-sway (Gatev et al 1999). Most recent studies propose that the actual postural control system during quiet stance adopts a control strategy that relies notably on velocity information and that such a controller can modulate muscle activity in an anticipatory manner without using a feed-forward mechanism (Masani et al 2003).

The velocity information is most accurate among proprioceptive sensory inputs (Jeka et al 2004).

2.3.2 Bipedal walking control

Walking is generally a forward progression compatible with dynamic equilibrium, adapting to potentially destabilizing factors by means of coordinated synergies of upper limbs, trunk, and lower limbs (Grasso et al 2000). Human biped walking has features summarized by Gilchrist and Winter (1997) as follows.

> First, during the whole walking process, the upper body remains close to the vertical, so that the posture helps control the body's COM with stable supporting area. Second, the movement at each joint must remain within its physiological range of motion. Third, a stance leg provides support at all times. Fourth, there must be forward progression with an alternating pattern of leg support, and finally, the swing foot must clear the ground until the body is suitably positioned for weight transfer.

A human gait can be divided into stance and swing phases. A gait retains about 60% of stance and 40% of swing in phase. Double support in stance phase charges a portion of 24% in a gait.

1. Transition from stance to swing:

   The proprioceptor at hip (maybe, from the muscle spindles in hip flexor muscles) detects the transition. Swing is evoked when the flexor muscles are stretched and the leg is unloaded. Extensor muscles sense force reduction, probably, by Golgi tendon organs. In midstance, ankle pantarflexors push off the ground to provide forward thrust. Especially Soleus (uni-articular plantar flexors) contributes to trunk forward progression and Gastrocnemius (bi-articular plantar flexors) to swing initiation (Zajac 2003). The limb will be unloaded through actions at ankle, but at the knee and hip in order. In fact, the plantar flexors hinder

progression before midstance. They increase the vertical energy of the trunk to support body before midstance.

2. Swing phase:

   The information of the movement of the body's COM with respect to the support foot is significant. It is because one leg only in contact with the ground should support the whole body and maintain stability. Thus, the primary endings of ankle muscle spindle presumably play a critical role to track a stable swing trajectory. In environmental changes, the afferent information is necessary to adjust the rhythmic locomotion pattern. In addition, the afferent information is used to determine swing interval enough for weight transfer from the one leg to the other in order not to lead to tripping or falling. Knee flexors decelerate the swing foot prior to heel contact at the end of the phase.

3. Transition from swing to stance:

   Knee extensors absorb the body weight when heel strikes the ground.

4. Stance phase:

   Muscles at each joint prepare for forward thrust production as well as support the body weight. Vasti group (uni-articular quadriceps) and gluteus maximus (uni-articular hip extensors) contribute to support and forward progression at the beginning of stance, and rectus femoris (bi-articular quadriceps) to forward progression in late stance (Zajac 2003). They accelerate the trunk and brake the leg in early phase, and then accelerate both trunk and knee in late phase.

In energy view, major positive mechanical energy is burst at stance to swing transition. Positive forward thrust at ankle plantarflexors is the primary factor. On the other hand, negative energy burst takes place at swing to stance transition. Ideally, the negative work by weight acceptance at this transition is equal to the positive work by push off at stance to swing transition. However, muscles must activate to compensate the energy loss as heat or some other dissipation. The rate of metabolic energy expenditure (calorie/min/kg) increases parabolically as walking speed increases.

When the rate is normalized by the distance traveled, an optimal walking speed is predicted at 80 m/min (Anderson and Pandy 2001). During a gait, a maximum of potential energy and a minimum of kinematic energy of the body come into play in middle of stance. At the midstance, the body's COM heightens most and walking speed is slowest. The converse situation is at the double support.

2.4 Examples of current models

Burgeoning interest in robot design as well as in the physiology of human motor control has stimulated computational investigations of natural upright balance and locomotor control. Some of recent works are summarized here.

2.4.1 Peterka's balancing model (Perteka 2003)

Peterka showed that principally a Proportional Integral Derivative (PID) controller can describe human sensorimotor control system of maintaining postural balance involving primarily ankle motion, which is represented by a link inverted pendulum, and the force feedback is influential at motion of low frequencies. The force feedback primarily influences postural behavior, a gain decline and phase advance by scaling proportionally to the integral of the sensed signal according to him. A gain decline means smaller steady error with respect to the gravitational vertical line. The force-related signal input may arise from the pressure distribution o the feet or muscle tension by Golgi tendon organs. However, balance maintenance in reaction to rapid external disturbances necessitates multi-joint, e.g., mixed hip and ankle, responses. And rapid disturbances may excite high-frequency dynamics that give rise to undesirable oscillations or destabilize a nonlinear system with delays or other phase lags. Peterka's model included neural transmittal delays, but did not provide the confidential details on neuroanatomical structure. What explicitly can the PID controller represent? The control gain values were obtained by regression of human experimental data. In addition, the investigation is limited to system output signals in time- and frequency- domains. Internal signals such as electromyography (EMG) are not

included. To further promote neuroanatomical plausibility of the model, such internal signals would need to be taken into account.

2.4.2 Kuo's balancing model (Kuo 1995)

An engineering model was developed that effectively describe aspects of human postural balance by Kuo. For disturbances of different magnitudes, human body dynamics can be linearized so that, in the context of effective full body state estimation/prediction by a linear internal dynamics model, human postural responses to platform translation speeds were described in terms of optimal linear (linear quadratic Gaussian) control. Adjustment of a control parameter evoked different postural strategies appropriately corresponding to platform translation speeds. Therefore, Kuo's model realizes the full range of human postural balancing behaviors without stepping.

However, the model was designed as if there were no delays or muscular coupling dynamics. Maintaining system stability with such phase lags or delays is a critical issue in the field of neural system models (Massaquoi 1999). In addition, like Perterka's, no specific neuroanatomical structure was not proposed. Instead, only optimal control structure represented the whole central nervous system. The optimality of human behaviors is controvertible. Even suppose human behaviors are optimal, its objective (or cost) function is beyond verification. The external disturbance was model kinematically, e.g., initial conditions of joints not dynamically, e.g., external forces.

2.4.3 Taga's biped walking model (Taga 1995, 1998)

Taga proposed a noteworthy neuro-musculo-skeletal model of biped walking. The model has eight body segments, ground contact elements, and 20 muscles. Its neural controller depends on a sequence of global states, which is defined by COM and COP. The sequence feeds inputs from neural oscillators, located to each joints, in order to generate stable limit cycles. The impedance controllers representing muscles help

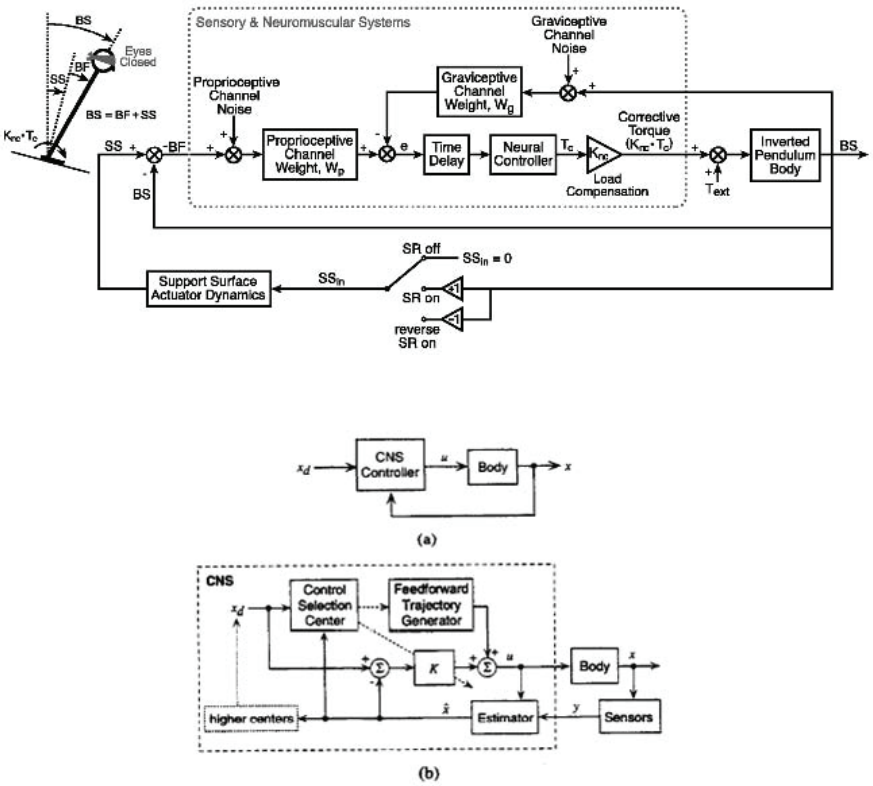

Figure 2-3: Peterka's postural balancing model (adapted from Perterka 2003) (top), and optimal control model used by Kuo (adapted from Kuo 1995) (bottom).

the construction of gait emergence in the sense of feedback. The integrative neuro-musculo-skeletal system interacting to the ground generated stable gait motions in the sagittal plane. Further studies (Taga 1998) demonstrated that the model generates robust walking motions against external perturbations, or variations in the terrain, and even more, speed can be controlled by a single parameter tonically exciting the neural oscillators, and step cycle can be entrained by a rhythmic input to the oscillators.

In the perspective of neurophysiological modeling, Taga's model is still in lack of explicit evaluation on plausibility. It is unknown yet whether humans use such global states to generate walking. Also, Taga's model attaches neural oscillator pairs to every joint. In reality, NPGs in the spinal cord level may not need provide such many local

rhythmic patterns separately. Muscle model is not biological neither. Each muscle is a simple spring-damper impedance controller without activation and contractile dynamics, and its parameter values are not based on physical muscular values at all. Most of all, neurophysiological phase lags such as neural signal delays or muscular excitation and contraction coupling were not included at all.

2.4.4 Ogihara and Yamazaki's biped walking model (Ogihara and Yamazaki 2001)

Another neuro-musculo-skeletal model by Ogihara and Yamazaki emphasizes NPGs and the neural feedback control system that consists of muscles, reflexes from muscle spindles, tendon organs, and foot tactile receptors. This model has much more biologically meditated structure, especially low nervous system, than Taga's. Muscle model includes dynamic properties of force-length-velocity relations with activation. However, high nervous system was not explicitly designed. A genetic algorithm decided the neural network weights by minimizing energy consumption per step. The neural control algorithm in this model is more complicated than Taga's, and its walking performance is less robust.

2.4.5 Kimura and Fukuoka's walking and running of a quadruped robot (Kimura and Fukuoka 2001)

Kimura and Fukuoka built a quadruped walking robot "Tekken" controlled based on biological concepts. Viscoelastic muscular structure activates the robot, and its neural system model consists of a NPG and reflexes. The equation of NPG is similar to that of Taga's. A modified proportional control-type vestibulospinal reflex controls body roll and pitch angles, and affects the phases in the NPG network. Muscular control gain can be adjusted based on the phase signal of the NPG so as to make adaptive walking. However, the control parameters are not biologically oriented. They demonstrated that the robot can walk on terrains of irregularity and change walking speeds.

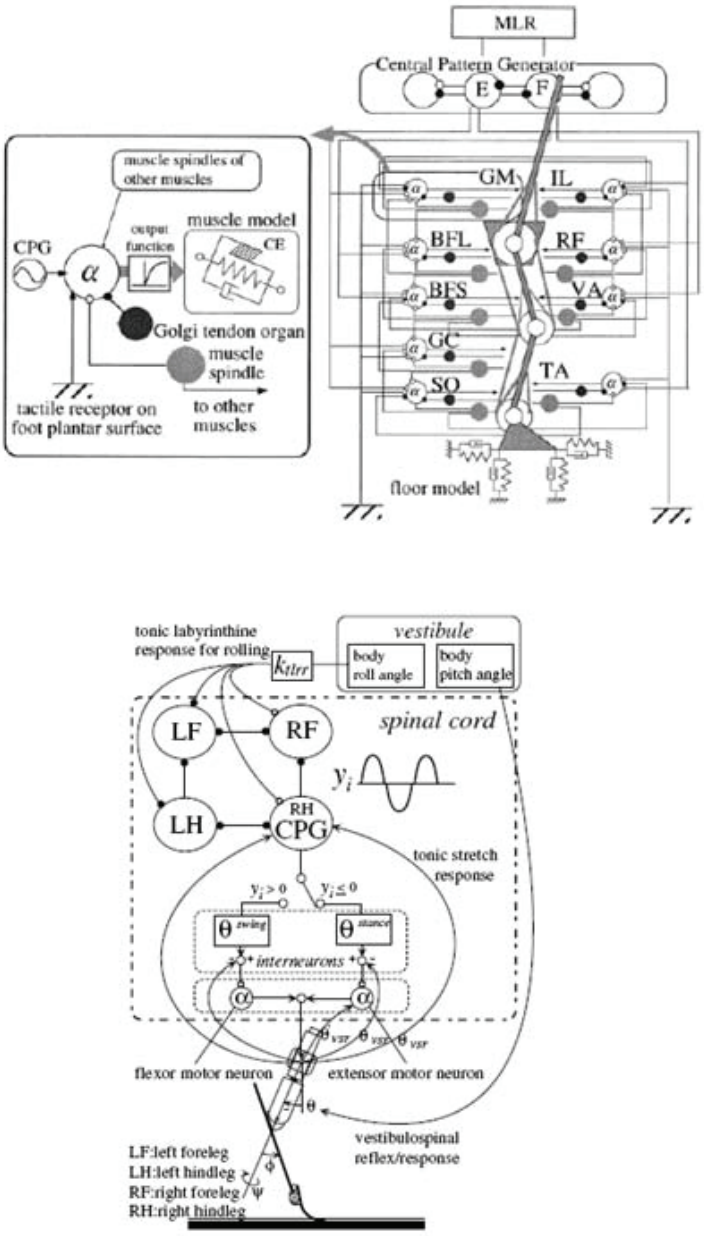

Figure 2-4: Diagram of a bipedal walking model (adapted from Ogihara and Yamazaki 2001) (top), and diagram of a quadripedal walking model (adapted from Kimura and Fukuoka 2001) (bottom).

These models show that qualitatively realistic bipedal walking kinematics can be achieved using biomorphic components. However, these models have not demonstrated the capacity to walk at different speeds or to balance upright when stationary

without changes in physical parameters. Also, the sensitivity to changes in physical characteristics and to disturbances has not been examined. Most of all, the nature of the higher levels of neural control of bipedal gait remains essentially unexplored.

2.5 Common principles of balance and walking

It has already been pointed out that the waking and postural balancing share common organizational principles (Lacquaniti et al 1997; Massion 1992). For both behaviors, the reference frame seems to be the vertical along gravitational field. The erect posture for both cases can minimize the effect of gravitational destabilization and therefore is energetically efficient. Secondly, the COM seems to be a critical control variable for both behaviors (Lacquaniti et al 1999; Grasso et al 2000; Winter 1995). For investigations on biped humanoid walking, the COM [1] relative to either static or dynamic equilibrium has already been considered as an important control factor to deal with dynamic stable walking (van der Kooij et al 2003; Sugihara et al 2002; Taga 1995). The COP, in other words, ZMP may be another critical variable for analysis of postural balancing (Winter 1995) as well as walking (Sugihara et al 2002). However, it is suspicious whether COP is really critical information used in the neural system. Freitas et al (2006) proposed two channels of posture, i.e., COM and truncal verticality, on basis of human postural balancing studies. Forward walking is to move COM forward intentionally with respect to foot on the ground to take a step. Third, both behaviors are closely mediated through afferent sensory feedback (Peterka 2003; Lacquaniti et al 1999; Grasso et al 2000; Brooks 1986). Sensory feedback information makes it possible to control responses robustly against unexpected disturbance. It has been experimentally observed that both behaviors depend seriously on afferent sensory information (Jeka et al 2004; Masani 2003; Gordon et al 1999; Pardoe et al 2004).

[1] From now on throughout this thesis, more precisely speaking, COM stands for COG, e.g. horizontal projection of COM.

2.6 Principal motor centers involved in balance and bipedal walking

The major neurophysiological sensorimotor control systems of interest in this thesis are cerebrum, cerebellum, and spinal cord. They are organized hierarchically and in parallel interacting with other systems such as thalamus, Basal ganglia and so on. The whole organization consists of feedback, feedforward, and adaptive mechanisms in hierarchical and parallel relations. Thanks to the hierarchical and parallel structure, movement is still possibly generated even with atrophy or malfunction of partial systems. Figure 2-5 illustrates significant pathways among those major systems. The highest level of sensorimotor system consists of cerebral cortices: motor cortex, premotor cortex, and somatosensory cortex. Consulting sensory information from the somatosensory cortex, the premotor (and/or supplementary motor (not shown in Figure2-5)) cortex coordinates and plans complex sequences of movement, and the motor cortex executes them. The cerebral cortices project directly to the spinal cord through corticospinal tract as well as indirectly through brain stem systems. The brain stem system modulates motor neurons and interneurons in the spinal cord. The cerebellum and the Basal ganglia improve the accuracy of movement by comparing descending motor signals and ascending sensed signals. Both transmit their monitoring signals to cerebral cortex through thalamus, which is the synaptic relay for information reaching the cerebral cortex. The cerebellum also acts on the brain stem connected to the spinal cord. The spinal cord principally receives descending signals from either the cerebral cortex or the brain stem. The spinal cord also projects ascending signals to higher motor systems via several different pathways.

A large number of systems potentially influence posture and gait including cerebral cortex (King 1927; Nielsen 2003; Dietz 1992), cerebellum (Dietz 1992; Morton and Bastian 2004), basal ganglia including subthalamic locomotor region (Zijlstra et al 1998; Shik and Orlovsky 1976; Dietz 1992), midbrain locomotor region (Grillner 1975; Shik and Orlovsky 1976; Kandel et al 2000) and spinal cord with segmental reflexes

(Duysens et al 2000; Knikou et al 2005; Brooke et al 1997; Grillner 1975; Dietz 1992; Shik and Orlovsky 1976). At least in primates, upright walking appears to require the integrity of cerebral cortical control of legs, midline cerebellum including at least the fastigial nucleus (Mori et al 2004) and possibly the interpositus (Armstrong and Edgley 1988), the brainstem and spinal cord. While basal ganglionic dysfunction leads to a host of walking deficits (Zijlstra et al 1998; Shik and Orlovsky 1976; Kandel et al 2000) it is not clear that explicit representation of basal ganglionic function is required to account for locomotion. Certainly in a supported decerebrate cat, highly coordinated walking motions can be elicited by stimulation of cerebellar or mesencephalic centers (Grillner 1975; Mori et al 1999; Shik and Orlovsky 1976; Kandel et al 2000). Thus, it may be proposed that rudimentary voluntary walking might be modeled by motor cortex supported only implicitly by intact basal ganglionic function.

Several studies suggest that locomotion results from net performance of spinal level circuits that are modulated and driven by higher systems. The precise partitioning of function has not yet been determined. However, several observations are relevant. Studies of frog spinal cord demonstrate synergistic patterns of muscle activities (Cheung et al 2005; d'Avella et al 2003). Such a mechanism collapses multiple muscle control to a lower degrees of freedom control for each leg. The lower dimensional control can still account for a wealth of frog leg EMG activity and behaviors including wiping, crawling and swimming. It is plausible that low level locomotion may use the same or similar spinal synergies.

2.6.1 Cerebrum

The cerebrum is the evolutionarily newest and largest part of the brain. It participates in many different functions such as perception, decision making, memory, motor control and so on. The cerebral cortex, the surface of the cerebrum, is composed of six neuronal layers, which locates on top of white matter pathways. It includes about 10 billion neurons. The most conspicuous features on the surface are numerous folds termed *gyri* which increase the surface area. The intervening grooves between the

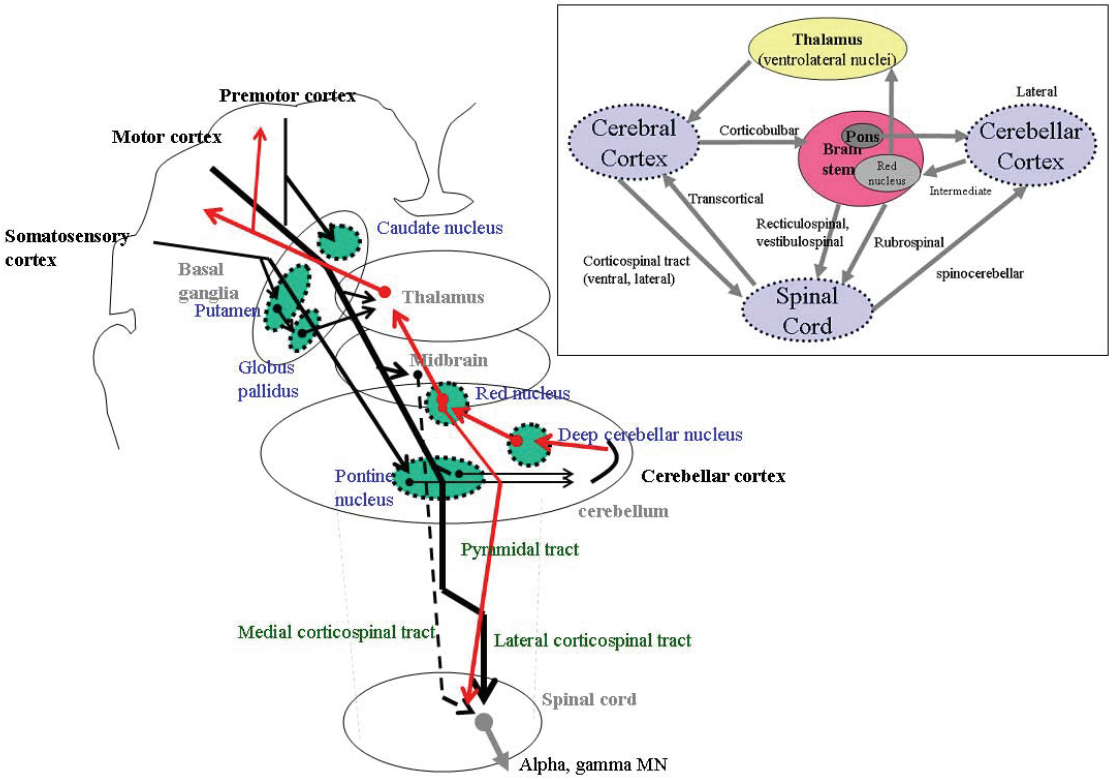

Figure 2-5: Neuroanatomical pathways between cerebral cortex, cerebellar cortex, and spinal cord (adapted from Kandel et al 2000). Box shows a simplified version.

gyri are called *sulci*.

The distinction between the six layers is based on architectonic structure (Figure 2-6). Layer 1 receives neural signals from the surface of the cortex. Layer 2 and 3 consist of a variety of excitatory pyramidal cells and even richer populations of interneurons. Layer 4 as the input layer of the cortex contains star-shaped excitatory neurons called stellate cells and inhibitory interneurons or basket cells. Layer 5 includes large excitatory pyramidal cells and two or more types of interneurons. Layer 6 is actively connected with sensory inputs from the thalamus. Layers 5 and 6 provide cortical outputs. Layer 5 pyramidal cells extend axonal connections to spinal cord and basal ganglia, and thalamic nuclei, and layer 6 pyramidal cells form a feedback pathway with the specific thalamic nuclei.

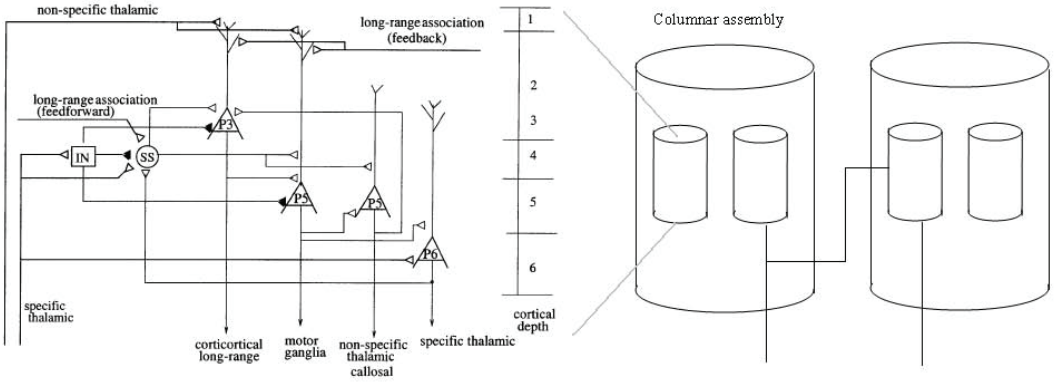

Figure 2-6: Basic connectivity of cortical circuit (left) (adapted from Karameh 2002), and columnar assemblies (right).

An interesting feature is that the spatial extent of pyramidal cell association collaterals approximately construct a columnar assembly. Each column may contain a specific feature presentation of sensory information such as orientation or a specific direction. An ongoing hypothetical thought is that each directional neuron population representation seems to be implemented in each column in sensorimotor cortical Area 3a (Karameh 2002; Huffman and Krubitzer 2001). For a specific piece of movement, a specific columnar firing may be distinguishably dominant. The activity dominated from the winner columnar assembly may be transmitted to other sensorimotor cortical columns and thence to cerebellum by larger TL5 pyramidal cells. Experimental observations have shown task-related neural activity in premotor and motor cortex. Neurons in motor cortices have a uniform distribution of "preferred directions" for reaching or tracking movements (Johnson and Ebner 2000). Neural activities of M1 cells in monkey are directionally tuned during an epoch of reaching task movement and the preferred directions of M1 cells were very different (Cisek et al 2003). It is known that activity population distribution in an ensemble of M1 neurons adequately points a specific direction, which is mathematically expressed by a unit vector though the discharge of single neurons rarely identifies any direction with accuracy (Georgopoulos 1988). These observations may be related to the function of the columnar assembly in cortex. Tanji (2001) argued that motor cortex plays important roles in

the temporal sequencing of multiple movements.

In this study, the cerebrocerebellar interaction is very simply modeled as the recurrent integral feedback loop, but no detailed model of the cerebrum is investigated. The cerebrocerebllar system in the proposed model proceeds with the specific components of sensory information or a linear combination of them rather than the whole sensory information. The representation of the sensory information may be explained with respect to hypothetical cortical mechanism of selection.

2.6.2 Cerebellum

It appears that in arm reaching, the cerebellum is responsible for coordinating and controlling movements. By extension, human studies and preliminary work (see section 3) suggest that the role of the cerebellum in balancing is to manage adaptive changes of postural control and in walking is to regulate balance dynamically. Specifically, it seems that the cerebellum participates in the generation of appropriate patterns of limb movements and adaptation of posture and locomotion through practice.

The cerebellum has three functionally distinct regions; anterior lobe, posterior lobe, and flocculonodular lobe. The three lobs are piled up and separated by fissures. In details, fissures divide the anterior and posterior lobes into nine lobules. The primary fissure divides the anterior and posterior lobes, and the posterolateral fissure the posterior and flucculonodular lobes. A more interesting division is on the basis of function. Two longitudinal furrows distinguish three mediolateral regions, e.g., the central vermis and the intermediate and the lateral regions. The three functional regions consist of the main body of the cerebellum, the anterior and the posterior lobes. The flocculonodular lobe is the most primitive and receives input primarily from the vestibular system and its major function is to control balance and eye movements and is called the *vestibulocerebellum*. The vermis receives most sensed signals such as visual, auditory, vestibular, and somatic sensory inputs. Its outputs reach indirectly proximal muscles of the body and limbs. Thus, the vermis is concerned

with posture and locomotion as well as gaze. The intermediate region is related to control the distal muscles of the limbs and digits. The vermis and intermediate are called the *spinocerebellum* because the regions receive somatosensory inputs from the spinal cord. The lateral region, most recent, is called the *cerebrocerebellum* because its input is from the cerebral cortex. The expected role of cerebrocerebellum is motor planning and mental process related with motor actions and movement errors.

The cerebellum is globally uniform in its structure. In microarchitecture, three layers, e.g., molecular, Purkinje cell, and granular layers, organize the cerebellar cortex and contain five types of neurons: granule cells make excitatory connections with all the other cells, and basket, stellate, and golgi cells are inhibitory neurons. Purkinje cells receive excitatory signals, but its output is inhibitory. Two types of inputs are conveyed to the cerebellum: Mossy fibers and Climbing fibers. Mossy fiber input produces a steam of simple spikes in Purkinje cells throughout relayed circuits. The firing rate of simple spikes is about several hundred spikes per second. The frequencies encode either peripheral sensory information or central commands. Climbing fiber input is error-type signals originating from the inferior olivary nucleus. Climbing fibers have powerful synaptic connection with Purkinje neurons and provoke a complex spike on the dentrites of the Purkinje cell, but its firing rate is so low (around 1 per second). Climbing fiber pathway is a "teaching" line for the adaptation at the parallel fiber-Purkinje cell synapse.

About 10^{11} granule cells, the most numerous, are in the cerebellum. They receive neural signals through mossy fibers and transmit output signals to the Golgi cells and parallel fibers. Signal information in mossy fibers is a bit different in different region of cerebellum. In the medial and the intermediate cerebellar cortical zones, the information is from vestibular, somatic, visual, and auditory sensory pathways and from sensorimotor cerebral cortex. In lateral zone of the cerebellar cortex, the mossy fibers carry information from prefrontal, premotor, and parieto-occipital association cortex.

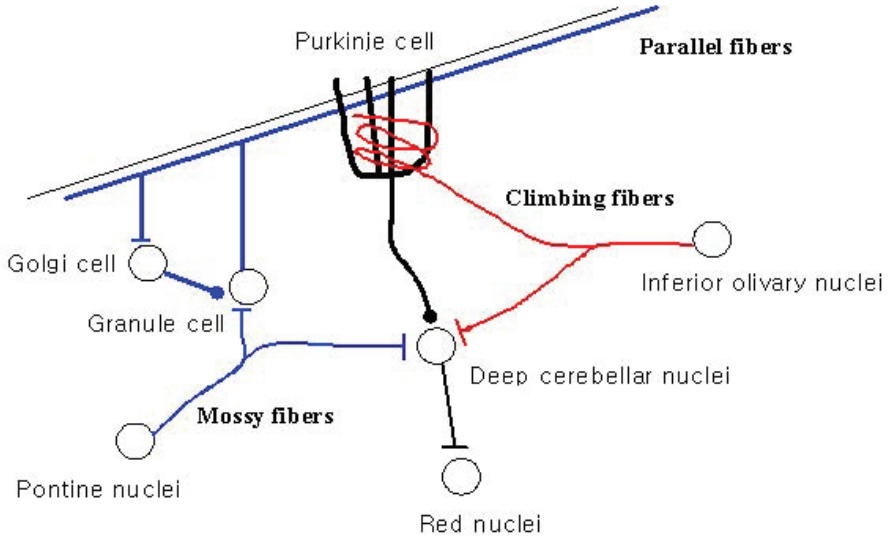

Figure 2-7: Neural circuit of cerebellar cortex: bar indicates excitatory synapse and filled circle inhibitory.

Golgi cells in the granule layer receive excitatory inputs from mossy fibers directly as well as granule cells. Inhibitory inputs from stellate, basket, and Purkinje cells are also conveyed to Golgi cells. Then, Golgi cells inhibit granule cells in the glomeruli. Signal conveyed to parallel fibers is relayed to Purkinje cells. The signal is a brief excitatory potential that evokes high frequency firing on the dentrites of the Purkinje cell at 0-500 spikes per second. Parallel fibers locate parallel to the long axis of the folia and perpendicular to the dendrites of Purkinje cells. Purkinje neurons have fan-like dendrites and project into the white matter under the granular layer. Its shape is like a palm tree. Purkinje cells provide the output signals of the cerebellar cortex to deep cerebellar nuclei. Purkinje cells also receive the other input to the cerebellum through climbing fibers. A feature is that a Purkinje cell receives input from only one climbing fiber. Stellate and basket cells modulate inhibitory connections with parallel fiber to Purkinje cell in the molecular layer.

The outputs of cerebellar cortex are sent to other areas exiting through deep cerebellar nuclei. The nuclei are called differently in different regions of cerebellum. Medial, intermediate and lateral regions, respectively, project via the fastigial, in-

terposed, and dentate deep cerebellar nuclei. The neural output signals reach either motor cortex via Thalamus (ventrolateral nuclei) or spinal cord via brain stem. Impairments related to the deep cerebellar nuclei indicate behavioral functional relationship (Thach 1998). The neural output signals from fastigials contain mainly the information on upright stance and gait. Interposed nuclei (Interpositus) are related to reaching movements or alternating agonist-antagonist muscle. Impairment of Dentate causes curved trajectory, overshoot on reaching movement, and incoordination of fingers in grasp/pinch.

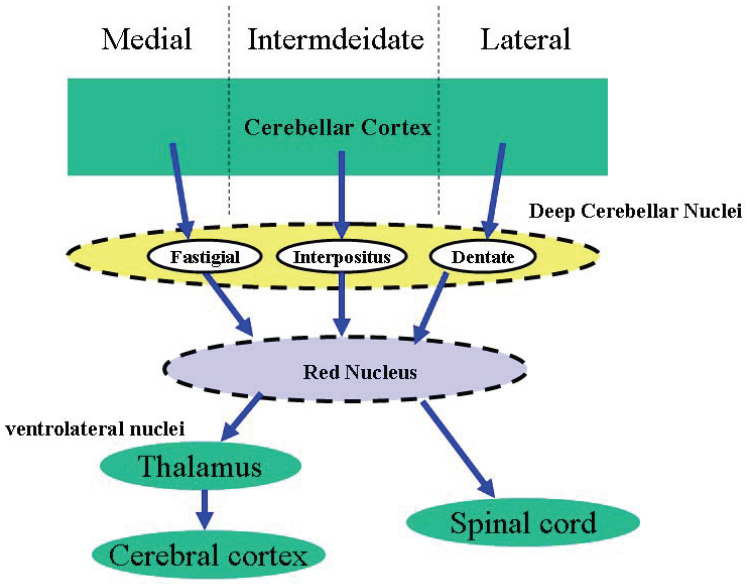

Figure 2-8: The outputs of cerebellar cortex.

The Ito's opinion on climbing fiber signal as a "teaching" line has been extensively studies in the vestibulo-ocular system and some other applications (Kandel et al 2000). The adapted state is retained and the phenomenon is called synaptic plasticity. Especially, conjunctive stimulation of both climbing fiber and mossy fiber pathways provokes excitation on the Purkinje cell but inhibition on the deep cerebellar nuclei for a while. The synaptic plasticity is called LTD (long term depression). The depression is postsynaptic and restricted to the interaction site between the two climbing fiber and mossy fiber inputs (Gao et al 2003). Some other possible adaptation processes

have also been suggested (Ito 2001). Granule cell-deep cerebellar nuclei line is a candidate. Stimulation of granule cell axions alone in the absence of climbing fiber stimulation evokes directly burst of excitation in the deep cerebellar nuclei (LTP: long term potential) (Frysinger et al 1984). Postinhibitory rebound of excitability in deep cerebellar nuclear cells is another. When coherent inhibition on deep cerebellar nuclear cells by Purkinje cell is terminated, the neurons within the deep cerebellar nuclei produce a rather pronounced burst of excitation by mossy fiber input. The effect may be that the deep nuclei are capable of driving neuronal populations to which it projects.

The cerebrocerebellar interaction model of this thesis is originated from planar arm reaching movement tasks (Massaquoi 1999; Massaquoi and Topka 2002). The model is termed the Recurrent Integrator Proportional Integral Derivative (RIPID) model. The model proposes the recurrent integrator loop between cerebellum and cerebrum to afford effective differentiation and thereby phase lead critical for long-loop stability. In addition, the model interpreted that the neural signal processing over the cerebellar cortex can be regarded as proportional scaling, differentiation and integration operations. The details are explained in section 3.4.3.

2.6.3 Vestibular system

The vestibular system is the sensory system that provides the dominant input about movement and orientation in space. Together with the cochlea, the auditory organ, it is situated in the vestibulum in the inner ear. As our movements consist of rotations and translations, the vestibular system comprises two components: the *semicircular canals*, which indicate rotational movements; and the *Otoliths*, which indicate linear translations. Therefore, the system regulates postural balance. The vestibular system sends signals primarily to the neural structures that control eye movements as well as to the muscles that keep us upright. Vestibular-ocular reflex participates in the eye movement control. Even subjects with significant vestibular dysfunction may be able to balance (Nashner et al 1982). The orienting mechanism can utilize multisensory

inputs. The most frequently reported symptoms of vestibular disorders are dizziness, unsteadiness or imbalance when walking, vertigo, and nausea.

In this research, a detailed vestibular system model is not pursued because the research is focused on the cerebrocerebellar control. Rather than that, vertical reference along gravitational field is assumed to be informed by vestibular system probably with corporation of other neural systems (Peterka 2003).

2.6.4 Basal Ganglia

It is known that the basal ganglia contributes to body posture and controlling the movement, even further, cognitive programs. It seems to play a major role especially in normal voluntary movement. An interesting point is that the basal ganglia is not directly connected to the spinal cord unlike most other motor systems. Therefore, its motor function is attributed via other systems, especially, motor areas of the cerebral cortex (Kandel et al 2000). Its input signals from the cerebral cortex through the striatum are conveyed by two different pathways, e.g., "direct" and "indirect" pathways. Neural signals through direct pathways reach the thalamus with net excitatory effect via the internal segment of *globus pallidus*, and those through indirect pathways converge to the thalamus with net inhibitory effect via the internal segment of globus pallidus after passing by the external segment of globus pallidus under the effect of a local loop between the external segment and subthalamic nucleus. Then, the thalamus excites the related areas of the cerebral cortex. The basal ganglionic neural circuit seems to do discrete operation of context-to-control mapping (Massaquoi and Mao, unpublished).

The basal ganglionic function is beyond the interest of this study. It is because this thesis focuses on less voluntary (postural) movements and responsive behaviors to environment or external disturbance mainly controlled by the cerebrocerebellar interaction.

2.6.5 Spinal cord and reflexes

The spinal cord consists of nerve cells as a part of the vertebrate nervous system. The cord conveys the spinal nerve pairs of the peripheral nervous system that contains sensory information as well as central nervous system pathways that innervate muscles. Reflex calls a stereotyped (involuntary) motor response elicited by a defined stimulus. Reflex participates effectively in motor control in order to either protect body or improve motions.

Principally the role of spinal cord seems supplementary to the higher sensorimotor system. This research pays less attention to the spinal cord for balancing tasks. However, as Bizzi et al (2000) indicated, the spinal cord level control networks may be effective for motion generation in terms of organization and modification (see section 3.2.3). Therefore, walking control model includes the spinal locomotor system, especially, with respect to neural pattern generators and motor primitives. The neural pattern generators term the neural networks generating rhythmic motor activity in the absence of sensory feedback. The rhythmic pattern generator networks are considered to be at the core of locomotor control system (Brooks 1986). The existence of the pattern generators in mammals has been observed (Kandel et al 2000): decerebrate cats can walk on a treadmill by stimulating a small region in the brain stem; the hind limbs can step on a treadmill even after the spinal cord is transected in a cat. These observations implicate that rhythmic patterns can be generated at the level of the spinal cord independently of sensory feedback and sophisticated command from the higher motor systems. Humans also possibly have such rhythmic pattern generators for locomotion. Some studies have proposed some evidences (Calancie et al 1994; Pinter and Dimitijevic 1999). The networks are regulated by signals from the higher nervous system or/and the proprioceptive information though they are not necessary. Reflexes also affect the pattern generation by adjusting limb positions or movement directions. The specific distinct neural activities, as modules, are called muscle synergies. They can be identified as the invariant amplitude and timing relationships among the muscle activations. Therefore, reversely the muscle activations can be

constructed by scaling different muscle synergies with appropriate time-dependent or -independent treatments (d'Avella et al 2005; Cheung et al 2005; Cajigas-Gonzalez 2003).

2.6.6 Muscle

A typical muscle consists of many thousands of muscle fibers working in parallel. Motor neurons convey descending commands to the muscle fibers. The bundle of muscle fibers innervated by only one motor neuron is called muscle unit. A single action potential in a motor neuron activates the muscle unit in synchrony. Accumulation of overlapping action potentials results a complex pattern of electrical potentials recorded as an *electromyogram* (EMG). A single muscle fiber microscopically contains many *myofibrils*, which consist of repeating cylindrical bands called *sarcomeres*. The sarcomeres are organized into a matrix of thick and think filaments repeatedly bounded by Z disks. The myofibrils in all muscle fibers tend to change length in concert as a result of the various noncontractile components that link them mechanically. This results the passive spring-like restoring force. It does not require energy consumption, but is induced by the mechanical properties of muscle fibers. In addition, the contractile machinery of the filaments produces contraction by the mechanism so called "sliding filament hypothesis". Cyclical interactions between the cocked myosin heads of the thick filaments and binding sites on the actin of the thin filaments work like rack and pinion by pulling or detaching repetition. This process is active energy consuming process. The contraction of the contractile component can stretch inactive muscle components, which produce the spring-like restoring force. Therefore, the total force produced by a muscle fiber consists of active and passive forces. Contractile force depends on the level of activation of each muscle fiber and its length and velocity.

A mathematical model, e.g., Hill model, captures the interrelations between length-to-force, velocity-to-force, and activation level-to-force. However, such a computational muscle model is not appropriate and too complicated to implement system

level simulation for real time or for practical purpose. Within reasonable range of muscle length change, a linearized spring and damper-like model may be good enough to facilitate implementation. Such simplified muscle models have popularly been used in neural computational model society (Katayama and Kawato 1993; Flash 1987). In this thesis, an improved activation-dependent nonlinear spring and damper-like muscle model is introduced (see section 4.2.2).

2.6.7 Overview of CNS control of the balance/locomoion control system

Theoretically and experimentally it is demonstrated that the intrinsic mechanical stiffness alone cannot stabilize posture during quiet stance (Loram and Lakie 2002; Morasso and Sanguineti 2002). The CNS should augment the system stiffness sufficiently to stabilize posture.

The high nervous system initiates and maintains appropriate locomotion patterns based on the circumstances. Stimulation of mesencephalic locomotor region (MLR) initiates walking in mammals. The strength of stimulation to MLR changes the gait and rate of stepping. Signals evoked in MLR is projected to medial reticular formation (MRF), and then, descends to the spinal locomotor system via the reticulospinal pathway. The signals in this pathway contribute to activation of muscle synergies by the spinal locomotor system. The spinal locomotor system is assumed to have pattern generators and receive afferents from muscles and also send efferent copies to cerebellum. The cerebellum also receives afferent proprioceptive signals through spinocerebellar pathway.

Without the cerebrum and cerebellum, the locomotor patterns are much simpler than normal stepping (Kandel et al 2000). The cerebellum is critical for balance and studies have shown that selective lesions of descending control from the motor cortex compromise irrevocably certain fine control of especially swing leg trajectory in the cat (Drew 1993). The motor cortex also has been shown to contribute to structure and

timing of step cycle during locomotion in the intact cat (Bretzner and Drew 2005). In humans, where fine integration of bipedal balance and stepping must be exquisite, disconnection of cerebral control of legs due to stroke or tumor evokes much devastating effects in postural balance and locomotion (Porter and Lemon 1993). Thus, normal bipedal function in humans appears to depend significantly upon activity in transcerebral pathways (Nielsen 2003; Peterson et al 1998; Nathan 1994). Work with decerebrate cats (e.g. (Mori et al 1998; Mori et al 1999; Hiebert and Pearson 1999)) confirms that important parts of cerebellar locomotor control system may not involve the cerebrum. However, in primates, the more direct system is shown to function usually together with the corticospinal pathways (Petersen et al 1998; Capaday et al 1999). Also importantly, it has been noted that most of cerebral activity during locomotion appears to be generated by sensory afferent feedback (Christensen et al 2000; Nielsen 2003).

It is known that the activity of both ventral (VSCT) and dorsal (DSCT) spinocerebellar neurons is rhythmically modulated with the different phases of locomotion. These neurons encode linear combinations of the changes in limb geometry. The coordination provides the basis for segmental feedback that may be essential for implementation of motor strategies to control limbs. Bosco and Poppele (2001) suggest that framework of DSCT proprioception might contribute to a possible regulation of joint angle covariance. It indicates that joint angle coordination is appropriate to represent neural signals in the pathway from muscle to cerebellum.

The cerebrocerebellar system plays a critical role especially during learning period of balancing and walking. Through repetitive training, the system would adaptively generate neural patterns which achieve stable and robust walking motions. Even after full adaptation, the descending command tunes basic spinal networks so as to produce dynamically the changes in amplitude and phase relationships of the spinal output, e.g., pattern generator, sufficient to achieve stable motions under uncertain environment. The climbing fiber activities in cerebellar cortex are correlated with

the step cycle and coupled to walking phase in the cat's cerebellar cortex (Kim et al 1987). Another study observed that a statistically significant adjustment of the climbing fiver activation at times immediately after the perturbation during ferret's locomotion (Lou and Bloedel 1992), and Pardoe et al (2004) also demonstrated that climbing fiber signals regulate depending on step cycle. All of the studies indicate that climbing fiber discharges are modulated with different phases of locomotion.

2.7 Abnormal control

The cerebellum seems to be important for regulating and adapting posture and locomotion through trial and error practice. As for balancing matters, subjects with cerebellar deficit, especially, cerebellar anterior lobe lesions, show increased postural responses with excessive and prolonged muscle activity, larger sway amplitude, and greater torque production (Horak and Diener 1994). As for gait matters, subjects with cerebellar deficit showed mainly gait ataxia, especially with a balancing deficit (Morton and Bastian 2003). The features of gait ataxia are reduced angular excursions, joint-joint decomposition (a series of single joint movements rather than multijoint movement.), increased stride-to-stride variability, and reduced speed. In addition, subjects with cerebellar deficit tend to a leg hypermetrica (excessive foot elevation) during walking or stepping (Morton and Bastian 2004). The medial zone of the cerebellum has been known to be the spot to control posture and locomotion (Kandel et al 2000). However, human walking is bipedal so much less stable than quadrupedal, therefore, probably additional cerebral cortical control from other area of cerebellum such as the lateral may also be important. The three primary factors can be required for the CNS to produce stable walking patterns (Grillner and Wallen 1985): 1) the principal rhythmic patterns to produce the basic motor synergies, 2) control of equilibrium for stability, 3) adaptation for locomotor control. Physiological studies have shown that the cerebellum contributes to each factor somehow. The cerebellum may modulate the timing, rate of muscle activity, and coordinate interaction between multijoint segments, and control upright posture during walking (Morton

and Bastian 2004). It appears that in arm reaching, the cerebellum is responsible for coordinating and controlling movements.

In principle, many models could achieve similarly realistic performance of nominal behaviors. Using the model to include pathological behaviors helps to constrain the choice of models. The abnormal performance realization promotes the plausibility of the model.

2.8 Outstanding questions in artificial and biological control of balance and locomotion

Bipedal walking robots like Honda ASIMO (Hirai et al 1998) were traditionally controlled by preprogrammed trajectory information provided by offline dynamic optimization algorithms. However, such techniques tend to be too inflexible to respond to large unexpected disturbances or varying situations. On the other hand, humans can walk adaptively and robustly maintaining stability under the same circumstances. Central questions are as below.

1. What accounts for this robustness of stability and ability to adapt?

2. Is it possible to achieve such flexible and robust behaviors without complicated computational control systems?

3. What, in particular, are the possibly simplest control systems that still satisfy biological plausibility?

The simplicity facilitates the application to robotic locomotion. To seek some answers to the above questions, it is useful to begin with the study of simple postural and locomotion tasks. More specific questions of this research are summarized.

1. Is a simple position and velocity-like feedback, possibly together with force feedback sufficient to control balance and locomotion?

2. Are internal forward or inverse dynamic models required?

3. How the system would change postural strategies against disturbances in postural balance?

4. Does the system change walking speeds, and exhibit robust performance with disturbances (pushing a body segment, change in body mass) in biped locomotion?

5. What does the model propose in the perspective of both neural and robotic engineering?

Postural balancing and walking mechanisms seem to be based on common principles (Massion 1992; see section 2.5). Therefore, a unified approach may supervise and execute both tasks. This thesis investigates possibly simple, but still flexible biological motor control systems to get closer to the seeking answers.

2.9 Roadmap

This thesis develops computational models which explain human postural balance and biped walking to answer the questions in section 2.8. Major concern is to develop models with minimal complexity, however, that enable sufficient explanation of human behaviors and their mechanisms. At first step, a postural balance model is investigated. And then, the model is extended to walking. The models do not violate each other with respect to neurophysiology and neural structure, and can be unified as a whole neural system without trouble.

Chapter 3 introduces a human postural balance model and demonstrates postural responses to external perturbations. Also, the chapter proposes the neural scheme to execute typical postural strategies. Chapter 4 describes a human biped walking model, using a combination of neurophysiological and biomechanical analyses. Chapter 5 demonstrates some examples of voluntary behavior during walking to evaluate

the usefulness of the proposed neural scheme. In Chapter 6, discussions over the investigations are presented.

Chapter 3

Postural balance model

Few have made specific proposals for how human postural balance control may be implemented by the CNS. In particular, the performance of CNS feedback control systems must be evaluated carefully given that transcortical round trip signal transmission delays to and from trunk and ankle are on the order of 60 to 80 ms, respectively, and additional phase lags occur due to neuromuscular excitation-activation coupling (Fuglevand and Winter 1993). Especially the latter have been frequently neglected which leaves in question some conclusions regarding the stability of some balance models. The issue of delay management in motor physiological feedback control has been specifically addressed by other investigators. Models differ with respect to whether they propose (Uno et al 1989; Miall et al 1993; Paulin 1993; Wolpert et al 1998) or do not propose (Lacquaniti and Soechting 1986; Massaquoi and Slotine 1996b; Kettner et al 1997) that the CNS incorporates internal dynamics models to achieve sufficient signal prediction for stabilization. In a number of these descriptions, the function of the cerebellum is represented prominently because of its established importance in both movement control and postural stabilization (Diener and Dichgans 1992; Thach et al 1992; Massaquoi and Hallett 1997). Internal dynamics model-based approaches to physiological state estimation/prediction, including those based on Kalman filtering (Kuo 1995; Paulin 1997), Smith predictors (Miall et al 1993) or other schemes (Uno et al 1989; Kettner et al 1997) are clearly powerful and well-motivated from an engineering viewpoint. Yet, while the CNS is presumably sufficiently complex include

circuits that could match the dynamic order and nonlinearity of the body itself, there is no specific evidence that such mechanisms are actually employed. Therefore, the question of whether the brain uses computational schemes that are simpler and/or more efficient in terms of neuronal processing remains an open one. For example, Ayaso et al (2002) have demonstrated that effective inverse kinematic modeling may be achieved implicitly using relatively coarsely specified gain settings within feedback control loops. Similarly, 'direct' control approaches (Goodwin and Sin 1984), including those linear schemes based on wave-variable processing (Massaquoi and Slotine 1996; Massaquoi 1999), or recurrent integrators (Massaquoi 1999), demonstrate that internal dynamics models are not necessary for stable delayed long-loop control.

The Recurrent Integrator Proportional Integral Derivative (RIPID) model of cerebrocerebellar control (Massaquoi 1999) posits a particularly simple mechanism for stabilizing long-loop proprioceptive feedback loops to achieve arm posture and movement and postural control in the horizontal plane. Specifically, it proposes that corollary efference-copy discharge (Hore and Vilis 1984) transmitted via a cerebellar integrator returns to the cerebral cortex to afford effective differentiation and thereby phase lead critical for long-loop stability. Once stabilized, linear scaling of same-joint and inter-joint feedback responses by linear gains is sufficient to manage plant dynamics. A number of features of human arm control, both for intact and compromised cerebellar function, appear to be well-described by the model. However, it is not clear that this type of mechanism would be able to properly address the nonlinear and inherently unstable dynamics of an upright multisegment plant. This work investigates and proposes a model to answer the question.

3.1 Musculoskeletal plant model

A three-segment kinematic chain with pivot joints representing the ankle, knee and hip was used to represent human rigid body dynamics in the sagittal plane (Figure 3-1). Positive angular motion was consistent with anatomical flexion at the hip, knee

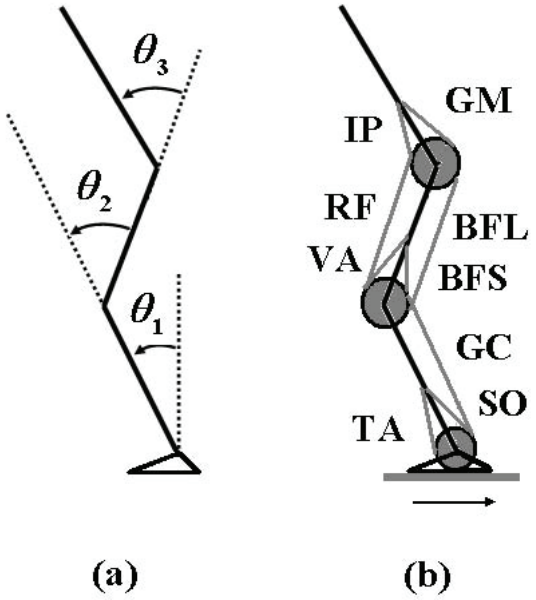

Figure 3-1: (a) Body segment parameters and body configuration angle conventions: $\theta_{ankle} = \theta_1, \theta_{knee} = -\theta_2, \theta_{hip} = \theta_3$. (b) Muscle diagram: GM:gluteus maximus, IP:iliopoas, BFL:biceps femoris long, BFS:biceps femoris short, RF:rectus femoris, VA:vastus intermedius, GC:gastrocnemius, SO:soleus, TA:tibialis anterior.

and dorsiflexion at the ankle. The feet were assumed to be always in flat stable contact with the ground (platform). After computation of motion, it was verified that ankle torques and center of mass location would not have caused heel lift or loss of balance. The body model's dynamics in response to applied total muscular and disturbance torques applied to the joints, $\tau_M(\Theta, \dot{\Theta}, u_\theta)$ and τ_D ($\ddot{D}$, Θ), respectively, is given by:

$$H(\Theta)\ddot{\Theta} + C(\Theta, \dot{\Theta}) = \tau_M(\Theta, \dot{\Theta}, u_\theta) + \tau_D(\ddot{D}, \Theta) + G(\Theta) \tag{3.1}$$

where $\Theta = \begin{bmatrix} \theta_1 & \theta_2 & \theta_3 \end{bmatrix}^T$, $\dot{\Theta} = \begin{bmatrix} \dot{\theta}_1 & \dot{\theta}_2 & \dot{\theta}_3 \end{bmatrix}^T$, and u_θ is the 3x1 central command vector from brain.

$H(\Theta)$ is the 3x3 symmetric configuration-dependent body inertia matrix, $C(\Theta, \dot{\Theta})$ is the 3x3 matrix related to centrifugal and Coriolis forces, $G(\Theta)$ is 3x3 gravitational effect matrix, and $\tau_D(\ddot{D}, \Theta)$ is the 3x1 vector related to external disturbance generated

by backward platform acceleration ($\ddot{D}$) .

Body model parameter values adapted from van der Kooji et al (1999) are summarized in Table 3.1.

	Trunk	Upper leg	Lower leg
Mass(kg)	49	7	4
Moment of inertia(kgm^2)	2.3	0.14	0.12
Length(m)	0.8	0.5	0.4

Table 3.1: Body model parameter adapted from van der Kooji et al(1999).

Joint torque is determined by the total muscular force (passive + active) $F(l, \dot{l}, u)$ and the moment arms of each muscle according to:

$$\tau_M(\Theta, \dot{\Theta}, u_\theta) = A^T F(l, \dot{l}, u) \tag{3.2}$$

$$A^T = \begin{bmatrix} 0 & 0 & 0 & 0 & -a_5 & a_6 & 0 & 0 & a_9^a \\ 0 & 0 & a_3 & -a_4 & 0 & 0 & a_7^k & -a_8^k & -a_9^k \\ -a_1 & a_2 & 0 & 0 & 0 & 0 & -a_7^h & a_8^h & 0 \end{bmatrix} \tag{3.3}$$

where a_i is the estimated average moment arm of the ith muscle in Table 3.2.

This formulation substantially follows that employed by Katayama and Kawato (1993) except that muscles are activated simply in relation to intended joint control and muscles undergo a simple step change in stiffness with activation. For biarticular muscles, superscript h, k and a represent moment arms at, respectively, the hip, knee and ankle. Flexor moment arms are negative reflecting the relationship between length change and direction of rotation.

Passive muscular force is expressed by:

$$F_p = [K_p(l_{eq} - l) - B_p\dot{l}]_+ \tag{3.4}$$

Muscle	Location	l_{eq} (m)	a_i (m)	PCA(cm^2)
Iliopsoas(IP)	mono,hip flexor	0.35	0.132	17
Gluteus Maximus(GM)	mono,hip extensor	0.30	0.092	30.4
Rectus femoris (RF)	bi,hip flexor, knee extensor	0.48	0.049(h), 0.025(k)	12.5
Biceps femoris long (BFL)	bi, knee flexor, hip extensor	0.46	0.054(h), 0.049(k)	15.8
Vastus(VA)	mono, knee extensor	0.26	0.04	30
Biceps femoris short(BFS)	mono, knee flexor	0.29	0.049	6.8
Tibialis anterior(TA)	mono, ankle dorsiflexor	0.30	0.023	9.1
Gastrocnemius (GC)	bi, knee flexor, ankle plantarflexor	0.56	0.050(k), 0.040(a)	30
Soleus(SO)	mono, ankle plantarflexor	0.35	0.036	58

Table 3.2: Length (l_{eq}), moment arm (a_i) , and physiological cross-sectional areas (PCA) of muscles used for postural balance model. The values are determined on basis of Ogihara and Yamazaki(2001), Delp et al (1999), and Winter (1990) .

where $[x]_+ = \begin{cases} x & x > 0 \\ 0 & x \leq 0 \end{cases}$ F_p is passive tension, K_p, B_p is passive muscle stiffness and viscosity, l_{eq} is muscle length at equilibrium; l is actual muscle length.

Active muscular force as a function of neural input to each muscle is represented by:

$$F_a = K_a(l(u))[l(u) - l]_+ - B_a(l(u))\dot{l} \tag{3.5}$$

where F_a is active tension, $l(u) = l_{eq} + pu$ where p is constant (activation-to-length gain), and u is neural input.(p is set to be 1 for simulation.)

$K_a(l(u)), B_a(l(u))$ active muscle stiffness and viscosity.

The active muscle stiffness and viscosity are functions of neural input.

$$\begin{aligned} K_a(l(u)) &= K_{act}\,(\mathrm{sgn}[l(u) - l]_+) \\ B_a(l(u)) &= B_{act}\,(\mathrm{sgn}[l(u) - l]_+)) \end{aligned} \tag{3.6}$$

where K_{act}, and B_{act} are constant coefficients, and $\mathrm{sgn}(x) = \begin{cases} 1, & x > 0 \\ 0, & x = 0 \\ -1, & x < 0 \end{cases}$

When both passive and active tensions are applied together,

$$F(l,\dot{l},u) = \Big[F_p(l,\dot{l}) + F_a(l,\dot{l},u)\Big]_+ \quad l = l_{eq} + A(\Theta - \Theta_{eq})u = Au_\theta \tag{3.7}$$

The positive brace means that a muscle feels force mainly when it is stretched. The activation of muscle force by neural input occurs according to low-pass dynamics that can be approximated by:

$$EC(s) = \frac{\rho^2}{(s+\rho)^2}, \qquad (\rho = 30\text{rad/sec}) \tag{3.8}$$

(Fuglevand and Winter 1993)

The model views the redundant muscle of the trunk and legs as operating together as functional groups of uni- and bi-articular flexors and extensors as shown in Figure 1b. Assuming that stiffness is proportional to physiological cross-sectional area (PCA) (Brand et al 1986), the relative muscle stiffness scaling is given based on morphmetric data in Table 2.1. The effective pre-set (e.g. before reflex neural activation) rotational stiffness of the ankle during standing is about 90 Nm/rad (Fujita and Sato 1998). This value was used to determine the absolute passive stiffness of each muscle given their relative scaling.

The muscle viscosity was set at one-tenth the muscle stiffness as has been done in arm modeling (Flash 1987). The passive stiffness is assumed to include the action of segmental reflexes as in the "lambda-model" of Feldman (Feldman 1986). The dynamics of series elasticity, filtering action of spindles, segmental proprioceptive and force feedback, and spinal processing by alpha motorneuron - Renshaw cell networks were not modeled explicitly, although it is likely that these could improve the accuracy of the simulations (Winters 1995). It was not felt that these features would bear significantly upon the question of FRIPID control feasibility. Finally, it was assumed that muscular activation simply doubled the modest passive stiffness and viscosity of each muscle, which increases the damping ratio by 40 %. This was considered based on human arm modeling where stiffness and damping ratio have been shown

to increase up to 500 % and 50 % respectively (Lacquaniti and Soechting 1986) with strong activation, this was considered conservative leaving a larger portion of the control to the CNS model.

3.2 Cerebellar computation model

It is hypothesized that the signal processing over the cerebellar cortex can be represented as positional-derivative control. An integral controller can also be implemented by the recurrent neural circuit between cerebellar corticonuclear complexes and precerebellar nuclei.

3.2.1 Cerebellar computation with mossy fiber inputs

During a sub-movement, a set of control gains is implemented in cerebellar cortex along the principal direction. Experimental observations have shown that the directional tunings of discharges in cerebellar cortex, motor cortex, and parietal cortex are strikingly similar during arm reaching tasks (Frysinger et al 1984; Kalaska et al 1983; Georgopoulos et al 1983). In addition, it is also reported that directional tunings of Purkinje cells, interpositus neurons, dentate units, and unidentified cerebellar cortical cells are pretty identical (Fortier et al 1989) so that it is assumable that the cerebellar system has uniform principal directions.

Those experimental observations support the proposed cerebrocerebellar mechanism along specific principal directions. Suppose that there are N groups of mossy fiber bundles, and each group conveys a neural signal with different population vector $w_{(i)}^T$, and magnitudes $MF_i = (w_{(i)}^T e)$, $i = 1, ..., N$, from cerebral cortex. Therefore, as a principal directional signal becomes dominant in cerebral cortex, the group of mossy fiber bundles receiving the signal becomes more active, and others get suppressed. Similarly in cerebral cortex, inhibition between different modules by stellate and basket cells accelerates competition to select a winner module. The winner module is the one that receives the principal directional signal in cerebral cortex.

In each module, the following signal processing is implemented (Massaquoi 1999).

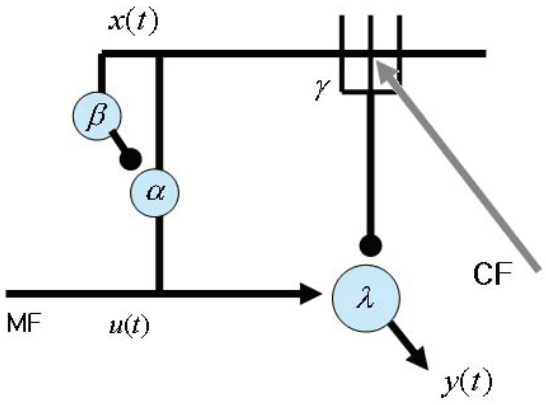

Figure 3-2: A model of the neural circuit in cerebellum, MF: mossy fiber, CF: climbing fiber (see the text for details on parameters and variables).

Input signal to the module by a bundle of mossy fibers is,

$$u(t) = w_{(i)}^{T} e(t) \tag{3.9}$$

Then, the ascending signal after granule and Golgi cells becomes:

$$x(t) = \alpha(u(t) - \beta u(t)) \tag{3.10}$$

where α is synaptic strength on mossy fibers to granule cells, and β synaptic strength on ascending fibers to Golgi cells.

The ascending signal is transmitted to a Purkinje cell. Depending on the distance between cells and fibers, there may exist neural transmission delay Δt on from mossy fibers to to Purkinje cell. When the delay is significantly considerable, the deep cerebellar nuclei output the neural signal $y(t)$ as follows.

$$
\begin{aligned}
&y(t) = \lambda u(t) - \gamma x(t - \Delta t) = \lambda u(t) - \gamma\alpha(u(t - \Delta t) - \beta u(t - \Delta t)) \\
&= (\lambda - \gamma\alpha(1 - \beta))u(t) + \gamma\alpha(1 - \beta)(u(t) - u(t - \Delta t)) \\
&\approx au(t) + b\dot{u}(t)
\end{aligned} \tag{3.11}
$$

where $a = (\lambda - \gamma\alpha(1 - \beta))$, $b = \gamma\alpha(1 - \beta)\Delta t$.

γ represents synaptic strength on parallel fibers to Purkinje cell, and synaptic strength on mossy fibers to deep cerebellar nuclei. If the delay is negligible,

$$
\begin{aligned}
&y(t) = \lambda u(t) - \gamma x(t) = \lambda u(t) - \gamma\alpha(u(t) - \beta u(t)) = (\lambda - \gamma\alpha(1 - \beta))u(t) \\
&= au(t)
\end{aligned} \tag{3.12}
$$

Therefore, equations above indicate that cerebellar cortex implements either Positional-Derivative or Positional controller.

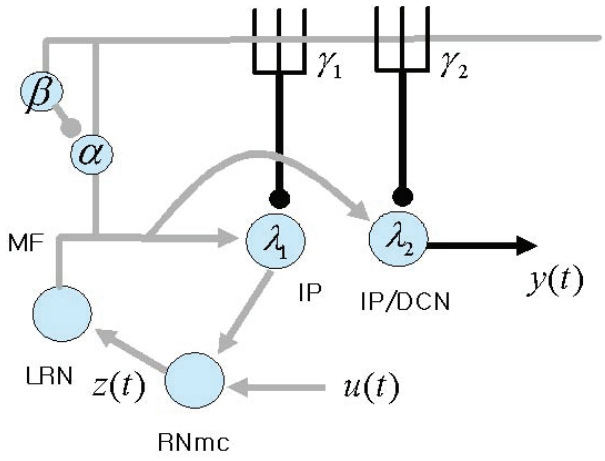

Figure 3-3: Integration neural circuit.

The integration may be afforded by interaction between cerebellar corticonuclear complexes in the medial cerebellum and certain precerebellar nuclei. Input $u(t)$ is transmitted by cells in magnocellular red nucleus (RNmc) and lateral reticular nucleus (LRN) to interpositus nuclear cells (IP) (Allen and Tsukahara 1974). RNmc units are modeled as leaky integrator with nontrivial time constant because of their large

size. Synaptic strengths on LRN and RNmc remain fixed to be unity for simplicity because the plasticity on those cells is not considered in model.

$$\frac{dz(t)}{dt} = u(t) + (\lambda_1 - \alpha\gamma_1(1-\beta))z(t) - \frac{1}{\tau}z(t) \tag{3.13}$$

$z(t) \approx \int u(t)dt$ for $(\lambda_1 - \alpha\gamma_1(1-\beta)) \approx 1/\tau$ by adaptive cancellation.

$$\begin{aligned} y(t) &\approx \lambda_2 z(t) - \alpha\gamma_2(1-\beta)z(t-\Delta t) \\ &= (\lambda_2 - \alpha\gamma_2(1-\beta))z(t) + \alpha\gamma_2(1-\beta)(z(t) - z(t-\Delta t)) \\ &= (\lambda_2 - \alpha\gamma_2(1-\beta))\int u(t)dt + \alpha\gamma_2(1-\beta)\Delta t u(t) \end{aligned} \tag{3.14}$$

The output is therefore approximately a scaled version of integral of input with a proportional term if Δt is not negligible. Finally combining derived equations, PID control gains are established with respect to the input and output of cerebellar cortex.

3.2.2 Cerebellar gainscheduling control

To complete a whole movement, the proposed model needs different cerebellar control gains for different principal directions. In this section, the gainscheduling or gain-switching mechanism is proposed. A new view of cerebellar cortical circuitry has been suggested (Bower 2002; Santamaria et al 2002) based on experimental observations. The new view is focused on ascending segment synaptic input from granule cells to the Purkinje cell distinct from parallel fiber input. Two populations of synapses on Purkinje cells, ascending segment synaptic input, and parallel fiber input, might have different physiological effects or functions. Two classes of activity in a same Purkinje cell were reported in 80's (Ebner and Bloedel 1981). A class is a strong positive correlation at short lag times, which decayed to baseline activity over greater than 50ms, and the other class is a positive correlation rapidly decayed within 10-15ms. Even though it is not sure that the two classes indicate ascending segment synaptic activity and parallel fiber activity, distinct activities on the Purkinje cell are observed. Bower (2002) put a suggestion that cerebellar cortical circuitry assures a balance between parallel fiber excitation and molecular-layer inhibition (by stellate

or basket cells).

An idea is proposed by induction from the experimental observations. Figure 3.M5 illustrates it based on recent experimental observations (Bower 2002). The author proposed two different functions of parallel fibers, *suppressor*, and *signal* parallel fibers previously. With the view of cerebellar cortical circuitry (Figure 3.M5 (a)), the signal parallel fibers may be equivalently the ascending fibers (AS). There are supportive experimental observations on it. It is reported (Gao et al 2003) that stimulation of the parallel fibers evoked a transverse beam of optical activity, and (Cohen and Yarom 1998) that stimulation of mossy fibers elicits a circular and nonpropagation patch of activity in Purkinje cell dendrite, and the stimulation does not activate the Purkinje cells along a transverse beam of parallel fibers. The observations implicate that the ascending segment synapses of the granule cell, and not its parallel branches, activates and defines the basis functional modules of the cerebellar cortex. Each Purkinje cell-to-deep cerebellar nuclei represents a set of cerebellar control gain. Therefore, switching a control gain set to another is equivalent to changing dominant excitement in a group of cerebellar nuclei to another group.

Gainscheduling stands for a sequence of control gain switchings during a whole movement. Once after fully trained, each cerebellar control gain set is set to each module. The author hypothesize that a specific principal directional control gain is selected and others are all off during each sub-movement. For a selected active module, inhibitions from other modules are strong so that Purkinje cell discharge can not be sufficiently strong to shut down the deep cerebellar nuclei activity. On the other hands, for any of inactive modules, inhibitions from other modules are weak so that Purkinje cell discharge excited by parallel fibers and ascending segment fibers are quite strong enough to deactivate deep cerebellar nuclei discharge. Thus, only activity of deep cerebellar nuclei in the selected active module is conveyed as control command to the lower CNS. The detail on selection mechanism is as follows.

Figure 3-4 shows a simple proposal for a gainset selection mechanism in which a "beam" of activity on parallel fibers (PF) inhibits (via basket cells, not depicted explicitly (Eccles et al 1967; Ito 1984)) Purkinje cells some distance away ("off beam"). This diminishes the net inhibition in those modules, allowing them to process the ascending segment input through mossy fibers (AS). Conversely, the beam activates local Purkinje cells, thereby suppressing the activity of "on beam" modules. The principal characteristic required of parallel fibers in this scheme is that unlike ascending segment fibers, they should contact Purkinje cells relatively more strongly than the corresponding cerebellar deep nuclear cells - if they contact the same DCN cells at all. This appears to be generally consistent with the studies of Eccles et al (Eccles et al 1974; Ito 1984). A prime candidate source for parallel fibers is the dorsal spinocerebellar tract (DSCT) elements of which are known to convey mixtures of proprioceptive and other information from multiple muscles within a limb (Oscarsson 1965; Bloedel and Courville 1981; Osborn and Poppele 1992) while typically maintaining a steady level of background firing in the absence of afferent input (Mann 1973).

These observations are formulized by proposing that the DSCT fibers transmit $[\bar{n}_i \cdot \bar{q} - n_{0i}]_+$ for many different values of directional unit vector n_i and offset n_{0i}. It would be expected that in vivo, $\bar{q}$ would be the average signal of a large number of primary afferents (Mann 1973) thereby reducing the noise transmitted to the cerebellum. Thus, certain parallel fibers become relatively more active when the sensed kinematic state is located in a region of the state space bounded by the plane perpendicular to n_i at distance n_{0i} from the origin. Depending upon the signs of n_i and n_{0i} , the region may include, or not include the origin. The net switching action can therefore be written:

$$G = G^{(1)}[1 - [1 - \gamma[\bar{n}_1 \cdot \bar{q} - n_{01}]_+]_+]_+ + G^{(2)}[1 - [1 - \gamma[\bar{n}_2 \cdot \bar{q} - n_{02}]_+]_+]_+ \quad (3.15)$$

where γ represents the strength of lateral inhibition provided by basket cells, and $G^{(i)}$ control gains.

This parameter regulates the steepness of the transition zone between scheduling regions. It is not clear yet what information $\bar{q}$ represents. It could be either estimated or sensed kinematic state, and/or contain force information. Anyway, a state space can be imagined and be constructed by coordinates that were the states or functions of the states. Then, switching region can lie in the state space, and be bounded by two switching surfaces described as $\bar{n}_i \cdot \bar{q} - n_{0i} = 0, i = 1, 2$.

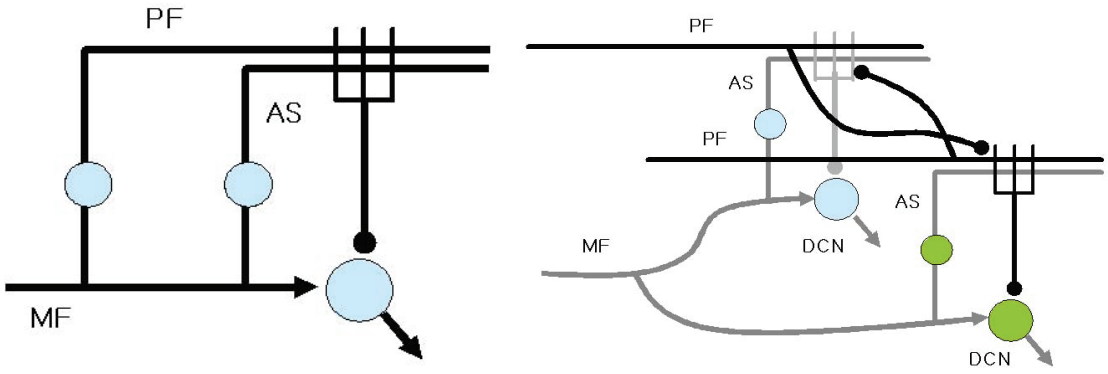

Figure 3-4: Two inputs to Purkinje cell dendrite: ascending segmental synaptic (AS) input, and parallel fiber (PF) input (see also Figure 5(B) in Bower 2002) (left), and proposed cerebellar gainscheduling Circuitry (right). DCN: deep cerebellar nuclei.

3.3 FRIPID cerebrocerebellar model

The hybrid Force feedback RIPID (FRIPID) model is shown in Figure 3-5. The model is an improved version of RIPID model by augmenting the force feedback loop. The FRIPID model formally contains a vertical reference signal (Θ_{ref}) to acknowledge the fact that the CNS presumably can compute body orientation with respect to vertical (Peterka 2003). As even subjects with significant vestibular dysfunction may be able to balance (Nashner et al 1982), the orienting mechanism can utilize multi-sensory inputs. For simple upright balancing on a horizontal platform, Θ_{ref} and τ_{ref} can be set to zero. We propose that the linear cerebellar PID processing shown in

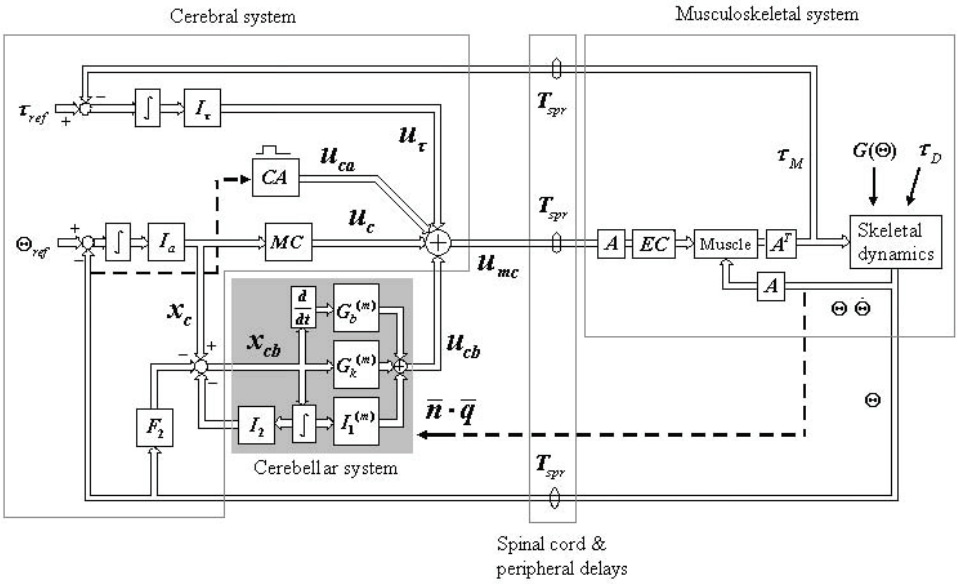

Figure 3-5: The Force feedback RIPID cerebrocerebellar balance control model (see the text for explanation of features).

section 3.4.3 can be extended directly to three-joint control such that the cerebellar output is given by:

$$u_{cb}(i) = \sum_{j=1,2,3} G_b^{(m)}(i,j)\dot{x}_{cb}(j) + \sum_{j=1,2,3} G_k^{(m)}(i,j)x_{cb}(j) + \sum_{j=1,2,3} I_1^{(m)}(i,j) \int x_{cb}(j) \tag{3.16}$$

where $\int x = \int_0^t x(\tau)d\tau$.

Here $G_k^{(m)}$, $G_b^{(m)}$, and $I_1^{(m)}$ are 3x3 matrices that belong to gainset m =1, 2 as described in the next section. Therefore, Equation 3.16 represents linear control for any m , and piecewise linear control overall. Empirically, differentiation of x_{cb} was found to be unnecessary for balance simulations. Therefore, the elements of $G_b^{(m)}$ were set to zero.

As in the basic RIPID model (Massaquoi 1999) the 3x3 matrices I_a and I_2 are proposed to represent scaling of signals related to hypothesized sensorimotorcortical integrators. The 3x3 diagonal matrices F_2 and MC affect the relative balance of

cortical and cerebellar circuitries. Proprioceptive feedback processing accesses the cerebellar system directly through F_2 . Descending signals from parietal or motor cortices that bypass the cerebellar cortex are scaled by MC .

A very similar scheme that includes activity related to a reverberating circuit between u_{cb} and x_{cb} involving pre-cerebellar brainstem nuclei (Allen and Tsukahara 1974) is taken to implement integration (Massaquoi 1999; Massaquoi and Topka 2002). This signal is scaled by the 3x3 diagonal matrix I_2, and projected to cerebral cortex in a recurrent feedback manner. The circuit has closed loop transfer matrix $sI(sI + I_2)^{-1}$ (where I is an identity matrix) and provides significant phase lead that is responsible for delay compensation.

In particular, examining for simplicity a single joint representation in terms of scalars g_k, i_1, i_2, f_2, i_a and mc in Figure 3-5, the transfer function from x_c to u_{cb} is given by $(sg_k + i_1)/(s + i_2)$, and the overall transfer function from Θ to u_{mc} is given by $-(sg_k f_2 + i_1 f_2 + g_k i_a + i_1 i_a/s)/(s + i_2) - i_a mc/s$, and therefore for $|s| << i_2$, this becomes $-(i_1 f_2/i_2 + g_k i_a/i_2) - (i_1 i_a/i_2 + i_a mc)/s - s(g_k f_2/i_2)$. Thus, for lower frequencies, proprioceptive control is approximately PID. However, it should be noted that inclusion of excitation-contraction muscular dynamics ($EC(s)$) renders the control between Θ and τ_M to be slightly more complex than PID even before force feedback is included.

The FRIPID model adds a torque feedback loop that represents force-related information from the pressure distribution on the feet or muscle tension sensed by Golgi tendon organs (Perteka 2003). For the moment, it is assumed that this signal traverses the cerebral cortex where force information is felt to arrive at the cerebral cortex via the VPL thalamic nucleus (Brodal 1981). By symmetry with the processing of proprioceptive information in the basic RIPID model and consistent with the predominantly low frequency effect of force feedback as explored by Peterka (2003), force feedback is processed by a (thalamo-) cortical integrator associated with 3x3 scaling matrix I_τ.

Closed loop transmission delays through spinal and peripheral nerves (T_{spr}) are conservatively taken to be 60, 70, and 80 ms for long-loop responses to and from the hip, knee and ankle respectively, based on 2 m height, 50 m/s neural conduction velocity and five synaptic delays of less than 1 ms.

It was also found empirically that use of feedforward muscular coactivation in concert with long-loop control improved the fit to some human data sets. It was assumed that for healthy subjects, the magnitude of this component should be comparatively small. However, it was suspected a priori based on clinical observations (Massaquoi and Hallett 1997) that coactivation might be increased to compensate for degraded cerebellar processing of long-loop responses. To accommodate this, the FRIPID was augmented by a hypothetical system that triggered a prespecified level (CA) and duration of muscular coactivation when a sufficiently large ankle velocity signal was detected at the cortex.

The cerebellar gainscheduling introduced in section is applied to implement different postural strategies depending on the amplitude of disturbance. Successful balancing reactions to the full range of tested disturbances were achieved by the FRIPID model using just two, slightly overlapping, gainscheduling regions in $\hat{\theta}_1 \times \hat{\theta}_3 \times \dot{\hat{\theta}}_1$ space. In principle, there is no reason to expect that the cerebellum does not access to the equivalent of full state information from all joints. However, we sought the smallest number of kinematic variables that could enable the model's switching mechanism to account for the data. The components $\hat{\theta}_1$ and $\hat{\theta}_3$ provide significant information about body's center of mass when there is little knee motion, and $\dot{\hat{\theta}}_1$ provides rapid information about platform velocity. Figure 3.7 depicts the projection of a low-velocity and high-velocity recovery trajectory into this subspace, and the scheduling zones determined by two closely-spaced planes. The planes are defined by the equations: $\bar{n}_i \cdot \bar{q} = 0$, i=1,2. The quantity $[\bar{n}_1 \cdot \bar{q}]_+$ is positive for sensed state space locations on the origin side of the outer plane. $[\bar{n}_2 \cdot \bar{q}]_+$ is positive at locations beyond the inner plane. The inner part of the space was considered the base region,

and its associated gain matrices $G_k^{(1)}$, $I_1^{(1)}$ yielded ankle strategy. The outer zone, designated the catching region, was associated with $G_k^{(2)}$, $I_1^{(2)}$ and generated mixed ankle-hip strategy.

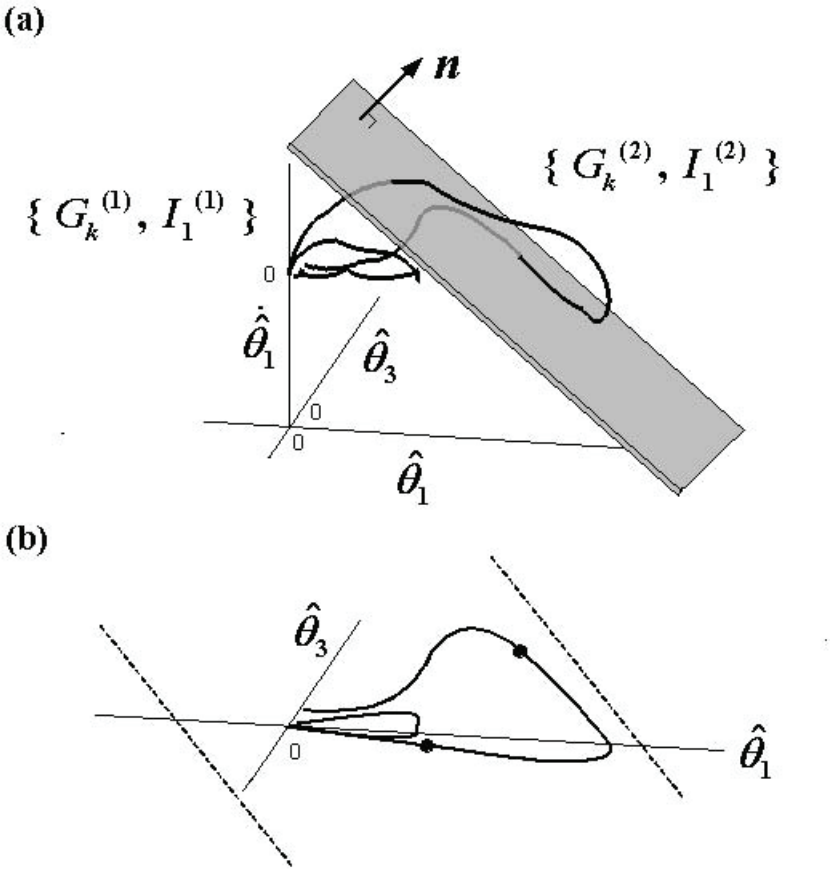

Figure 3-6: (a) Sensed recovery trajectories and one of two closely parallel switching planes in $\hat{\theta}_1 \times \hat{\theta}_3 \times \dot{\hat{\theta}}_1$ space. (b) Projection of sensed trajectory onto $\hat{\theta}_1 \times \hat{\theta}_3$ space with two large points corresponding to points of their intersection with switching plane. Dashed lines show approximate limits of feasible balance region as in Figure 3-8.

3.4 Simulation task

Several experimental methods have been employed to study human balance control (Horak and Nashner 1986; Nashner and McCollum 1985) including platform translations. Humans have been noted to exhibit characteristically different balancing kine-

matics that emphasizes either ankle or hip motion depending upon the magnitude and speed of the platform disturbance. Backward platform movement and kinematic data in Henry et al (1998), Runge et al (1999) and Park et al (2004) covered a fairly wide range of disturbance velocities, but were not identical. Also, platform kinematics were not reported in detail. These studies were used to establish a useful set of nominal model gains with respect to which other changes were made as described.

For simulations, platform movements were 2.97, 4.50, 5.94, 6.75, and 9.00 cm displacements lasting 300 ms and were sigmoidal in time. An important check on the presumed cerebellar locus of the control system is whether simulated lesions of the system yield balance control deficits that correspond to clinical findings. In particular, diffuse cerebellar injury, especially of the anterior lobe that results in general loss of cerebellar tissue (atrophy) would be expected to reduce the strength of the cerebellar gains. It is also conceivable that this deficit might engender increased active muscular stiffness to compensate for the loss of long-loop control.

No attempt was made to obtain precisely optimal fits according to any abstract mathematical cost function. Rather, representation of human behavior was obtained to be visually satisfactory. The tuning procedure involved first obtaining a stabilizing linear quadratic regulator (Franklin et al 1994) that approximated human behavior for small disturbances. Then, the behavior was tuned manually to fit human data with force feedback and muscular coactivation.

3.5 Results

A number of human studies show the same basic patterns of body movement in relation to platform translation (Henry et al 1998; Runge et al 1999; Park et al 2004; Allum and Honegger 1992; Horak and Nashner 1986; Nashner and McCollum 1985). Figure 3-7 shows the model tuned to most closely approximate the data of Henry et al (1998). Attention is paid here to the relative amplitudes and timings of the joint excursions, and smoothness of settling. The simulated vertical projection of

the center of mass onto the ground remains within the base of support assuming a length from the ankle to the first metatarsophalangeal joint of at least 8 cm, which is a conservative estimate. And the peak ankle torque remains below 60 Nm, a value which Park et al (2004) found to be consistent with the heels remaining flat on the platform. From this point on, we will refer to the parameter settings used in 3-7 top left as the base FRIPID scheduled control model.

Attention is paid here to the relative amplitudes and timings of the joint excursions, and smoothness of settling. It is noteworthy that although the joint angle vs. time plot of the data of Henry et al did not show initial hip undershoot, the ankle-hip body configuration trajectory plot did (figure 2 in Henry et al 1998). We consider the possibility that in this study the feature was variable and was averaged out in the time domain plot Other studies have typically shown initial hip motion undershoot (figure 5 in Park et al 2004; figure 3 in Runge et al 1999) as does the simulation. The simulated vertical projection of the center of mass onto the ground remains within the base of support assuming a length from the ankle to the first metatarsophalangeal joint of at least 8 cm, which is a conservative estimate. And the peak ankle torque remains below 60 Nm, a value which Park et al (2004) found to be consistent with the heels remaining flat on the platform. From this point on, we will refer to the parameter settings used in Figure 6 top left as the base FRIPID scheduled control model.

The responses of the scheduled FRIPID model to displacements of different velocities are shown in Figure 3-8. If the generally small variation in knee angle motion is neglected, the body configurations that are consistent with balance can be determined to lie approximately between the diagonal dashed lines shown. Slow disturbances result in comparable peak excursions at the ankle and hip. In this case, because the body center of mass is much farther from the ankle than the hip, ankle motion has the dominant control over COM positioning, and therefore over balance ("ankle strategy" (Nashner and McCollum 1985)). On the other hand, rapid disturbances yield

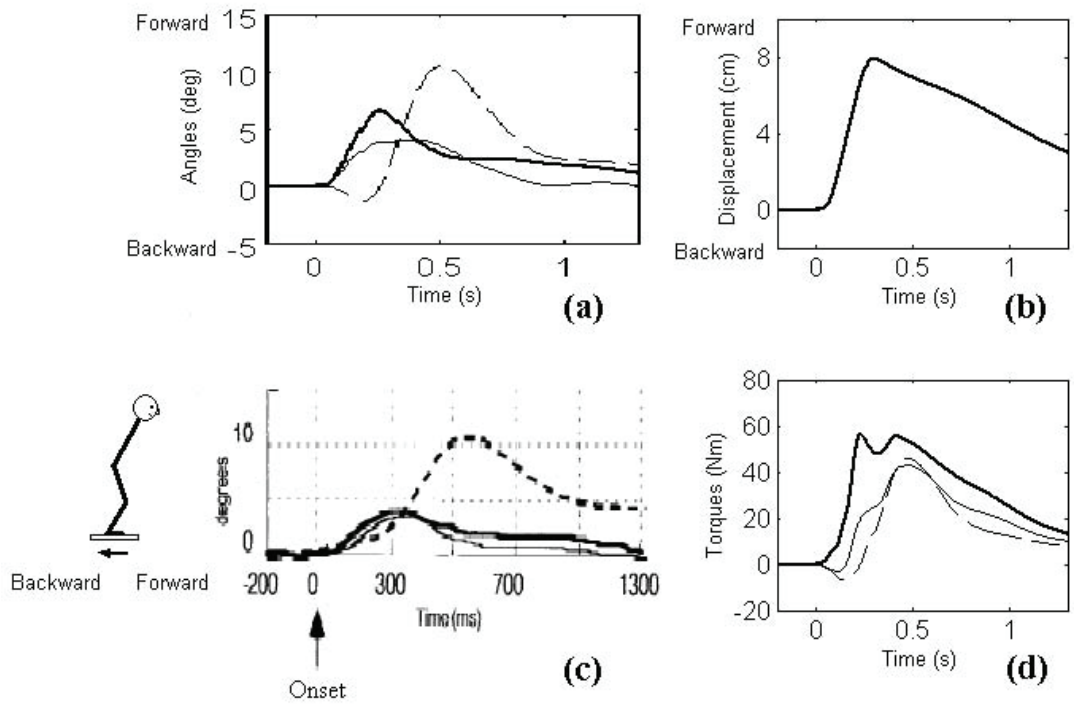

Figure 3-7: (a) Simulated and (c) actual (Henry et al 1998) kinematics showing ankle (thick solid line), knee (thin solid line) and hip (dashed line) motion in response to backward platform movement (left). (b) Simulated COM trajectory and (d) simulated torque profiles (right).

progressively greater hip motion until both joints contribute more equally to balance, especially later within the recovery motion ("mixed ankle-hip strategy"). It enables the body to remain within the feasible balance configuration region by limiting ankle movement, and restricting ankle torque to levels consistent with maintaining heel contact with the platform (Figure 3-8(a)). The flexion at the hip and extension at the ankle that promote COM recovery are aided by the abrupt deceleration of the platform at all translational velocities, as was described by Runge et al (1999). The base FRIPID scheduled control model settings produce a distinct transition between strategies at a platform velocity of about 25 cm/s, qualitatively similar to the data of Runge et al (1999) (Figure 3-10).

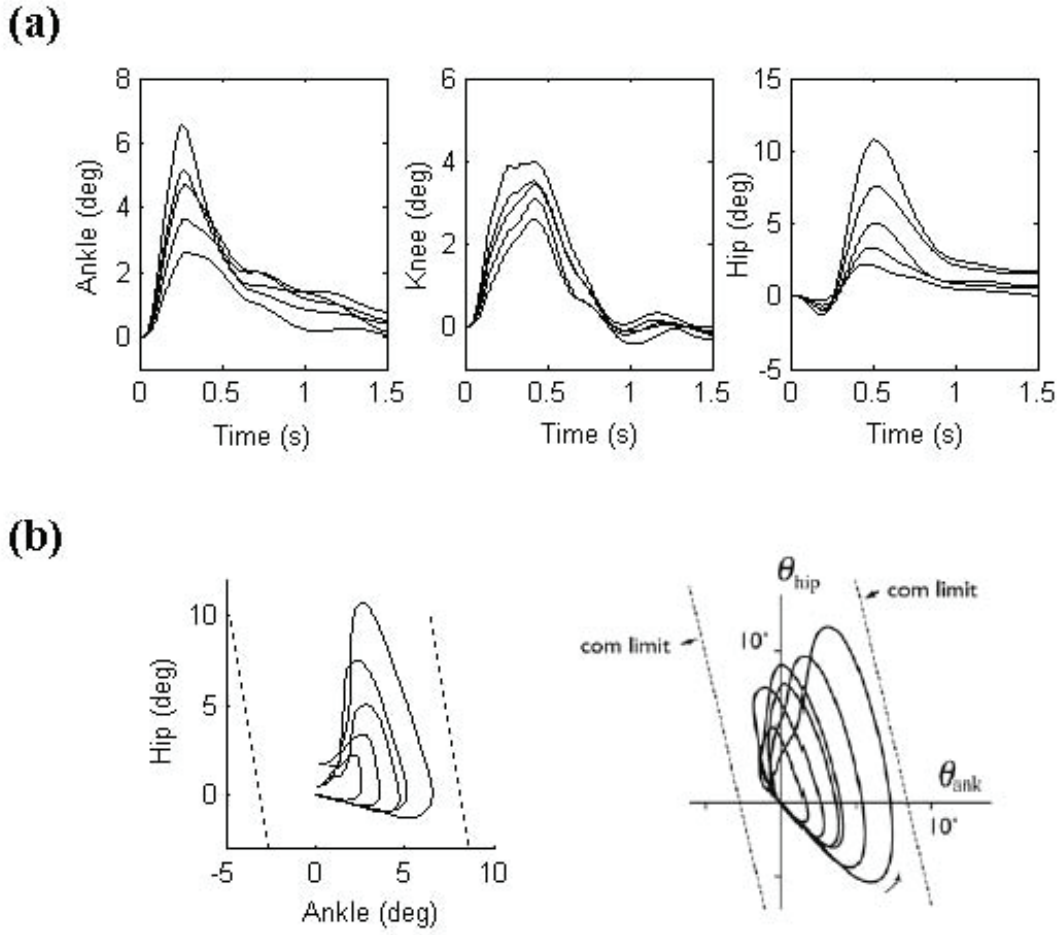

Figure 3-8: (a) Simulated joint trajectories for a family of different sized disturbances, (b) simulated ankle vs. hip configuration plots (left), and configuration plot (right) adapted from Park et al 2004. Dotted lines indicate boundaries in ankle-hip joint space where the COM remains within feasible region for balance.

Figure 3-11 shows the distribution of simulated electromyogram (EMG) activity: $\text{sgn}([l(u_k) - l_k]_+)(l(u_k) - l_k)$, for six muscles, k. Horak and Nashner (1986) recorded hip joint EMG from rectus abdominis (RA) rather than iliopsoas, and from paraspinals (PS) rather than gluteus maximus. The RA and PS have mechanical functions very similar to the PS and GM and were found to show similar EMG patterns. Simulated EMG patterns demonstrate typical pattern features explained in section 2.3.1 (Figure 2-2).

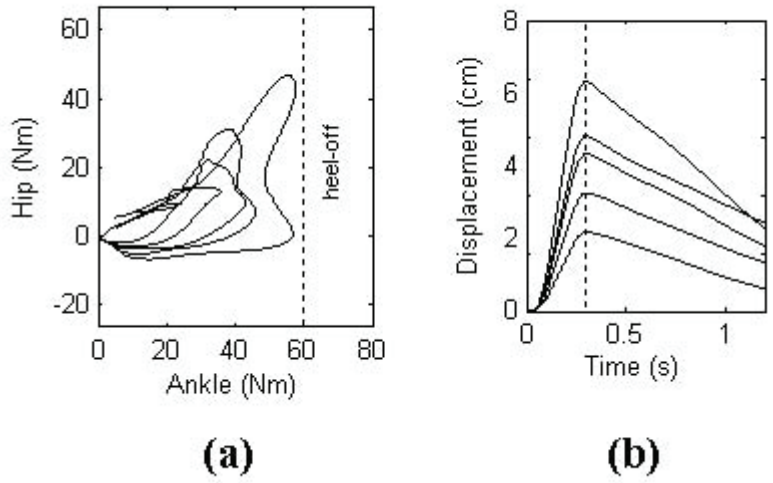

Figure 3-9: (a) Simulated hip vs.ankle joint torque trajectories. Dotted line indicates the maximum allowable ankle torque for which feet remain flat on the ground (as indicated in Park et al 2004). (b) Trajectories of COM forward displacement corresponding to different platform velocities. Dotted line indicates time that platform movement ends.

The FRIPID model qualitatively reproduces the postural disturbance responses of persons with cerebellar disease, especially of the anterior lobe as in nutritional deficiency-related cerebellar degeneration (Massaquoi 2002) in Figure 3-12. To simulate cerebellar disease, the magnitudes of cerebellar control gains ($G_k^{(m)}$, $I_1^{(m)}$) were reduced by 40 %. This would correspond to loss of deep cerebellar nuclear cells, mossy or parallel fibers with or without Purkinje cell loss. On the other hand, muscular coactivation was increased to simulate the apparent typical compensation strategy employed by patients. A relatively mild ramp platform displacement of 3 cm over about 300 ms was applied to qualitatively reproduce experimental observations of Horak and Diener (1994). Consistent with clinical observations, patients develop significantly larger amplitude ankle and hip motions but only relatively minor disturbance in COM location. Thus, patients tend to oscillate, but not to fall, unless they trip. In simulations, it was also noted that body oscillation may become more sustained, yielding a typically 2 to 3 Hz postural tremor termed titubation (Massaquoi 2002). It is apparently engendered by the muscular coactivation and/or by reduction

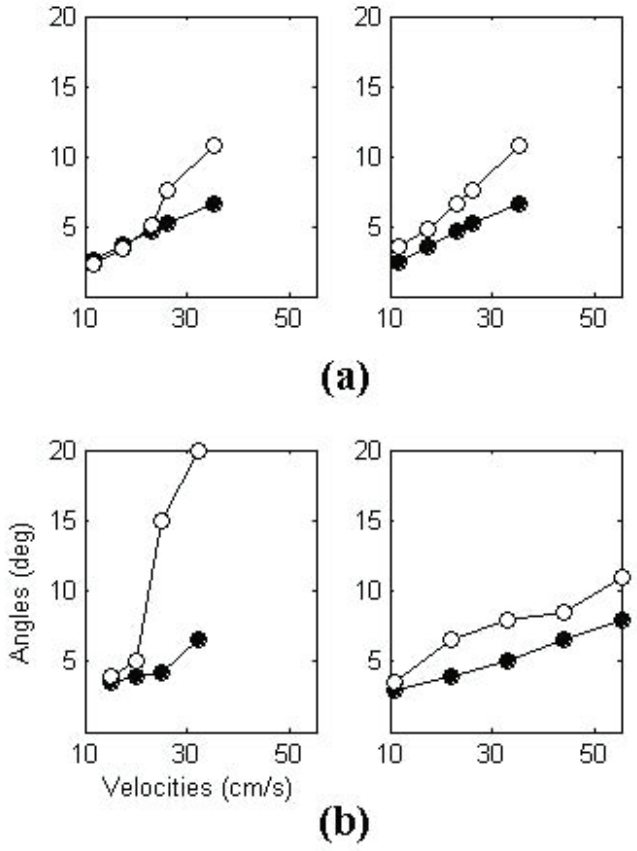

Figure 3-10: Peak values of ankle (solid) and hip (open) angles vs. platform velocity: (a) simulations, (b) actual data from Runge et al 1999 (left), and Park et al 2004 (right).

in recurrent integrator function associated with reduced I_2 (Massaquoi and Hallett 1998).

Aside from the changes in parameters that correspond to damage to the cerebellum itself, the sensitivity of the model to other components was explored as shown in Figure 3-13. Principal observations are: first, as expected, model function is most sensitive to the integrity of the recurrent integrator path gain (I_2), and the gain of direct long-loop feedback to cerebellum (F_2). The former may be reduced by interruption of cerebellar outflow destined for the cortex as often occurs in multiple sclerosis and gives rise to a violent, destabilizing tremor that may affect arms or

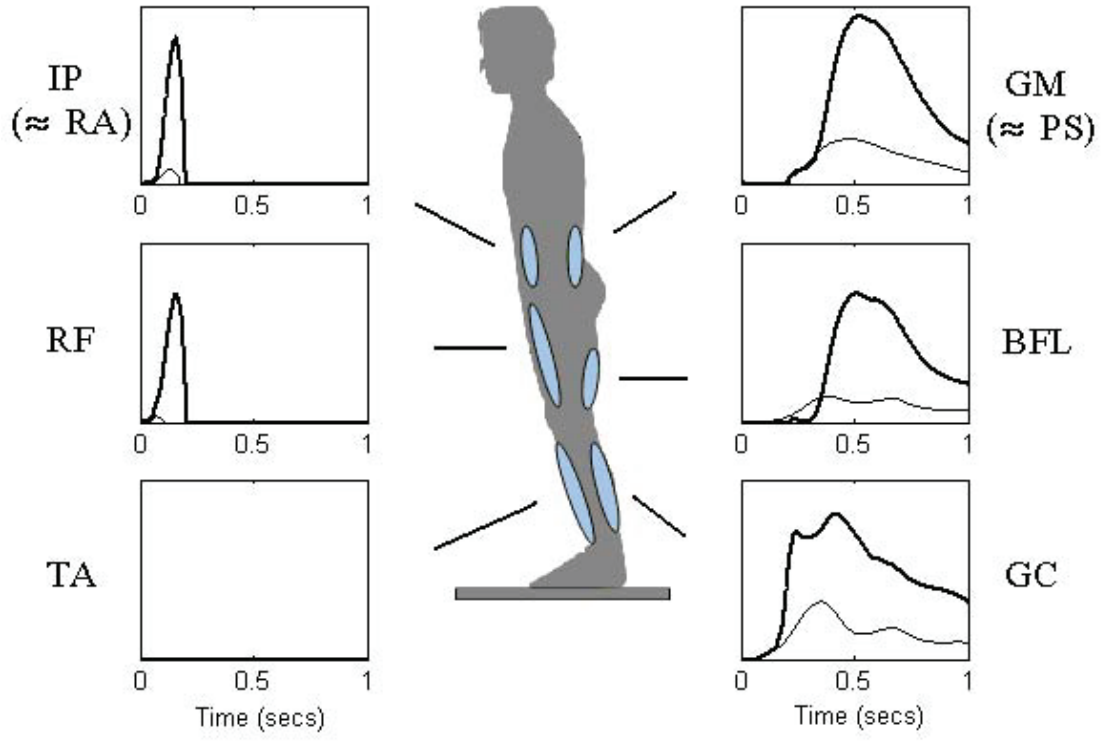

Figure 3-11: Simulated EMGs in low velocity (thin lines) and high velocity (thick lines) platform disturbances (Compare with Figure 2-2). PS: paraspinals, RA: rectus abdominis.

body. Attenuation of the latter signal as occurs with deafferentation by peripheral sensory nerve or spinal disease may be compensated for by visual input to some extent. Eye closure results clinically in the catastrophic fall depicted here. Moderate changes in the cerebellar gainsets or switching in general provide appreciable, but generally modest changes in balancing motion trajectory. This is appropriate for an adaptive control mechanism. The relevance of gainset switching is shown by raising the switching plane to greater than 200 % of its setting in the base model. In this case, only ankle strategy occurs. Although the COM excursion increases only slightly, the peak ankle torque rises to 70 Nm thereby exceeding the criterion for maintaining heel contact on the platform. The marked robustness of the control system to increases in neural signal transmission delays is demonstrated by the less than 2 % increase in COM excursion engendered by a 40% increase in loop transmission time. Force

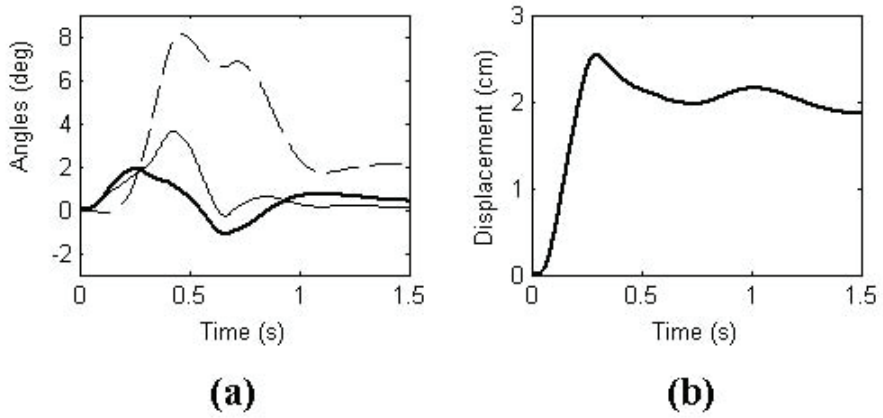

Figure 3-12: Predicted response of person with cerebellar disease to a low velocity (11.55 cm/s) backward platform disturbance: (a) simulated joint trajectories: ankle (thick solid line), knee (thin solid line) and hip (dashed line), and (b) simulated COM trajectory.

feedback is necessary to prevent violent recoil of the ankle that could otherwise be destabilizing as described earlier. Finally, muscular coactivation is not necessary for balance recovery. However, it does enhance the speed of COM return to zero.

3.6 Preliminary conclusion

A recurrent integrator PID model is augmented with long-loop force feedback and gain scheduling to describe the control of human upright balance. The cerebellar component of the controller is represented by two sets of gains that provide linear scaling of same-joint and inter-joint long loop stretch responses between ankle, knee and hip. The cerebral component of the model includes a single set of same-joint linear force feedback gains. Responses to platform translations of a three-segment body model operating under this hybrid proprioception and force based long-loop control were simulated. With low-velocity platform disturbances, "ankle-strategy"-type postural recovery kinematics and EMG patterns were generated. With faster disturbances, balance was maintained by employing a second set of cerebellar control gains that yielded "mixed ankle-hip strategy"-type kinematics and EMG patterns.

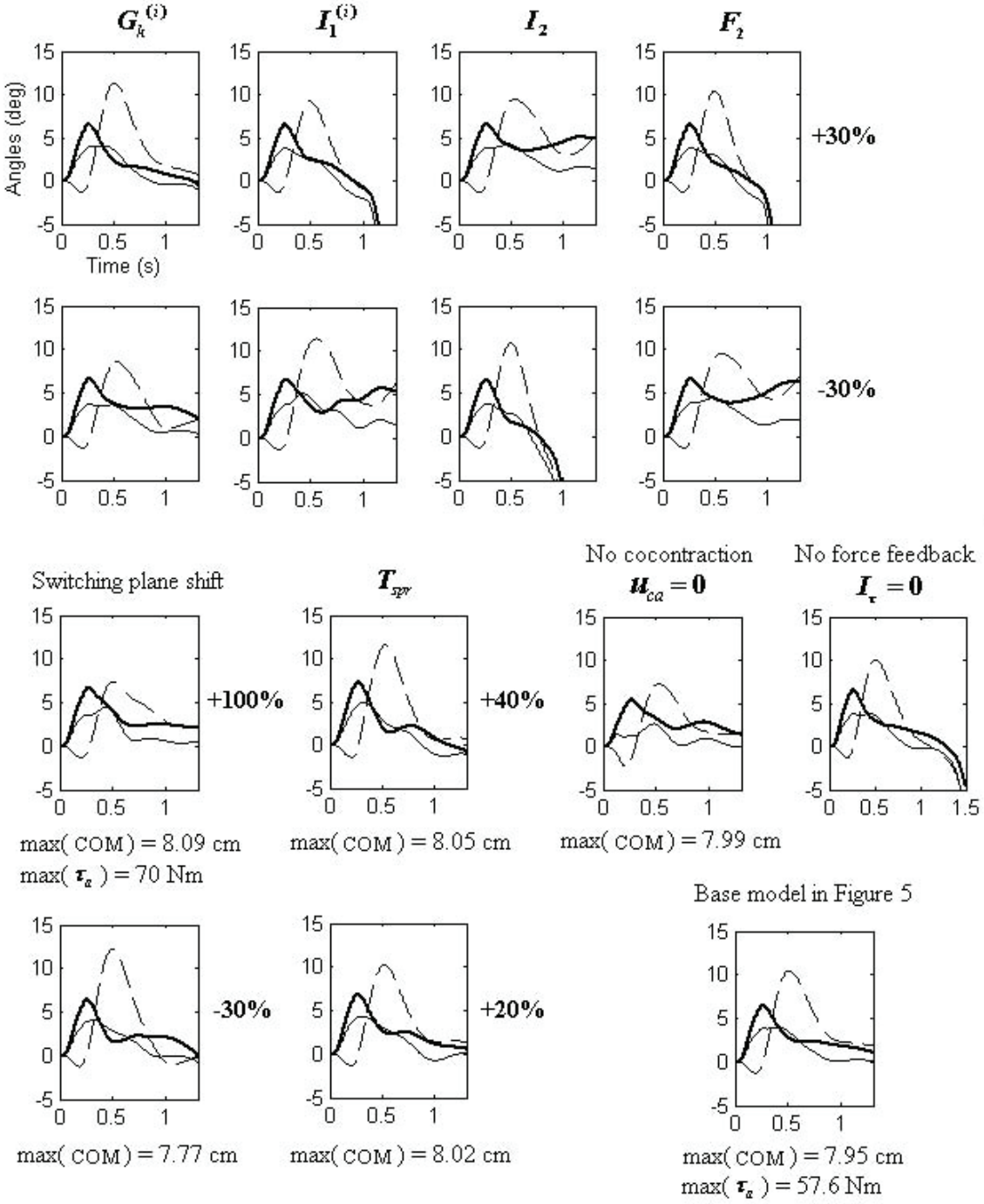

Figure 3-13: Sensitivity to several parameters: ankle (thick solid line), knee (thin solid line) and hip (dashed line) motions. max(COM): the maximum value of forward COM displacement, max(τ_a): the maximum value of ankle torque trajectory.

The addition of small amounts of simulated muscular coactivation improved the fit to certain human data sets. It is proposed that the cerebellum switches control gainsets as a function of sensed body kinematic state. Reduction of cerebellar gains with a compensatory increase in muscular stiffness yielded posture recovery with abnormal motions consistent those found in cerebellar disease. The model demonstrates that stabilized hybrid long-loop feedback with gainscheduled linear scaling may effect realistic balance control in the absence of explicit internal dynamics models, and suggests that the cerebellum and cerebral cortex may contribute to balance control by such a mechanism.

The present study demonstrates that the combination of stabilized, scheduled long-loop proprioceptive and force feedback could provide flexible and powerful control to facilitate postural defense despite the presence of significant signal transmission delays and phase lags. The findings also suggest that the body's control could be substantially linear within regions of the kinematic state-space with switching driven by a small number of sensed variables. The control segmentation need not be fine-grained and there is apparently no requirement for precise prediction of body state that would necessitate an internal forward dynamics model.

Chapter 4

Biped walking model (SBBW model)

The previous chapter showed that realistic control (FRIPID model) of upright balance can be accounted for in terms of stabilized long-loop (trans-cerebrococerebellar) proprioceptive and force feedback . This system affords energetic efficiency because muscular coactivation and associated active body stiffness can be reduced, as well as flexibility and automaticity of response patterns because feedback gainsets can be applied according to sensed changes in body state. The model also manages robustly the potentially destabilizing effects of long-loop neural signal transmission delays and muscular excitation-activation phase lags that have not been heretofore included in neuromorphic locomotor control models. At the same time, considerable work on spinal physiology has shown that certain basic muscle activations patterns (*synergies*) may be coded within the cord (Tresch et al 1999). Simulation of muscle synergies in a model of the frog hindlimb with simple switch-like commands have been shown to generate a range of movements consistent in both kinematics and muscle activations with real behaviors (Cajigas-Gonzalez 2003). d'Avellar et al showed that combinations of a few number of distinct neural activities underlie the variety of muscle patterns and generate different behaviors such as kicking, swimming, walking and so on (d'Avellar et al 2003; d'Avellar et al 2005). Similar experimental results are reported in postural tasks. A limited set of muscle synergies are extracted from cat's

active balance control against perturbations (Ting and Macpherson 2004). Especially, muscle activation during human walking could be account for by five underlying signal component waveforms. A systematic phase shift of all five factors was observed in the same direction as the shift in the onset of the swing phase.

Animal locomotion is characterized by rhythmic neural activity and the use of multiple degrees of freedom. The idea of the mechanism was primitively studied to explain the lamprey swims by means of periodic muscle contractions (Kandel et al 2000). Even for regular biped walking pattern, biological inspiration suggests the concept of the spinal pattern generator, which is presumably neural networks at the spinal cord level of vertebrates. Such rhythmic pattern generators in the spinal cord regulate muscle activity periodically around a single joint. Each NPG is programmed to govern individual muscle synergies and generate periodic sequences of the synergies. Human biped walking is expected to be accounted for by similar rhythmic patterns, e.g., repeating gait cycles. Pinter and Dimitijevic (1999) have provided two examples for the existence of the rhythmic pattern generator in humans. In the case of incomplete spinal cord injury, the human lumbar cord isolated from brain influence can be trained to respond with rhythmic EMG activity to peripheral afferents which are activated by externally induced stepping movements where the subject was suspended over moving treadmill. They also conducted a study on six subjects with completer long-standing spinal cord injury in which an electrical train of stimuli were applied over the second lumbar segment of the spinal cord. This stimulation induced rhythmic, alternating stance and swing phases of the lower limbs (Pinter and Dimitijevic 1999). Theoretical studies have suggested that the rhythmic interaction between muscles triggered by NPGs creates human walking (Taga 1995; Kandel et al 2000; Ogihara and Yamazaki 2001; Wadden and Ekeberg 1998). The typical periodic patterns could be thought as stable limit cycles (periodic orbits) in a viewpoint of stability of dynamic system. A cyclic sequence of joint states constitutes a global pattern of movement in a gait cycle at the joint. In the NPG, the periodic cycles are generated without considering disturbance from outside or afferent inputs from higher

level. The NPG, therefore, has a characteristic of feedforward system. However, the lower nervous system essentially receives the afferent proprioceptive information as well as NPG signals in constructing locomotion. Thus, generation of rhythmic locomotion is mutually coordinated by both afferent signals form joint receptors and NPG signals. The mechanism enhances system stability against external disturbance.

Given the intimate relationship between upright balance and bipedal locomotion, and the wealth of physiological data that indicates important cerebral, cerebellar, brain stem and spinal roles in balance, patterned leg motion and locomotion, an integrated model describing the hierarchical neural control of both balance and walking appears valuable. In particular, it may be expected a priori that long-loop control may afford similar functional advantages to locomotor control as it does for standing balance. It may also be suspected that recruitable muscular synergies organized at a spinal level may help to reduce control demands upon higher level systems.

The control of upright posture during walking is similar to that exerted during stationary balance except that it is transient and/or weaker. It is natural therefore to consider beginning with the upright balance FRIPID model explored in previous chapter. However, it is possible to walk or even run with the trunk bent forward or backward, and during running the trunk is maintained erect even while there is no ground contract. Therefore, it is plausible that control trunk pitch and overall COM control are managed by separate circuits. This is consistent with recent experimental work by Freitas et al (2006) and appears to be a necessary model extension. The FRIPID model showed that smooth switching or scheduling cerebellar gains associated with PID (propotional-integral-derivative) control circuits as a function of sensed body state enabled the cerebrocerebellar system to automatically modify its responses according to disturbance strength. The switching system was argued to be easily compatible with known cerebellar cortical microcircuitry. Importantly, interpolation between just two gainsets was sufficient to account for the full range of balancing strategies. The current model considers that possibility a single or small

set of cerebellar gains would also be sufficient for walking control.

The availability of spinal synergies also enables an important simplification of the cerebellar control in the SBBW model with respect to that proposed in the FRIPID model. Under the assumption that certain signals ascending the spinal cord e.g. via spinocerebellar tracts, may consist of linear combinations of proprioceptive information (see (Osborne and Poppele 1992)), the presence of synergies in the efferent path allows multiple joints to be both sensed and controlled by single cerebellar modules. Specifically, one single input single output (SISO) channel can engage a synergy spanning ankle, knee and hip to control the trunk and stance leg to enable tracking of the intended center of mass position as specified in the cerebral cortex. An independent SISO channel can engage muscles at the hip to control trunk pitch relative to vertical based on ankle, knee and hip angle and an assumed pitch for the stance surface. Such decoupling is similar to that used recently to control robotic locomotion (Hofmann 2006). Hence, in the SBBW model, balance control is implemented by 2x2 diagonal matrices rather than full 3x3 matrices. On the other hand, the SBBW model is not designed to account for all features of human upright balancing such as postural strategies because the model focuses on walking.

Other experiments have pointed out the role of peripheral neural input in modulating the locomotor pattern. The most important influences appear to be a) detection of ground contact which is used to gate trans-cerebellar long-loop postural control of supporting leg, b) the monitoring of hip angle which appears to be associated with releasing or triggering the forward step transition (thrust to retraction, in Figure M6) (Knikou et al 2005; Kriellaars et al 1994; Duysens et al 2000), c) the peripheral phase-dependent modulation of reflex (Baxendale and Ferrell 1981; Brooke et al 1997; Duysens et al 2000; Rossignol et al 2006).

Ultimately, it is of conceptual interest to determine the simplest formulation that is consistent with recognized functional anatomy and normal and pathological balance and gait. Central questions then concern the relative roles of feedforward input and

feedback systems necessary to invoke and maintain stable gait. Specifically: What are the sufficient feedforward command variables? Given the signal transmission delays inherent in long-loop responses, how complex must feedforward signals be to manage body dynamics during walking? What types of long-loop and segmental feedback processing are necessary and sufficient to support the basic motor command? In particular, how may sensory information be integrated? What are possible roles of spinally organized muscle activation synergies and what is their relationship to central NPGs?

In this chapter, a basic model of Sagittal control of Bipedal Balance and Walking (SBBW) is investigated consistently by extending the postural control system. Here a parsimonious mechanism is sought with the intention of identifying the minimal or near-minimal neural control requirements for human-like bipedal gait. It shows that long-loop responses if stabilized and modulated by cerebral, and cerebellar interaction can afford sufficient upright balance to allow basic walking to be driven at different speeds simply by adjusting the frequency and amplitude two five-state rectangular pulse generators that engage four time-invariant muscular synergies. Peripheral reflexes provide modulation that improves walking efficiency, but are not fundamentally required for the basic gait pattern. Simulated lesions of the cerebellar and peripheral feedback systems give rise to certain control defects that are grossly similar to those observed clinically.

In summary, the SBBW model assumes:

PA-1) The feedforward action of brainstem and spinal cord in locomotor muscle patterning can be summarized as a five-state activation/relaxation process that drives time-invariant muscle activation synergies. This process controls the intensity and frequency of synergy activation.

PA-2) The influence of peripheral input can be considered to consist most importantly of a) indicating which leg is in contact with the ground, b) modulating synergies to improve step morphology by altering a spinal muscle activation

threshold via presynaptic inhibition.

PA-3) The control afforded by the cerebrocerebellar long-loop circuitry is implemented by three independent channels. One continuously operating to regulate trunk verticality, and two others that represent independent, parallel control of respectively left and right leg postures at stance needed to regulate intended relative COM position. Detection of ground contact (PA-2a) is used to gate trans-cerebellar long-loop COM control to the supporting leg (Duysens et al 2000; Nielsen 2003; Zehr and Stein 1999; Morton and Bastian 2003).

4.1 Sponomusculoskeletal plant model

4.1.1 Skeletal system and ground contact

A seven-segment kinematic chain with pivot joints representing each joint was used to represent human walking in the sagittal plane (Figure 4-1). Positive angular motion was consistent with anatomical flexion at the hip and knee, and dorsiflexion at the ankle. Each leg incorporates nine muscles.

Body physical parameters				
	Body segment, H_B=1.8m, M_B=80kgm			
	Trunk	Upper leg	Lower leg	Foot
Mass(kgm)	$0.678M_B$	$0.1M_B$	$0.047M_B$	$0.015\mathrm{M}_B$
Moment of inertia(kgm^2)	$0.031M_BH_B^2$	$6.262\times10^{-4}M_BH_B^2$	$2.566\times10^{-4}M_BH_B^2$	$4.976\times10^{-6}M_BH_B^2$

Table 4.1: Body segment's masses and moments of inertia calculated based on Winter (1990).

The natural locking of the knee that prevents hyperextension is modeled by a high impedance damped elasticity:

$$\tau_{i,lock} = \begin{cases} \max(K_k(\theta_{i,\min} - \theta_i) - B_k\dot{\theta}_i, 0), & \text{if } \theta_i<\theta_{i,\min} \\ \min(K_k(\theta_{i,\max} - \theta_i) - B_k\dot{\theta}_i, 0), & \text{if } \theta_i>\theta_{i,\max} \end{cases} \tag{4.1}$$

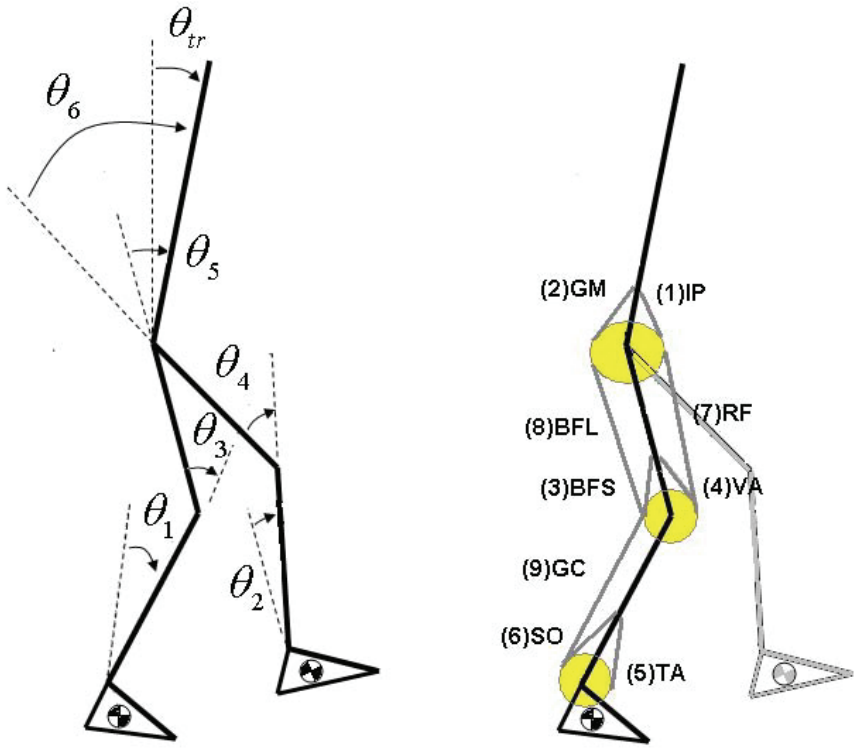

Figure 4-1: Body configuration angle convention (left): arrows indicate directions where angle values increase. Muscle diagram (one leg for simplicity)(right) with muscles identified in Table 4.2. The length of each segment is represented with respect to the total body's height H_B (Figure 4-2). Each segment's mass and moment of inertia are calculated with respect to H_B and the body's mass M_B in Table 4.1. The position of center of mass at feet is detailed in Figure 4-2(bottom).

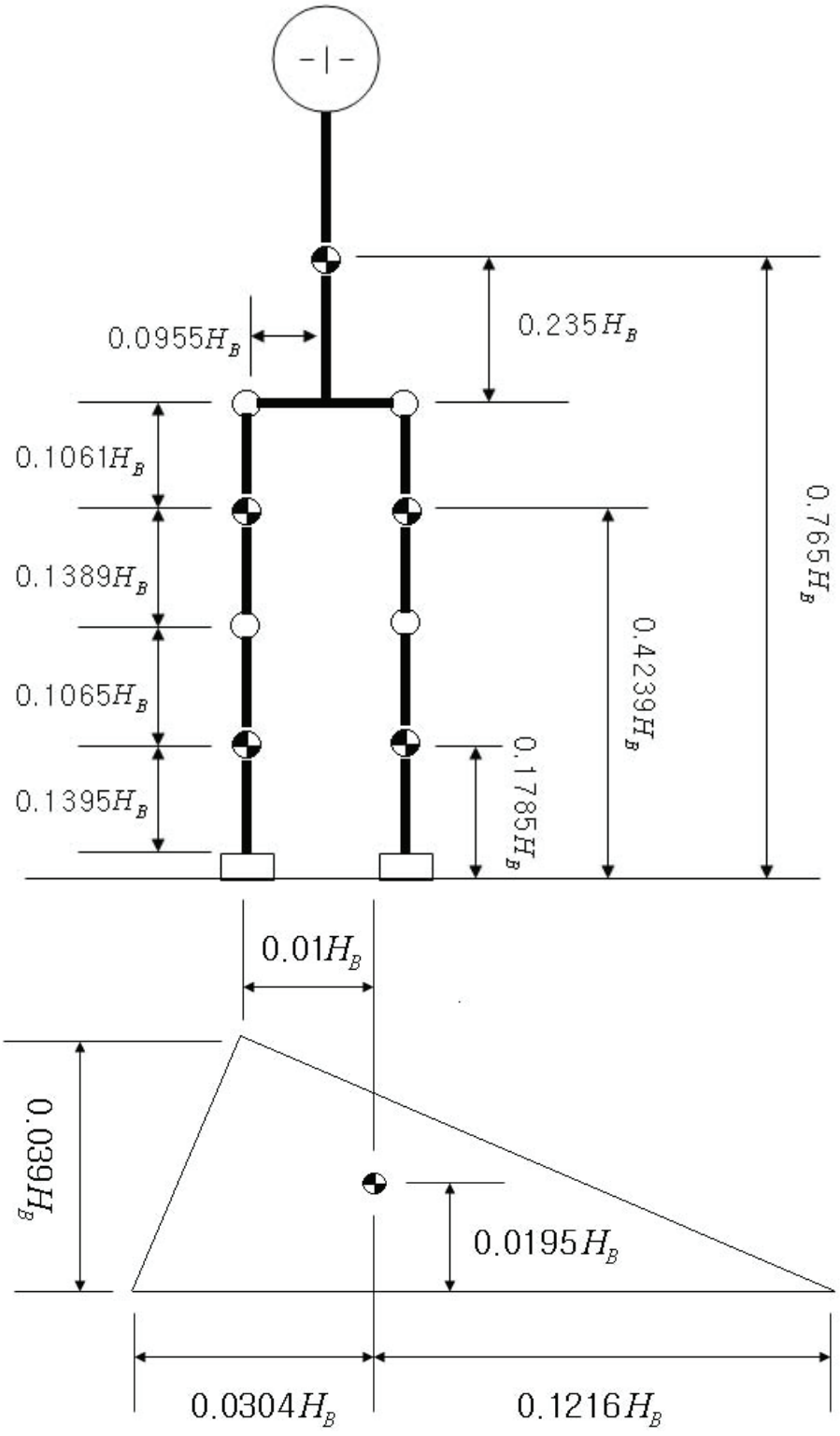

Figure 4-2: Body segment length (top) and foot dimensions (bottom) (Winter 1990). Centers of component masses are indicated by small checkered discs.

where K_k, B_k are respectively spring and damper coefficients, $\theta_{i,\min}$ is a minimum knee angle, and $\theta_{i,\max}$ is a maximum knee angle, and θ_i is an actual knee angle $(i = 3, 4)$. For this research, $\theta_{i,\min}$ is set to be -160 degrees, and $\theta_{i,\max}$to be zero degree.

The body model's dynamics in response to applied total muscular and ground reaction torques applied to the joints, $\tau_M(\Theta, \dot{\Theta}, \text{act})$ and $\tau_R(F_{gx}, F_{gy}, \Theta)$, respectively, is given by:

$$H(\Theta)\ddot{\Theta} + C(\Theta, \dot{\Theta}) = \tau_M(\Theta, \dot{\Theta}, \text{act}) + \tau_R(F_{gx}, F_{gy}, \Theta) + G(\Theta) \tag{4.2}$$

where $\Theta = \begin{bmatrix} \theta_1 & \theta_2 & \theta_3 & \theta_4 & \theta_5 & \theta_6 \end{bmatrix}^T$, $\dot{\Theta} = \begin{bmatrix} \dot{\theta}_1 & \dot{\theta}_2 & \dot{\theta}_3 & \dot{\theta}_4 & \dot{\theta}_5 & \dot{\theta}_6 \end{bmatrix}^T$, and $\text{act} = \begin{bmatrix} act_1 & act_2 & \dots & act_9 \end{bmatrix}^T$ represents the muscle activations defined below (Equation 4.11), $H(\Theta)$ is the symmetric configuration-dependent body inertia matrix, $C(\Theta, \dot{\Theta})$ is the matrix related to centrifugal and Coriolis forces,$G(\Theta)$ is the gravitational effect matrix, and $\tau_R(F_{gx}, F_{gy}, \Theta)$ is the torque generated by horizontal and vertical reaction forces to the ground at heel and toe (the details in section).

The dynamics are executed using Simmechanics in Matlab (MathWorks Inc., Natick, MA).

4.1.2 Muscle structure and activation

Muscular torque is determined by the total muscular force (passive + active) $\mathrm{F}(\mathrm{l}, \dot{\mathrm{l}}, \text{act})$ and the moment arms of each muscle according to:

$$\tau_M(\Theta, \dot{\Theta}, \text{act}) = \mathrm{A}^{\mathrm{T}}\mathrm{F}(\mathrm{l}, \dot{\mathrm{l}}, \text{act}) \tag{4.3}$$

$$\mathrm{A}^{\mathrm{T}} = \begin{bmatrix} 0 & 0 & 0 & 0 & -a_5 & a_6 & 0 & 0 & a_9^a \\ 0 & 0 & a_3 & -a_4 & 0 & 0 & a_7^k & -a_8^k & -a_9^k \\ -a_1 & a_2 & 0 & 0 & 0 & 0 & -a_7^h & a_8^h & 0 \end{bmatrix} \tag{4.4}$$

Where a_i^{jo} is the estimated average moment arm over the usual range of motion

of the ith muscle in Table 4.2. $jo = a, k, \text{or}, h$ to distinguish ankle, knee and hip joint moment arms, respectively, in biarticular muscles. Flexor moment arms are negative reflecting the relationship between length change and direction of rotation.

Muscle	Location	l_{eq} (m)	a_i^{jo} (m)	PCA(cm^2)
Iliopsoas(IP)	mono,hip flexor	0.35	0.132	17
Gluteus Maximus(GM)	mono,hip extensor	0.30	0.092	30.4
Rectus femoris (RF)	bi,hip flexor, knee extensor	0.48	$0.049(h)$, $0.025(k)$	12.5
Biceps femoris long (BFL)	bi, knee flexor, hip extensor	0.46	$0.054(h)$, $0.049(k)$	15.8
Vastus(VA)	mono, knee extensor	0.26	0.04	30
Biceps femoris short(BFS)	mono, knee flexor	0.29	0.049	6.8
Tibialis anterior(TA)	mono, ankle dorsiflexor	0.30	0.023	9.1
Gastrocnemius (GC)	bi, knee flexor, ankle plantarflexor	0.56	$0.050(k)$, $0.040(a)$	30
Soleus(SO)	mono, ankle plantarflexor	0.35	0.036	58

Table 4.2: Length (l_{eq}), moment arm (a_i^{jo}) , and physiological cross-sectional areas (PCA) of muscles used for biped walking model. The values are determined on basis of Ogihara and Yamazaki (2001), Delp et al (1999), and Winter (1990) .

The model views the anatomically redundant muscles of the trunk and legs as operating together as functional groups of uni- and biarticular flexors and extensors as shown in Figure 4-1. Assuming that stiffness is proportional to physiological cross-sectional area (PCA) (Brand et al 1986), the relative muscle stiffness scaling is given based on morphmetric data in Table 4.2.

Passive muscular force is expressed by:

$$\mathrm{F}_{pass} = \left[\mathrm{K}_{pass}(\mathrm{l}_{eq} - \mathrm{l}) - \mathrm{B}_{pass}\dot{\mathrm{l}}\right]_{+} \tag{4.5}$$

where F_{pass} is passive tension vector, $\mathrm{K}_{pass}, \mathrm{B}_{pass}$ is passive muscle stiffness and viscosity matrices, l_{eq} is muscle length vector at equilibrium; l is actual muscle length vector.

Active muscular force as a function of neural input to each muscle (act) is represented by:

$$\mathrm{F}_{act} = \mathrm{K}_{act}(\mathrm{l(act)})[\mathrm{l(act)} - \mathrm{l}]_{+} - \mathrm{B}_{act}(\mathrm{l(act)})\dot{\mathrm{l}} \tag{4.6}$$

where F_{act} is active tension vector, $\mathrm{l(act)} = \mathrm{l}_{eq}+\mathrm{act}$.

$\mathrm{K}_{act}(\mathrm{l(act)})$ and $\mathrm{B}_{act}(\mathrm{l(act)})$ are the active muscle stiffness and viscosity matrices which are functions of muscular activation.

$$\begin{aligned} \mathrm{K}_{act}(\mathrm{l(act)}) &= \mathrm{K}_{a}\left(\alpha[\mathrm{l(act)}]_{+}+\beta\min(\gamma[\mathrm{l(act)}]_{+}, 1)\right) \\ \mathrm{B}_{act}(\mathrm{l(act)}) &= \mathrm{B}_{a}\left(\alpha[\mathrm{l(act)}]_{+}+\beta\min(\gamma[\mathrm{l(act)}]_{+}, 1)\right) \end{aligned} \tag{4.7}$$

where K_a , B_a are constant matrices, and α , β , and γ are constant coefficients.

When both passive and active tensions are applied together,

$$\mathrm{F}(\mathrm{l}, \dot{\mathrm{l}}, \mathrm{act}) = \left[\mathrm{F}_{pass}(\mathrm{l}, \dot{\mathrm{l}}) + \mathrm{F}_{act}(\mathrm{l}, \dot{\mathrm{l}}, \mathrm{act})\right]_{+} \tag{4.8}$$

$$\mathrm{l} = \mathrm{l}_{eq}+\mathrm{A}(\Theta - \Theta_{eq}) \tag{4.9}$$

where Θ_{eq} is joint angle vector at equilibrium.

The positive brace means that each muscle is constrained to exert only contractile force. This formulation substantially follows that employed by Katayama and Kawato (1993).

The effective pre-set (e.g. before reflex neural activation) rotational stiffness of the ankle during standing is about 90 Nm/rad (Fujita and Sato 1998). This value was used to determine the absolute passive stiffness of each muscle given their relative scaling. It was assumed that $\mathrm{K}_a = 2.5\mathrm{K}_{pass}$ and $\mathrm{B}_a = 2.5\mathrm{B}_{pass}$. This was considered based on human arm modeling where stiffness and damping ratio have been shown to increase up to 500% and 50% respectively (Lacquaniti and Soechting 1986) with strong activation, this was considered conservative leaving a larger portion of the control to the CNS model. In general, muscle viscosity was set at one-tenth the muscle stiffness as has been done in arm modeling (Flash 1987).

The activation of muscle force by neural input occurs according to low-pass dynamics that can be approximated by:

$$EC(s) = \frac{\rho^2}{(s+\rho)^2}, \qquad (\rho = 30\text{rad/sec}) \tag{4.10}$$

(Fuglevand and Winter 1993),

and

$$\text{act} = EC(s)\,(\text{u}_\alpha) \tag{4.11}$$

meaning that the filter is applied to u_α that is the alpha motor neuronal output. The dynamics of series elasticities, filtering action of spindles, segmental proprioceptive and force feedback, and spinal processing by alpha motorneuron - Renshaw cell networks were not modeled explicitly, although it is likely that these could improve the accuracy of the simulations (Winters 1995). However, it was not felt that these features would bear significantly upon the basic neuromuscular mechanisms of gait control.

4.1.3 Foot interaction with the ground and tactile receptor

When the heel or toe touches the ground, the horizontal and vertical reaction forces at the heel and toe are generated. The vertical reaction force is modeled by

$$F_{gy}^i = \left(K_{gy}\left(y_{gy}\left(x^i\right) - y^i\right) - B_{gy}\dot{y}^i\right)\max\left(y_{gy}\left(x^i\right) - y^i, 0\right) \tag{4.12}$$

where (x^i, y^i) indicates the positions of either heel or toe with $i = heel, toe$.

$y_{gy}\left(x^i\right)$ represents the ground profile as a function of x^i. F_{gy}^i is always nonnegative. The horizontal reaction force is modeled as a dynamic friction force.

$$F_{gx}^i = -\mu_k F_{gy}^i \text{sgn}(\dot{x}^i) \tag{4.13}$$

where μ_k is the dynamic frictional coefficient. If the toe or heel reaches zero horizontal velocity, the horizontal reaction force is modeled by a spring and damper

system instead of Equation 4.13 as long as the horizontal reaction force is smaller than the maximal friction force.

$$F_{gx}^{i} = \left(K_{gx}\left(x_{o}^{i} - x^{i}\right) - B_{gx}\dot{x}^{i}\right)\max\left(y_{gy}\left(x^{i}\right) - y^{i}, 0\right), if\left|F_{gx}^{i}\right| \leq \left|\mu_{s}F_{gy}^{i}\right| \quad (4.14)$$

where x_{o}^{i} is a location where either heel or toe touches the ground initially and μ_{s} is the static frictional coefficient.

However, if the horizontal reaction force is larger than the maximal friction force, Equation 4.13 describes the horizontal reaction force. As a result, the total vertical and horizontal reaction forces between foot and ground are respectively.

$$F_{gy} = F_{gy}^{toe} + F_{gy}^{heel}, \quad \text{and} \quad F_{gx} = F_{gx}^{toe} + F_{gx}^{heel} \quad (4.15)$$

The interaction between foot and ground is detected by tactile receptors on the foot. The signal from the receptor is expressed by R_{t}.

$$R_{t} = 1\left[F_{gy}^{toe} + F_{gy}^{heel} - \delta_{F}\right] \quad (4.16)$$

where δ_{F} is an offset (a small amount of force).

For simplicity, detection is based on the total reaction force on the foot, which is a sum of reaction forces on the toe and heel. R_{t} is 1 when foot receive reaction force and 0 otherwise. Therefore, the tactile receptors inform of whether each leg is at either swing or stance phase.

4.2 Central neural control model

4.2.1 Spinal pattern generator

Combining the neural pattern generator and muscle synergy concepts comes to a suggestion that each specific neural pattern plays a role of the synergy, and only a small number of patterns are sufficient to implement distinct motor behaviors. Each

of NPGs governs individual muscle synergies. Those are programmed. The activation signals recruited from the NPGs are motor primitives, which are interpreted to be fixed groups of muscles, their motor neuron pools and their afferent regulatory circuits, which together act as a unit to produce a fixed motor output.

A periodic activation can be modeled in the form of

$$u_{PG,i}(t) = m_{PG} \cdot 1\left[\cos(2\pi f_{PG} t - \phi_i) - h_i\right]_+, i = 1, 2, 3, 4. \tag{4.17}$$

f_{PG} determines the pattern frequency, m_{PG} is a magnification factor, ϕ_i is the phase shift, and h_i activity discharge threshold of the ith spinal command signal $u_{PG,i}(t)$. The values used for ϕ_i and h_i in simulation are given in Table 4.3. The values of ϕ_i and h_i were found empirically to yield a) no command overlap, b) the most realistic gait patterns subject to constraint a). As a further simplification, the intensity of $u_{PG,i}(t)$ is intentionally set to zero to correspond to an almost completely passive swing phase of each leg. Two identical pulse generators were used, one for each leg. A phase difference of 180 degrees between the generators was enforced artificially as gaits other than simple walking were not entertained in this study.

	$u_{PG,1}$	$u_{PG,2}$	$u_{PG,3}$	$u_{PG,4}$
ϕ_i	0.38	1.2	0.705	0.5275
h_i	$\cos(0.16\pi)$	$\cos(0.2\pi)$	$\cos(0.23\pi)$	$\cos(0.125\pi)$

Table 4.3: Parameters for periodic pattern generation: schematic representation of the membrane potential of a hypothetical neuron within an oscillating circuit. Action potential pikes representing output are fired when a threshold is crossed, and firing rate (intensity) is modeled by a rectangular pulse that occurs when threshold is traversed.

It is proposed that NPG commands $\mathrm{u}_{PG} = \begin{bmatrix} u_{PG,1} & u_{PG,2} & u_{PG,3} & u_{PG,4} \end{bmatrix}^T$ are distributed to the muscles according to a spinal locomotor control synergy network represented by the matrix W_{PG} (Figure 4-5 and Appendix A.2) according to four or five functional tasks during the gait cycle. The fifth task, active control of swing leg is for the moment ignored moment as indicated above.

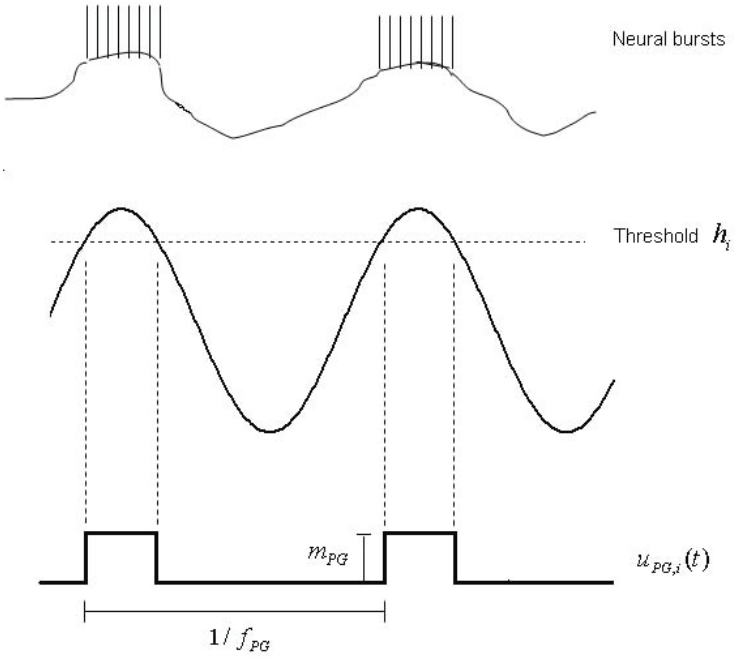

Figure 4-3: Periodic pattern generation.

$$\mathrm{u}_{SP} = \mathrm{W}_{PG}\mathrm{u}_{PG}(\mathrm{t} - \mathrm{T}_{pr}) \tag{4.18}$$

where $\mathrm{T}_{pr} = \begin{bmatrix} T_{pr,a} & T_{pr,k} & T_{pr,k} \end{bmatrix}^T$ represents the neural transmission delay from the spinal cord to muscles.

The combination of spinal pulse generator and control synergy distribution matrix is considered a NPG. To develop a minimal model, synergies involving the mono-articular muscles alone were formed. Thus, the spinal activations $u_{SP,j}(t)$ are defined for $j = 1, ..., 6$ in Figure 4-4. The signals for $j = 7, 8, 9$ were initially assumed to be zero, and later formed empirically from components of the mono-articular commands. As discussed later, simple walking was comparatively much less sensitive to biarticular activation.

Each rhythmic spinally generated muscle command $u_{SP,j}(t)$ is thus a train of rectangular pulses. Empirically, the primary function of each pulse is approximately:

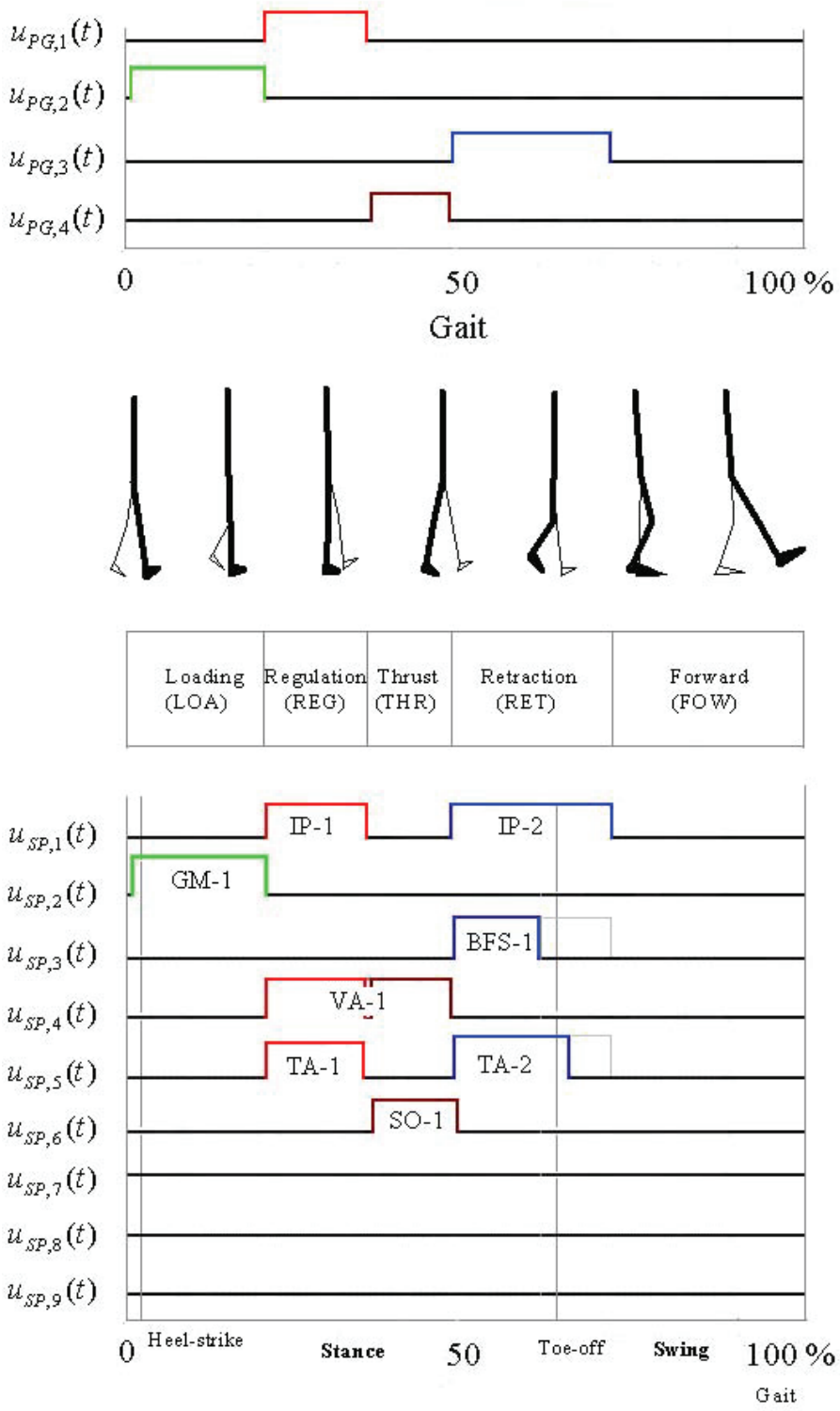

Figure 4-4: Decomposed spinal locomotor signals and a model of the neural network. (top) Spinal pulse output commands and (bottom) proposed control epochs and spinally generated command by muscle and phase of gait.

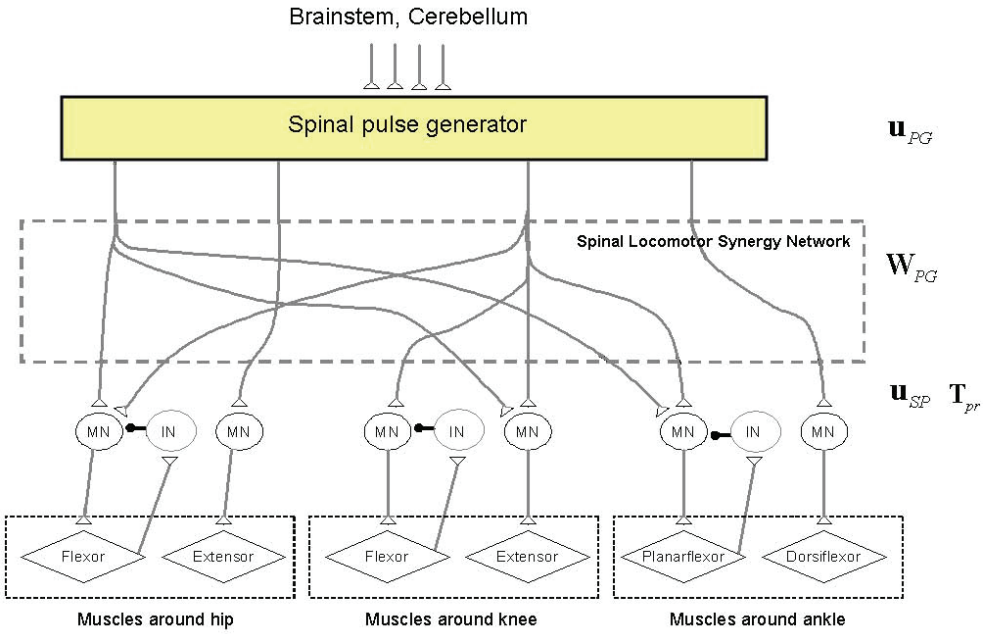

Figure 4-5: Hypothetical model of connection between spinal pulse generator and muscle.

- IP-1: to prevent the upper body from falling backward.
- IP-2: to trigger swing around hip.
- GM-1: to prevent the upper body from forward rotation just after heel strike.
- BFS-1: to help a swing leg foot avoid ground contact stay by bending its knee.
- VA-1: to maintain the body support of a stance leg by stretching its knee at mid-stance.
- TA-1: to help COM move forward so as to insure enough step size.
- TA-2: to help a swing leg stay in the air by rotating its foot.
- SO-1: to push a stance leg forward to initiate a swing phase and provide forward thrust.

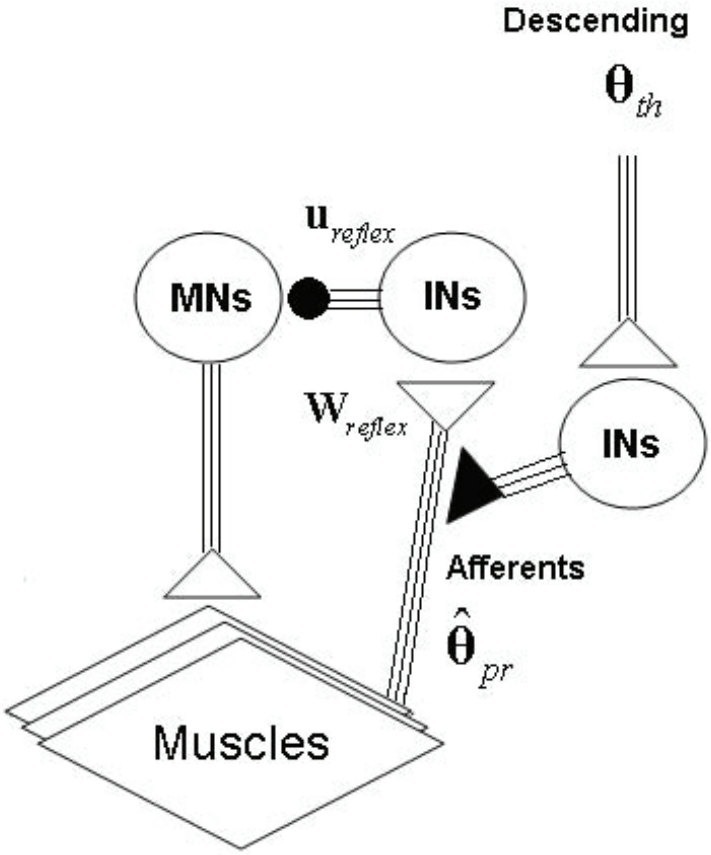

Figure 4-6: Presynaptic inhibition: depolarization of an afferent terminal (presynaptic inhibition) is indicated by the filed triangle ending on afferent pathway, inhibitory effect by the filled circle. MN: motorneuron, IN: interneuron.

As detailed in the results, it was assumed that a separate additional pulse could be delivered (superposed on other commands) to IP to launch walking from a standing start. The physiological basis of such a pulse is not specified. However, as discussed below, it may be of cerebral origin.

Finally, the SBBW model proposes that peripherally triggered spinal inhibition can help to modify certain synergy components. One possible neural circuit involves presynaptic inhibition (Baxendale and Ferrell 1981; Brooke et al 1997; Rossignol et al 2006; Duysens et al 2000) as shown in Figure 4-5 and in greater detail in Figure 4-6. A descending signal conveys a tonic excitation $\theta_{th,jo}$, ($jo = a, k, h$: ankle, knee, and hip respectively) that inhibits the proprioceptive afferent θ_{jo}. Once $\theta_{th,jo}$ is superseded by θ_{jo} , the interneuron is activated and the motor neuron activity is suppressed. It is assumed here that such a mechanism could truncate BFS-1 and TA-2 activity in early FOW to prevent excessive leg retraction. This mechanism is useful to implement the right timing between knee and ankle stretching motions in order not to touch the ground during swing phase. The reflex action is therefore modeled as:

$$\mathrm{u}_{reflex}(\mathrm{t}) = -\mathrm{W}_{reflex} \cdot 1\left[\theta(\mathrm{t} - \mathrm{T}_{pr,jo}) - \theta_{th}\right]_{+} \tag{4.19}$$

where $\theta = \begin{bmatrix} \theta_a & \theta_k & \theta_h \end{bmatrix}^T$, and $\theta_{th} = \begin{bmatrix} \theta_{th,a} & \theta_{th,k} & \theta_{th,h} \end{bmatrix}^T$, and W_{reflex} is a 9 x 3 matrix (see appendix A.2) that scales and distributes joint-related signals from the uniarticular muscles to the other muscles via the 9 element vector u_{reflex}.

4.2.2 Suprasegmental control

The second piece of the central neural control system consists of long-loop feedback pathways that add considerable stability. Two control channels are modeled. The first is concerned with tracking the commanded position of the body's COM as specified by a tonic reference signal COM_{ref}. The second concerns maintaining the trunk-head segment vertical at all times. The pitch angle of the trunk-head segment is represented as θ_{tr} (Figure 4-1) and therefore its position is set to be $\theta_{tr,ref} = 0$. The cerebrocere-

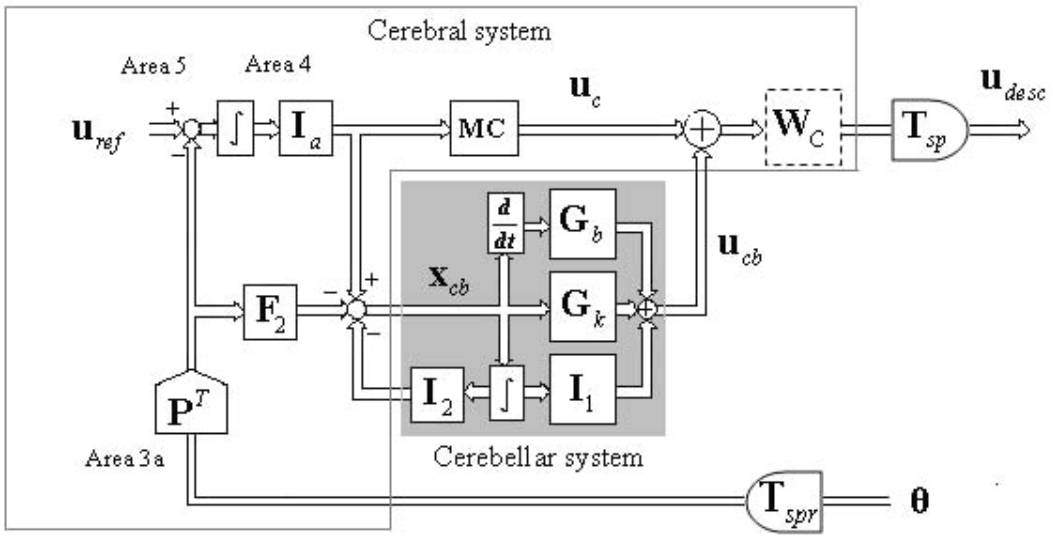

Figure 4-7: The RIPID cerebrocerebellar control model.

bellar control model (Figure 4-7) is simplified from the FRIPID model in that no high speed "catching" gainset or force-feedback are employed. This is because the SBBW is not designed to cope with rapid foot slippage or translation of the support surface. Physiologically, it is also quite possible that important long-loop feedback control operates via sub(cerebral)cortical levels. However, from the perspective of managing long signal transmission delays the most challenging possibility is if significant processing occurs via trans(cerebral)cortical loops as it does in arm control. For conservatism, therefore, trans(cerebral)cortical long-loop feedback is modeled.

During simulated walking $COM_{ref} = 25$ cm and this is compared to a linear estimate of COM position relative to the stance foot computed as:

$$\begin{aligned}
&\hat{x}_{com} = \tfrac{m_1}{(m_1+m_2+m_3)} r_1 \sin\theta_a(t - T_{aff,a}) + \tfrac{m_2}{(m_1+m_2+m_3)}(l_1 \sin\theta_a(t - T_{aff,a}) + \\
&r_2 \sin(\theta_a(t - T_{aff,a}) + \theta_k(t - T_{aff,k}))) + \tfrac{m_3}{(m_1+m_2+m_3)}(l_1 \sin\theta_a(t - T_{aff,k}) \\
&+ l_2 \sin(\theta_a(t - T_{aff,k}) + \theta_k(t - T_{aff,k})) + r_3 \sin(\theta_a(t - T_{aff,a}) + \theta_k(t - T_{aff,k}) + \theta_h(t - T_{aff,h}))) \\
&\approx \tfrac{(m_1 r_1 + m_2(l_1+r_2) + m_3(l_1+l_2+r_3))}{(m_1+m_2+m_3)} \theta_a(t - T_{aff,a}) + \tfrac{(m_2 r_2 + m_3 l_2)}{(m_1+m_2+m_3)} \theta_k(t - T_{aff,k}) \\
&+ \tfrac{m_3 r_3}{(m_1+m_2+m_3)} \theta_h(t - T_{aff,h})
\end{aligned} \tag{4.20}$$

Therefore,

$$\hat{x}_{com} = p_{11}\theta_a(t - T_{aff,a}) + p_{21}\theta_k(t - T_{aff,k}) + p_{31}\theta_h(t - T_{aff,h}) = \mathrm{p}_1^T\hat{\theta} \qquad (4.21)$$

where $\hat{\theta} = \begin{bmatrix} \theta_a(t - T_{aff,a}) & \theta_k(t - T_{aff,a}) & \theta_h(t - T_{aff,h}) \end{bmatrix}^T$, and

$\mathrm{T}_{aff} = \begin{bmatrix} T_{aff,a} & T_{aff,k} & T_{aff,h} \end{bmatrix}^T$ are the afferent signal transmission delays including spinal and peripheral components, and $\mathrm{p}_1 = \begin{bmatrix} p_{11} & p_{21} & p_{31} \end{bmatrix}^T$ are constants. The scaling factors p_{i1} were obtained by linearizing trigonometric relationships and neglecting contributions of the swing leg as detailed in the appendix. The determination of which leg is in stance or in swing is made by ground contact force sensing (see section 4.2.3).

The estimate of θ_{tr} is presumed to depend upon a similar linear estimate:

$$\hat{\theta}_{tr} = \mathrm{p}_2^T\hat{\theta} \qquad (4.22)$$

where $\mathrm{p}_2 = \begin{bmatrix} p_{12} & p_{22} & p_{32} \end{bmatrix}^T$.

The derivation of the p_{i2} assumes for the moment a horizontal walking surface also specified in the appendix. In the case of non-horizontal surfaces, the trunk-head segment pitch estimate is presumably adjusted on the basis of or replaced by visual and/or vestibular input. However, this issue is not examined here.

When x_{cb} is the input, u_{cb} is the output, and we take $\mathrm{I}_1 = 0$ in Figure (4-7), we can describe cerebellar control as :

$$\mathrm{u}_{cb} = [\mathrm{G}_{CB}\mathrm{x}_{cb}]_+ = [\mathrm{W}_{CB}\,[\mathrm{diag}(gk_i + gb_i d(\cdot)/dt)\mathrm{x}_{cb}]]_+\,, \qquad i = 1, 2 \qquad (4.23)$$

and

$$\begin{aligned} \mathrm{x}_{cb} &= \left(\mathrm{I} + \mathrm{I}_2 \int\right)^{-1} \left(\mathrm{I}_a \int \left(\mathrm{u}_{ref} - \mathrm{P}^T \hat{\theta}\right) - \mathrm{F}_2 \mathrm{P}^T \hat{\theta}\right) \\ &= L^{-1} \left\{ (s\mathrm{I} + \mathrm{I}_2)^{-1} \left(\mathrm{I}_a \left(\mathrm{u}_{ref} - \mathrm{P}^T \hat{\theta}(s)\right) - s\mathrm{F}_2 \mathrm{P}^T \hat{\theta}(s)\right)\right\} \end{aligned} \tag{4.24}$$

where s is the Laplace variable, L^{-1} is the inverse Laplace transform, I is the identity matrix, $\mathrm{P} = \left[\begin{array}{cc} \mathrm{p}_1 & \mathrm{p}_2 \end{array}\right]$,$\mathrm{u}_{ref} = \left[\begin{array}{cc} COM_{ref} & \hat{\theta}_{tr,ref} \end{array}\right]^T$,gk_i and gb_i are, respectively, proportional and derivative control gains, $d(\cdot)/dt$ is the differentiation operator, $\int$ is the integration operator, and W_{CB} is a distribution network in either cerebral cortical area 4 or in the spinal cord (for current purposes the location does not matter).

Thus, matrices G_k and G_b in Figure 4-7 are diagonal and G_{CB} is 9 x 3 and represents the total processing by the cerebrocerebellar system of joint-specific proprioceptive signals. The net command signals are also constrained to be always positive. Finally, we take MC = 0 in Figure 4-7, therefore

$$\mathrm{u}_{desc} = \mathrm{u}_{cb}(\mathrm{t} - \mathrm{T}_{sp}) \tag{4.25}$$

The two control variables, i.e., position of COM, and truncal verticality, are regulated for postural balance during walking. The cerebrocerebellar feedback control over COM during stance phase affects on muscular activation as in Figure 4-8. Red muscle parts are activated by the feedback control to achieve a proper posture during walking. Truncal verticality is controlled by muscular activations around hip in a similar way.

The cerebral cortex is presumably the spot where each (population) vector p_i is implemented. In sensorimotor cortical area 3a, the spatial extend of a pyramidal cell association collaterals over the layers approximately construct a columnar assembly (Karameh 2002). It is highly expected that each column contains a specific feature presentation of sensory information (Huffman and Krubitzer 2001). The specific presentation can be hypothetically described by a weighted linear combination of sensory information, which is a form of the inner product of a population vector p_i and a vector of sensory information as in Equations 4.21 and 4.22. Hypothetically, a

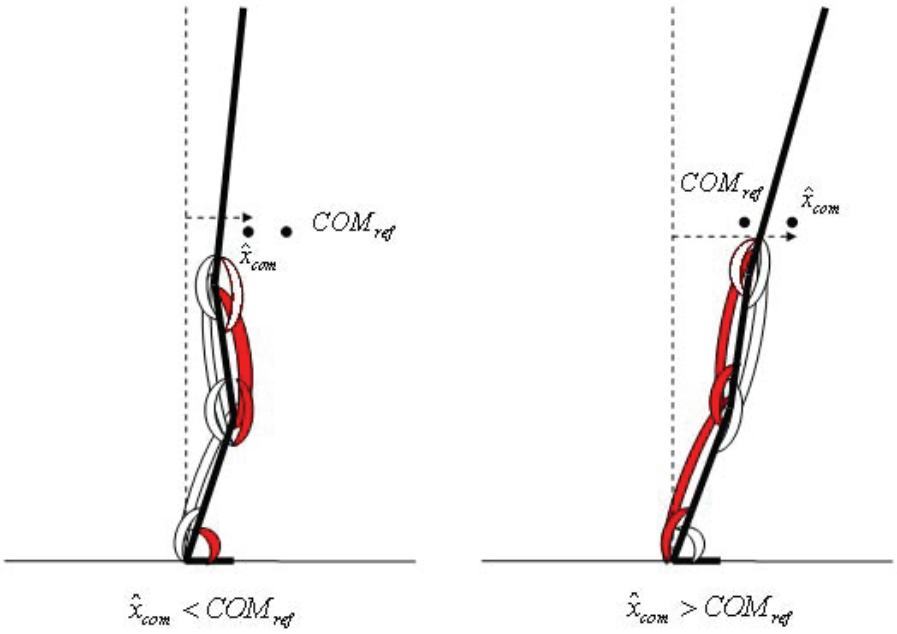

Figure 4-8: Muscular activation by the cerebrocerebellar system over position of COM.

columnar activity is represented by a unit population vector $\hat{\mathrm{p}}_i$ parallel to p_i.

$$\mathrm{p}_i = k\hat{\mathrm{p}}_i \tag{4.26}$$

where k is a scalar that represents the intensity of neural activity.

4.2.3 Summary of neural control model

Figure 4-9 summarizes the hierarchical neural control of the SBBW model. Alpha motor neuronal output u_α is then represented by a nine component vector. From Equations 4.18, 4.19, and 4.25,

$$\mathrm{u}_\alpha(\mathrm{t}) = \mathrm{u}_{desc}(\mathrm{t} - \mathrm{T}_{pr}) + \mathrm{u}_{sp}(\mathrm{t} - \mathrm{T}_{pr}) + \mathrm{u}_{reflex}(\mathrm{t} - \mathrm{T}_{pr}) \tag{4.27}$$

The cerebellum presumably plays a role in the generation of appropriate patterns of limb movements, dynamic regulation of balance, and adaptation of posture and locomotion through practice (Morton and Bastian 2004). The last function is not

relevant to the present model, but the first two are involved in. The cerebrocerebellar system controls the COM and trunk verticality, and implicitly descends neural signals affecting the parameters in the pattern generator, which implicate a presetting or adjustment of the gain of proprioceptive reflexes and a sequence of feedforward programs. Supraspinal control including the cerebellum also adjusts the tonic excitation $\theta_{th,jo}$ which coordinates the retraction of a leg. In this perspective, the cerebellar system demonstrates the first two functions.

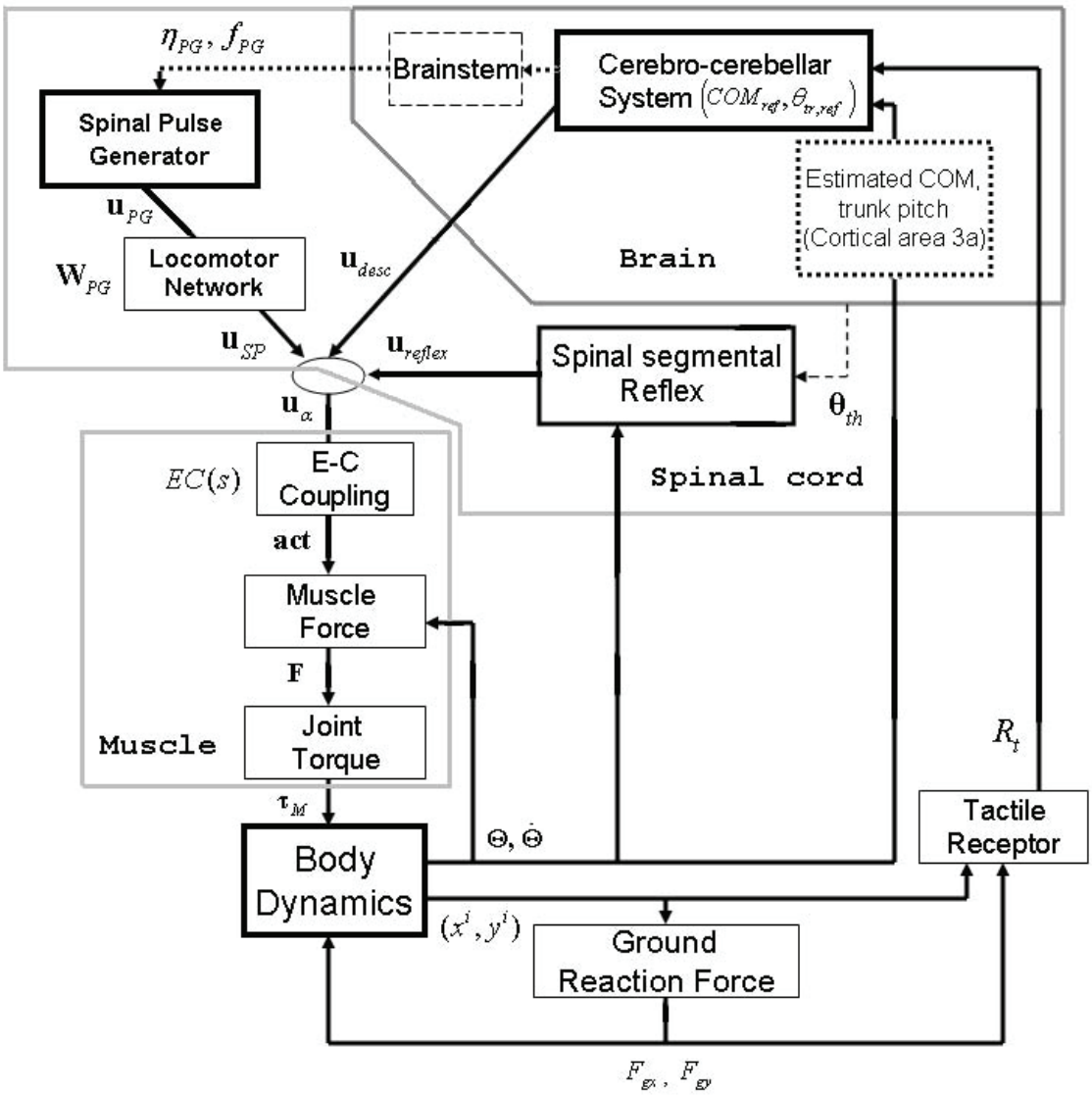

Figure 4-9: Diagram of hierarchical neural control of walking.

4.3 Implementational assumption and model evaluation

For tractability of the initial study, and to evaluate minimal requirements for active, moderately stable locomotion, the following implementational assumptions have been made:

IA-1) Movements will be driven by mono-articular muscle pairs.

IA-2) Spinal synergy activation will be driven by a strictly sequential train of on-off pulses.

IA-3) Inter-leg coordination is achieved by artificially enforced 180 degree phase difference between the pulse generators controlling each leg, rather than modeling interactive circuitry.

IA-4) For movement initiation from a standing start, it was assumed that a single additional pulse could be applied to hip flexors to flex the leading hip transiently.

The implications of these assumptions are considered in the discussion.

The SBBW model was then evaluated first in terms of its steady state walking features both kinematic and neuromuscular. Specifically, clinical investigators have defined the determinants of normal and pathological gait by observing features of human locomotion pattern that minimize displacement of the body's COM. This has yielded the six determinants of normal gait (Saunders et al 1953; Della Croce et al 2001). However, all but one – knee bending at foot impact – are not observable in the sagittal plane and therefore are not immediately useful for analysis of the SBBW. As an alternative, the model was examined to determine whether it exhibits any of nine pathological gait features (Perry 1992). Next, the robustness of its performance was assessed by determining its ability transition to steady state walking at different speeds from a standing start, and to subsequently slow to a stop. Stability robustness was tested by subjecting the model to forward and backward impulsive disturbances

during different phases of the gait cycle, and by simulating sudden additions of mass to the trunk. Finally, the sensitivity of the model behavior to several simulated neural and muscular lesions was observed. During the simulations, all model parameters were held fixed unless explicitly stated otherwise.

4.4 Results

4.4.1 Basic kinematic features of walking

After an initial transient, body kinematics converged to a consistent walking pattern that was qualitatively very similar across a range of speeds. Figure 4-10 shows a typical human speed of about 1.21 m/s that is simulated with $f_{PG} = 1.3$ and $m_{PG} = 1.2$. Initiation is discussed below and initial conditions are specified in appendix. It takes several steps to converge to steady state walking motion. The steady state motion displays a number of the kinematic features (Saunders et al 1953; Perry 1992) of natural human walking. The ankle joint trajectory (Figure 4-10bottom) includes a valley corresponding to toe push off. In Figure 4-11 (d, e, f), this motion at the end of ground contact can also be seen as a rapid transient. Small bending motions at knee joint during a gait cycle correspond to impact at the transition from swing to stance, while large bending motions correspond to the retraction phase. During each cycle, the hip has a monophasic oscillation in the anterior-posterior direction. Each joint motion approximates a limit cycle. The coordination of the joints is shown pairwise in Figure 4-11(a)-(c). During simulated steady walking at 1.21m/s with the nominal sets of parameters, each leg spends about 59% of each cycle in stance and the rest in swing. Double support phase accounts for about 9% of each cycle. These values mirror those of 60% and 10%, respectively, measured in humans (Perry 1992).

It has been suggested that at least 9 features can be identified in defective human gait (Perry 1992). Seven of these are observable in the sagittal plane:

1. Foot slap on the ground during loading response.

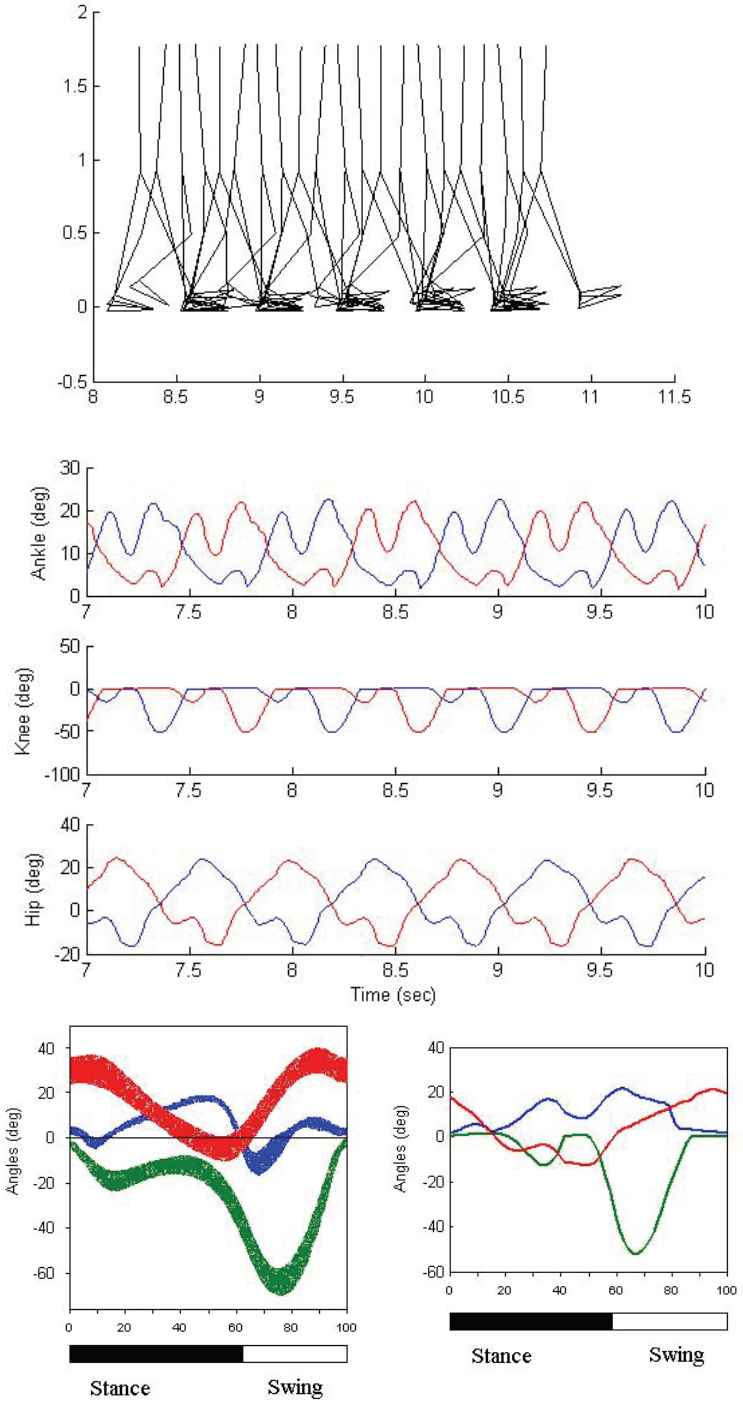

Figure 4-10: Steady state walking at 1.21m/s. (top) Stick plots sampled every 10msec. (middle) Simulated time courses of hip, knee and ankle joints: blue line indicates joints in right leg, and red in left leg. (bottom) Averaged time courses of hip (red), knee (green) and ankle (blue) joints during a gait cycle, (left): experimental data adapted from CGA normative gait database (http://guardian.curtin.edu.au/cga/data/index.html), (right): simulation.

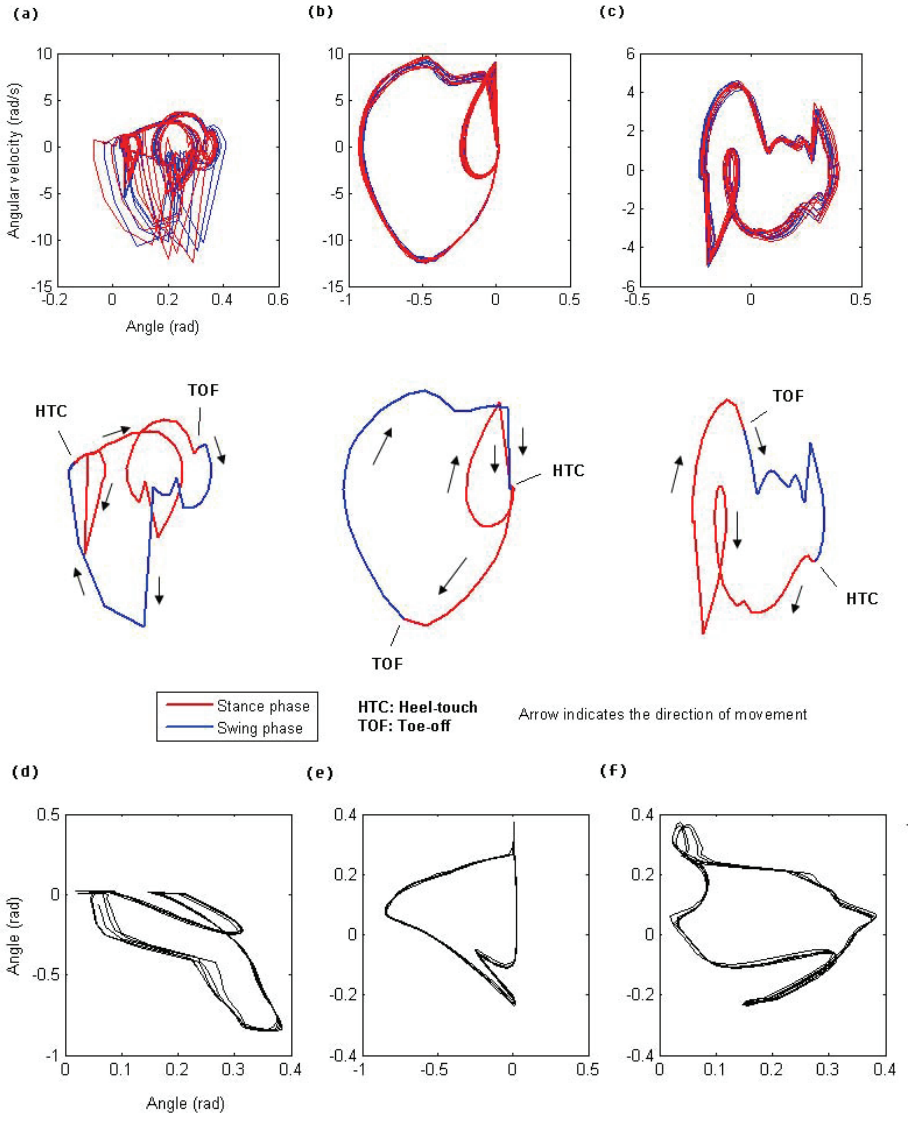

Figure 4-11: Steady state walking kinematics: joint phase-plane behavior: (a) ankle, (b) knee, and (c) hip (top), and joint coordination plots: (d) ankle vs. knee, (e) knee vs. hip, and (f) ankle vs. hip (bottom).

2. Flat foot contact at transition from swing to stance.

3. Knee hyperextension from loading response to midstance.

4. Inadequate knee flexion during swing.

5. Excessive forward lean of trunk during stance.

6. Backward lean of trunk during loading response.

7. Asymmetrical step length.

The third pathological feature is the complement of the third determinant of normal gait. Model steady state walking shows none of the above features. The simulated motion is also qualitatively smooth.

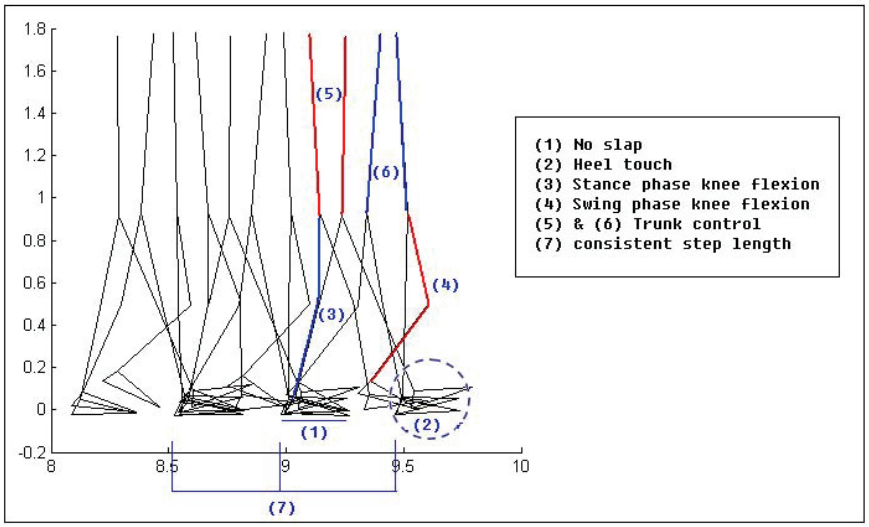

Figure 4-12: Gait analysis with respect to defective gait features.

4.4.2 Walking initiation

While a human maintains standing posture, the erect body tends to tilt slightly forward around ankle about 2 to 5 degrees to maintain the center of mass within stable supporting area (Loram et al 2004). Therefore, an initial postural condition is

set to be $\theta_a = 0.05, \theta_k = \theta_h = 0$ for both legs. Walking can be initiated from stance by applying pulses of muscular activity to hip flexors (Figure 4-13(b)) and then starting the NPG. The added pulse may be interpreted as a walking trigger from CNS. Figure 4-13(a) shows that there is a transient initial response. The first step is with the right leg while the left leg supports body. Steady state walking is substantially achieved by the third gait cycle.

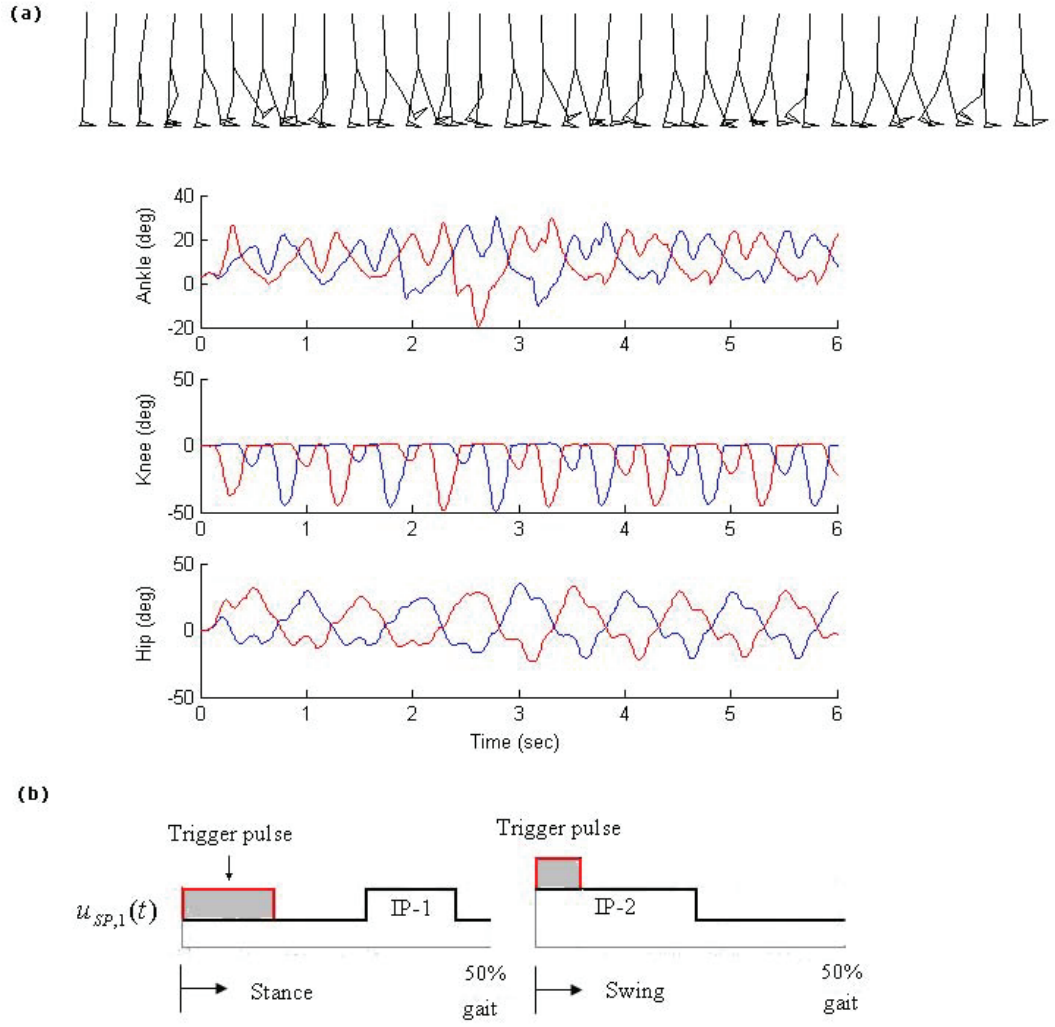

Figure 4-13: (a) Stick figure plot and joint trajectories of simulated walking initiation from stance. In the stick figure plot the motion is sampled every 100msec and separated horizontally for clarity. Solid red line indicates right leg joints in stance phase, and blue swing. Dashed black line, left leg joints. (b) Neural pattern for initiation: Trigger pulses are added to $u_{SP,1}(t)$ in Figure 4-4 in order to initiate walking at only first step.

4.4.3 Reaction force and muscular activation

Dynamic realism is confirmed in Figure 4-14 where both components of the reaction force waveform are biphasic with values of appropriate magnitude (Winter 1990). The horizontal reaction force is negative just after heel contact the ground, indicating a backward horizontal friction force. Then, the force becomes positive, indicating the forward reaction as the foot to pushes backward against the ground. The vertical reaction force shows a rapid rise at heel contact in excess of body weight (80kg) to account for vertical deceleration. As the knee flexes during midstance, the force is below body weight. At push-off, a second peak greater than body weight is caused by plantarflexors. The second peak in simulation is greater than the first, which is not physiologically typical. This is due to force at the heel that is not fully realistic as will be discussed.

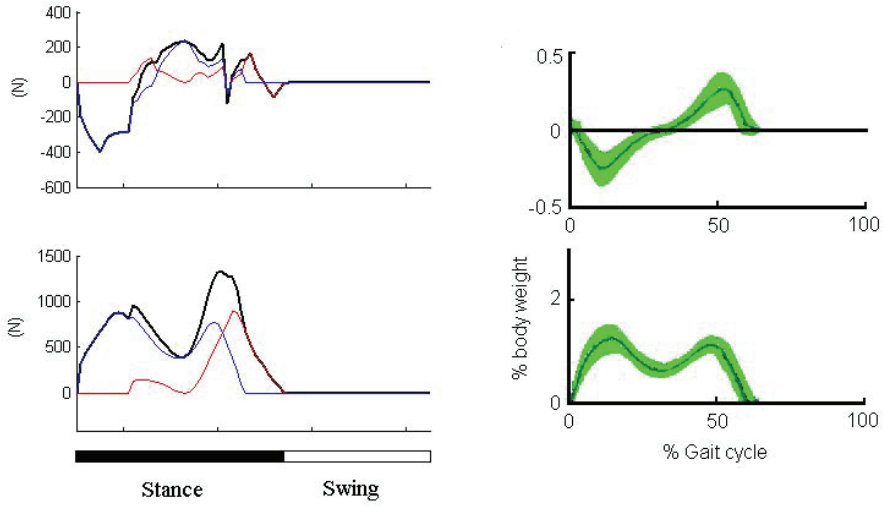

Figure 4-14: Left: simulated reaction forces on the ground in steady state, and Right: typical force profiles adapted from Neptune et al (2004). Top: horizontal reaction force, and Bottom: vertical reaction force: components of the reaction force are shown: black indicates the total force, blue force at the heel, and red force at the toe.

The patterns of muscular activation during steady state walking are shown in Figure 4-15. Examining first the physiological data from Ivanenko et al (2006, 2004), activation of GM, VA, and RF corresponds to the LOA control epoch. Activity of

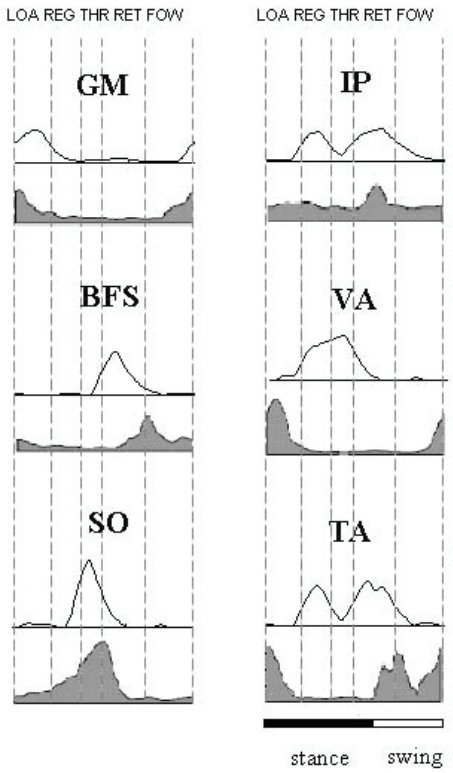

Figure 4-15: Simulated (upper trace) and observed EMG patterns (bottom filled gray) during a gait cycle arranged anatomically. Data is adapted from Ivanenko et al 2006.

SO and GC occur most strongly during the THR epoch, while that in IP and to some extent RF occur during RET, just before or during the onset of forward leg swing. BFS, TA and BFL operate during retraction and forward swing to prevent the swinging foot from touching the ground.

The activities of GM, BFS and SO are best predicted by the model. Except for minor phase shifts the waveforms are quite similar in simulation and data. IP and GC are also fairly similar. However in these muscles, the model predicts, unrealistically, activation roughly during the REG control epoch. In experimental data, there is little muscular activity during this period in any muscle. GM, BFS, SO and IP are mono-articular muscles and appear to be responsible for the bulk of the basic leg motion during walking and apparently account for much of the functional realism of the SBBW model. Biarticular muscles BFL and VA responsible for flexing and extending the knee, and uniarticular muscle TA which is responsible for lifting the foot to provide ground clearance, are least well predicted. The former are redundant from a control perspective and therefore may be inherently less predictable. The TA in vivo appears to stay active during the FOW control epoch while in simulation this was not necessary to afford ground clearance.

Principal component analysis (PCA) was applied to total 18 simulated muscle commands act. Four principal components (PC1 - PC4, Figure 4-16) captured over 98% (52.2%, 36%, 5.6%, 5.1% respectively) of the variance in the signals. These components resemble major factor waveforms derived from published muscle activity data during human walking (Ivanenko et al 2004; Davis and Vaughan 1993; Olree and Vaughan 1995). PC1 is comparable with FACTOR 1 in Ivanenko et al 2004, and PC2 with FACTOR 2, PC3 with FACTOR 3, and PC4 with a combination of FACTOR 1 and 5 and negative FACTOR 4. Olree and Vaughan (1995) also retained four major factors and one of them included a combination of FACTOR 4 and 5. According to Olree and Vaughan (1995), it was inferred that FACTOR 1 presents propulsion, and FACTOR 2 loading or weight acceptance, and suggested

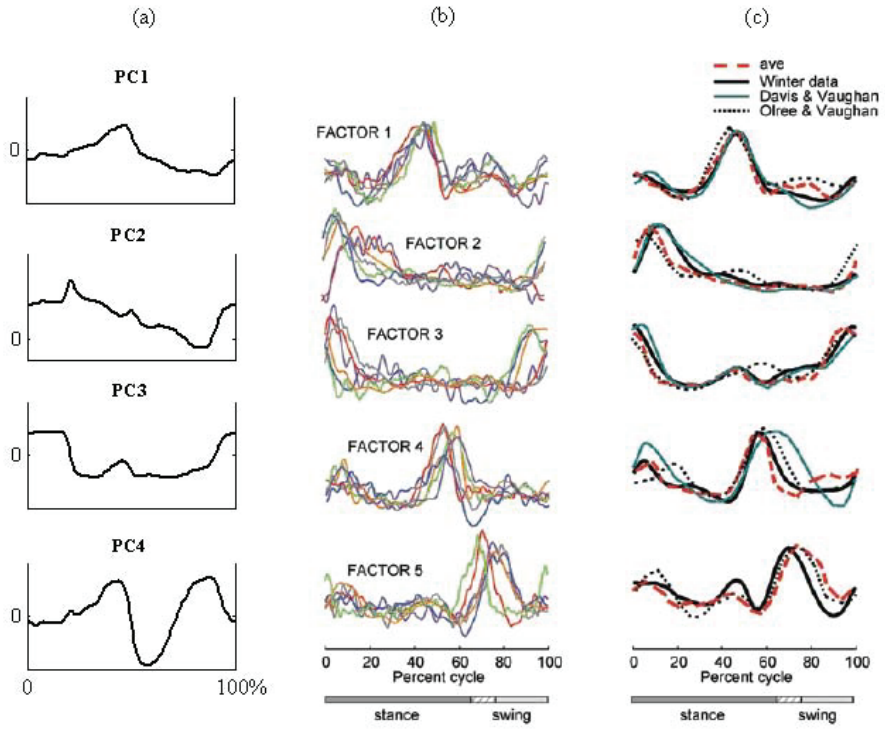

Figure 4-16: (a) Principal components of simulated EMG patterns in a gait cycle. (b) and (c) Factors summarized from human EMG data: (b) Several individual subjects from Ivanenko et al 2004 (b). (c) Comparison of principal factors from other studies (Winter 1991; Davis and Vaughan 1993; Olree and Vaughan 1995).

that FACTOR 1 and 3 were in fact the same as FACTORS 2 and 4, phase shifted by 50% of a step cycle so that there are only three basic factors. They referred to FACTOR 5 as the coordinating factor because it maintained the phase shift between the left and right sides. Temporarily, FACTOR 4 corresponds to retraction of the leg. Presumably, this closely predicts the timing of loading of the opposite leg and thus may be involved in inter-limb coordination. These results indicate that despite the SBBW model's somewhat unrealistic activity during the REG control epoch, it captures overall EMG activity fairly well. It is then also interesting that some of Ivanenko's subjects displayed EMG activity in REG (red and blue traces in FACTOR 2, Figure 4-16, column (b)).

4.4.4 Control of walking speed

Several parameters affect walking speed. Increase in the frequency f_{PG} and magnitude m_{PG} of neural pattern generator signal causes faster walking. Control during the REG and THR epochs is responsible. Enhancement of IP, VA and TA, via muscle activation components IP-1, VA-1 and especially TA-1 (Figure 4-4), the dorsiflexor action are found to be potent. These help move the COM forward during stance. Figure 4-17(a) shows the range of steady state walking speeds from 0.33 to 1.53 m/s by adjusting only parameters f_{PG} and m_{PG} with several intensities of TA-1. Smaller pulse TA-1 causes lower speed. Interestingly, the model walks most easily either within the speed range 0.5 - 0.8 m/s or 0.9 - 1.6 m/s, not especially well in between. At $f_{PG} = 0.8$, and $m_{PG} = 0.9$ without component TA-1, kinematics do not converge to a limit cycle, though the model also does not fall (* in Figure 4-17(a)). Its average walking speed is 0.55m/s. The body wobbles forward and backward. At steady state walking speed of 0.33 m/s, the heel rises unnaturally high with a straight leg during the forward stepping reminiscent of a wooden soldier and falls slightly backward reducing the step size.

Different walking speeds induced only by different intensities of TA-1 under the same other parameter values are demonstrated in Figure4-17(b). In 10secs, the stick

figure in top reaches less than 8m, but the one in bottom about 12m. Speed can also be increased within narrower limits by augmenting GC and SO action during the thrust epoch (component SO-1 in Figure 4-4). However, this eventually has the undesirable effect of lifting the body off of the ground. The SBBW model is not equipped to tolerate this occurrence. Presumably, however, this effect could be useful in the control of running.

Appropriately, speed is also partially controllable using the reference signal COM_{ref}. Increasing COM_{ref} causes the body to accelerate forward slightly during the REG epoch. For example, $COM_{ref} = 0.18$ with $f_{PG} = 0.8$, and $m_{PG} = 0.9$ generates steady state walking speed of 0.65m/s, while $COM_{ref} = 0.25$ with the same f_{PG} and m_{PG} yields a speed of 0.72m/s. The acceptability of increasing alone is limited, however. Unless f_{PG} and m_{PG} are changed concordantly, the model eventually falls forward.

EMG patterns are phase-invariant over walking speeds, however, in general, intensity of their activities increases as the walking speed increases (Ivanenko et al 2005; Hof et al 2002). The magnification of intensity depends on phases (Hof et al 2002). Even though this study does not rigorously investigate the effect of each EMG profile on walking speed, the function of EMG on walking speed is demonstrated by tests with pulse TA-1. A hypothetical neural mechanism of speed control in terms of pattern generator can be proposed as in Figure 4-17(c).

4.4.5 Stability to push disturbances

The application of 200msec duration forward and backward force impulses to the center of mass of the trunk-head segment were simulated at 0%, 25%, 50%, and 75% of the gait cycle. At each gait cycle fraction, the maximal force levels from which the model could recover steady state walking were determined. Figure 4-18(a), and (b) show the effects of a 70N maximal forward impulse applied at 0% phase (toe-off) and a 75N maximal backward push applied at 50% phase (mid-stance). Figure

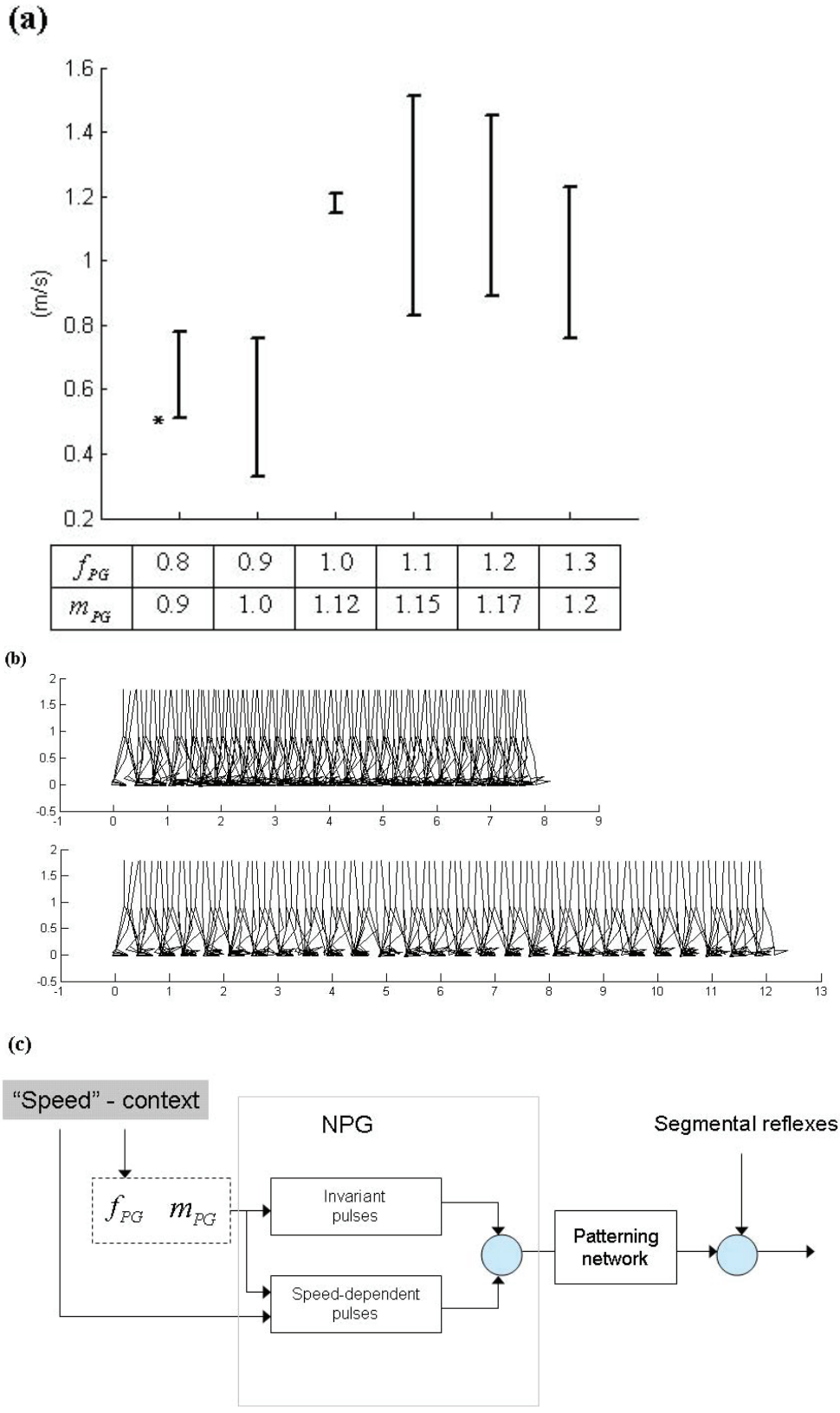

f_{PG}	0.8	0.9	1.0	1.1	1.2	1.3
m_{PG}	0.9	1.0	1.12	1.15	1.17	1.2

Figure 4-17: (a) Different steady state walking speeds: bars indicates possible steady walking speeds by changing the magnitude of pulse TA-1 with f_{PG} and m_{PG} given, (b) an example of different walking speeds and (c) hypothetical neural network to explain speed control based on the findings.

4-18(a) demonstrates forward pushes cause more distance, and backward pushes less distance to be traveled within a given time. In Figure 4-18(b) indicates that such a push disturbs primarily ankle motion (of the stance leg) transiently. The model tolerates forward disturbances slightly better than backward disturbances except at mid-stance when resistance to backward pushes is slightly better (Figure 4-18(c)). After an initial deviation, the COM motion pattern is recovered within 3 or 4 gait cycles modulo a fixed phase lag or gain (Figure 4-18(d)) that demonstrates again the absence of absolute position control shown in Figure 4-18a).

The model was also tested by changing the mass of the trunk-head segment, and, therefore, also its moment of inertia, without alteration of feedforward neural commands. Thus, this change tested the inherent viscoelastic and neural feedback mechanisms. It was found that up to a 10kg increase (18.5% of the trunk mass) could be tolerated without falling. Figure 4-19(b) shows the effect in the phase plane. It is evident that the walking speed is lower with the increase of mass. Phase plots indicate that different limit cycles result at ankle and hip.

4.4.6 Sensitivity to simulated system lesions

Figure 4-20 shows the effects of removing trans-cerebellar long-loop control of COM and trunk pitch, weakening the recurrent integrator and eliminating the peripheral modulation of synergies.

In (a), (b), and (c), the body fails to maintain a sufficient step size so as to cause the forward trip. (d) demonstrates that swing leg retraction is not fully achieved due to inappropriate large knee excursion so that toe eventually scratches the ground. That causes the forward trip again.

4.5 Preliminary conclusion

The SBBW model incorporates non-linear muscle mechanics having activation level -dependent impedance, scheduled cerebrocerebellar interaction for control of center of

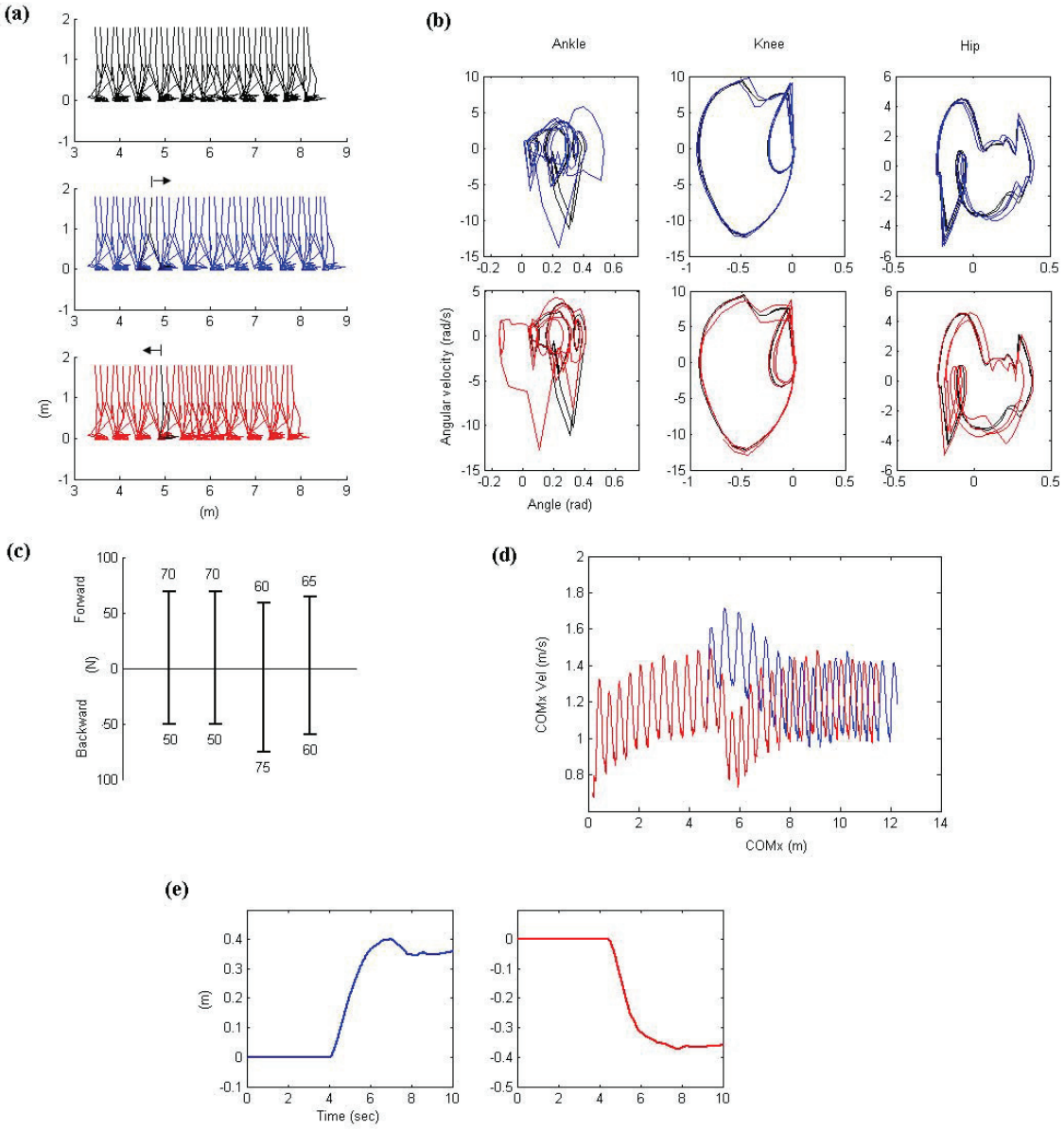

Figure 4-18: (a) Simulations of disturbed and normal walking: (top) undisturbed; (middle, blue) walking pushed forward by 70N at 0% phase, (bottom, red) walking pushed backward by 75N at 50% phase; the black figures indicate the timing of the impulse applications in duration of 20msecs (b) corresponding phase plane plots of ankle, knee, and hip of left leg. (bottom) Walking pushed backward by 75N at 50% phase, disturbed walking (red) vs. normal walking (black), (left leg only), (c) maximal tolerated forces at each phase, (d) Phase plane plot for COM with disturbed walking: Response to 70N forward impulse at 0% phase (blue), 75N backward impulse at 50% phase (red).(e) Trajectory of COM deviation between disturbed and normal walking, (left): walking pushed forward by 200msec, 70N pulse at 0% phase - normal walking, and (right): walking pushed backward by 75N at 50% phase - normal walking.

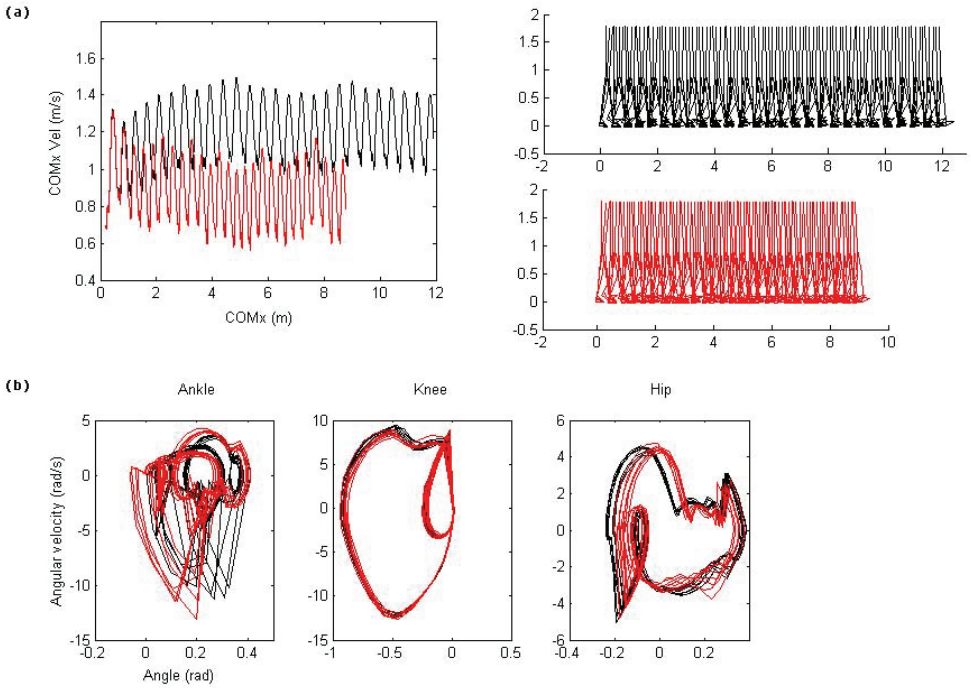

Figure 4-19: Simulations of normal and increased trunk mass walking: (a) COM patterns (forward COM position vs its velocity), (b) phase plots of ankle, knee, and hip from left to right (left leg only); nominal walking pattern (black), increased trunk mass (red).

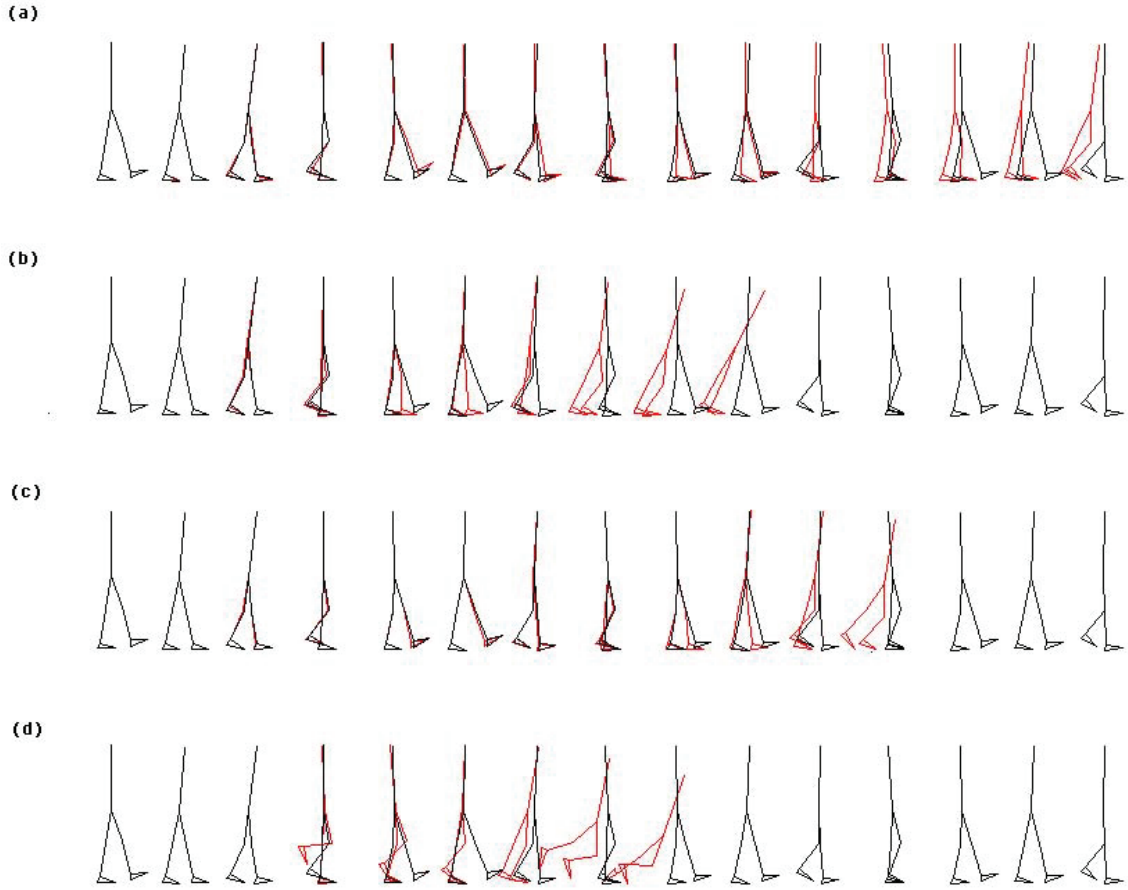

Figure 4-20: Stick plots (red) of (a) no trans-cerebellar long-loop control of COM, (b) weakened trans-cerebellar long-loop control of trunk pitch, and (c) weakened recurrent integrator; (d) eliminated segmental reflex in comparison with normal walking (black). Each motion is sampled every 100msec, but is horizontally relocated for clarity. Thick blue line indicates the ankle trajectory, the dotted green the knee, and the thin red the hip.

mass position and trunk pitch angle, scaled rectangular pulse-like feedforward commands from a brainstem/spinal pattern generator, and segmental reflex modulation of muscular synergies to refine inter-joint coordination. When undisturbed, the model can stand, though only with enhanced muscular coactivation at the ankle. When initiation trigger activates, the model can transition from standstill to walking at 1.5 m/s. Simulated natural walking displays none of seven sagittal plane pathological gait features. And simulated neural lesions result in several features of pathological gait. The walking is stable to modest pushes in the forward and backward directions at most up to 70 and 75 N, respectively, and to sudden changes in trunk mass up to 18.5%. The model shows that control of basic human-like walking can be achieved using stabilized-long loop feedback, and rudimentary, hierarchical feedforward, synergy-mediated control. In particular, internal models of body dynamics are not required. The reproduction of basic clinical gait deficits supports the model's proposed functional-anatomical correspondences.

The SBBW model attempts to account for the primary kinematic, dynamic and physiological features of peripheral and central human locomotor control with a formulation that is simple in structure and control principles. This is approach is motivated by the assumption that nature may often prefer simple, robust solutions to motor control problems. The work continues along the lines of Taga (1995) and Ogihara and Yamazaki (2001), and provides more detail regarding possible neural control mechanisms and more extensive evaluation of the stability and performance characteristics that result. Specifically, it is demonstrated that when balance is stabilized by long-loop stretch responses, stable walking with many realistic features can be afforded by a five state central pattern generator that distributes activation to muscles organized in four synergies. Model walking demonstrates natural convergence to a consistent steady-state gait pattern over a fair range of movement speeds and simultaneously displays significant resistance to pushes and weight changes. The simulated muscle activation patterns share important similarities to experimental observations, but also show differences that remain to be reconciled. Successful walking

is demonstrated to depend on the intactness of most components of the control system suggesting that the model is of fairly minimal complexity. Importantly, there is no apparent requirement for internal models of body dynamics, detailed programming of joint motions or computations based on sensed or estimated force. Also, it appears that muscle synergies, together with composite signal feedback, can enable multi-joint feedback control to be implemented by simple Single-Input Single-Output (SISO) modules. The proposed control is argued to be broadly consistent with cerebrocerebellar, and spinal/brainstem systems.

Chapter 5

Extended walking model with voluntary modulation (eSBBW model)

In previous chapter, the alpha motor neuronal output u_α is represented as follows.

$$u_\alpha(t) = u_{desc}(t - T_{pr}) + u_{sp}(t - T_{pr}) + u_{reflex}(t - T_{pr}) \tag{5.1}$$

This implies that muscular activation is determined by a simple linear combination of the signals on the right hand side. A major feature of SBBW model is that body control is divided between command channels significantly decoupled within the hierarchical neural structure even though the command effects are not perfectly separate. The spinal pattern generator provides the primary control of gait motion while the supraspinal system exerts major control over postural regulation (Figure 5-1). Spinal segmental reflex at the level of spinal cord helps modulate interlimb movement. In the SBBW model, The cerebrocerebellar system controls two substantially independent variables, i.e., the relative location of COM with respect to foot position and truncal verticality. The cerebrocerebellar channel that controls the location of COM exerts its greatest effect at the ankle. Control of truncal verticality is accomplished primarily at the hip. A change in trunk angle does affect COM position, but only weakly

relative to that in ankle angle. When the body responses to environment or elicit a new behavior, the effectively decoupled control makes it possible to provide a strategy of motion variation without the overall complicated computation of the behavior. The chapter will demonstrate computationally the scheme's potential. The chapter proposes that a linear superposition is a simple realization of such scheme. If this is true, this will be quite powerful in terms of behavioral modification or adaptation.

One of questions that can be raised in the previous chapter is about how voluntary modifications of nominal gait can be implemented by supraspinal control during normal walking. This chapter tries to answer the question at least by demonstrating that given the SBBW architecture, some tasks could be controlled by superposition of simple feedforward signals and arguing its possible mechanism. Given that nominal walking motion is implemented by a motor program in CNS, it is hypothesized that the execution of behavior requires no complicated programming such as mode-based estimation when voluntary modulation is presented but temporal and not seriously possessed over gaits. In this chapter, kicking and obstacle avoidance during walking are selected as test examples.

With no perturbation, a sequence of pulse activations in NPG are distributed to muscles via a neural network so as to generate normal walking patterns. suprasegmental and spinal segmental feedback systems help the stable maintenance of walking patterns (see Chapter 4). The neural networks in a fully trained person is expected to reserve the principal pulse patterns for locomotion and have no difficult in generation of nominal walking. Once if any context intends to modify kinematic or kinetic patterns corresponding to voluntary modulation, e.g., further excursion of a swing leg to step over an obstacle on the ground during locomotion, CNS may generate additional neural signals which were not activated during nominal walking. The new neural signals will affect some specific muscular activations so as to produce appropriate kinematic or kinetic patterns. A possible representation of the new signal activation could be additional simple new pulse-like commands as did in the spinal pattern

generator.

Ivanenko et al 2006 analyzed voluntary modulations of nominal gait using the principal component analysis and found that their muscular activations can be decomposed. In comparison with nominal walking, voluntary modulation included an additional principal factor in EMG waveforms, and similar other factors. Even though the investigation does not prove the plausibility of an additional pulse-like command in CNS, the command scheme would be hypothetically attractive because of its simplicity. Moreover, the scheme conserves the property of superposition. This modification implies no change of the principle of the model mechanism at all. The primary functional performance of each neural system still remains consistent.

This chapter does not intend to verify the proposed scheme yet due to lack of knowledge, but demonstrate that it may be consistent with human behaviors.

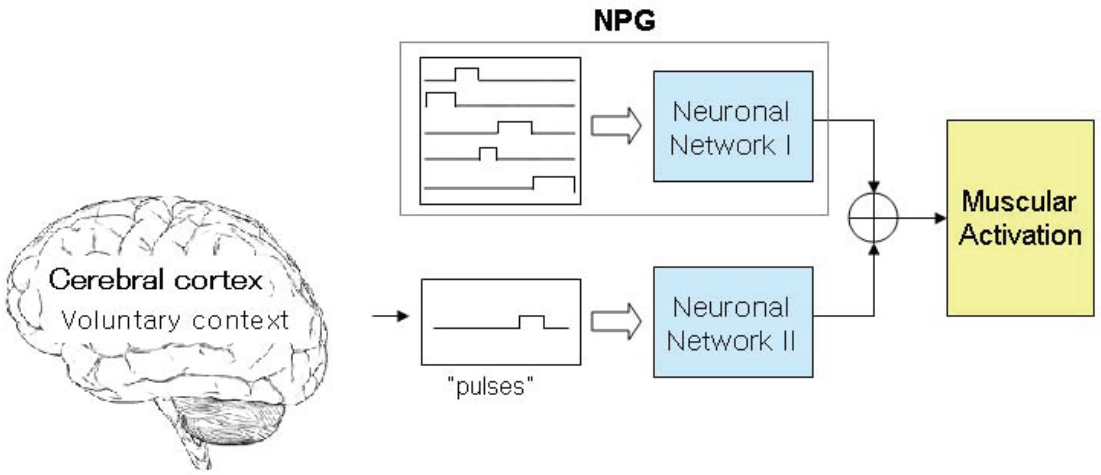

Figure 5-1: Superposition scheme: other neural systems are omitted.

5.1 Model

5.1.1 Spinal pattern generator

The SBBW model demonstrated normal kinematic and neuromuscular features during steady state walking (chapter 4). The normal walking patterns are implemented by a set of spinal pattern pulses. It was proposed that the spinal pulse activations were pretty much invariant (or stereotyped) over the range of walking speeds. The spinal cord pattern generator in SBBW model is extended here to have five nonzero states instead of four. It is called the extended SBBW (eSBBW) model. This allows for active rather than passive control of the swing leg. It is consistent with the appearance of EMG activity during swing in human datasets (Ivanenko et al 2005). The eSBBW model structure is the same as in the SBBW model except the modification of the spinal pulse states. In comparison with Equation 4.17 and Figure 4-4, a new pulse is introduced as follows.

A periodic pulse activation can be modeled in the form of:

$$\begin{aligned} &u_{PG,i}(t) = m_{PG} \cdot 1\left[\cos(2\pi f_{PG} t - \phi_i) - h_i\right]_+ , \mathrm{i} = 1,2,3,4 \\ &\text{and} \\ &u_{PG,5}(t) = m_{PG} \cdot 1[1 - u_{PG,1}(t) - u_{PG,2}(t) - u_{PG,3}(t) - u_{PG,4}(t)]_+ \end{aligned} \tag{5.2}$$

where $u_{PG,5}(t)$ is the new fifth pulse (see Figure 5-2).

5.2 Model evaluation

The voluntary perturbation of normal walking is tested with the eSBBW model: stepping over an obstacle, and kicking a ball during walking. These voluntary tasks are chosen because the tasks have been experimentally observed (Ivanenko et al 2005). In addition, a different style of walking, i.e., walking with trunk bent forward, is tested. The bent walking is also experimentally observed (Grasso et al 2000). These test examples are to evaluate the usefulness of substantial decoupling between neural

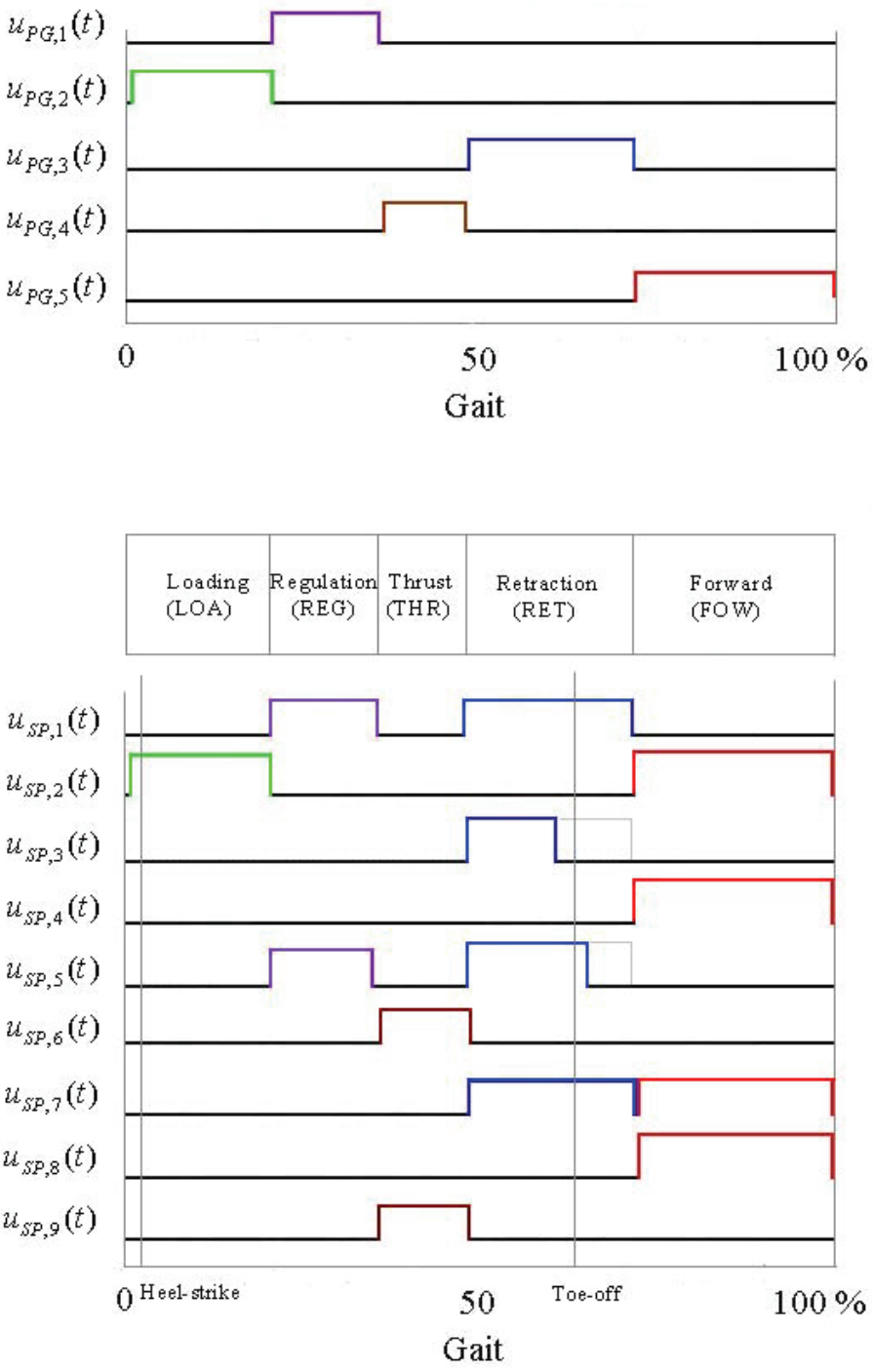

Figure 5-2: Decomposed spino-locomotor signals and a model of the neural network. Neural signals from the pattern generator (top), and neural signals to muscles (bottom).

systems, and that of superpositional neural network.

During the simulations, all model parameters were held fixed unless explicitly stated otherwise. No optimization of performance is intended because this investigation goals the potential explanation of the principles behind the system and its performance not accurate manipulation of performance. In fact, it is not yet confirmed whether human walking is according to a specific optimization criterion even though energy cost is popularly chosen for studies of human walking (Anderson and Pandy 1992).

5.3 Results

5.3.1 Generation of normal walking pattern

Kinematic pattern

The eSBBW model generates normal human-like walking motion at natural speed (detailed model parameters in Appendix A.3). After an initial transient response, body kinematics converges closely to a consistent normal walking pattern. Figure 5-3 shows walking at a typical human speed of about 1.15 m/s, that is simulated with $f_{PG} = 1.3$ and $m_{PG} = 1.2$. Figure 5-4 verifies its kinematic performance.

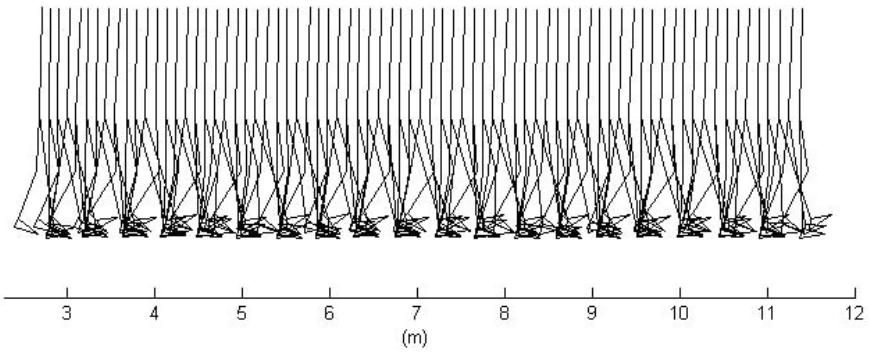

Figure 5-3: Steady state walking: stick plot is sampled every 10msec.

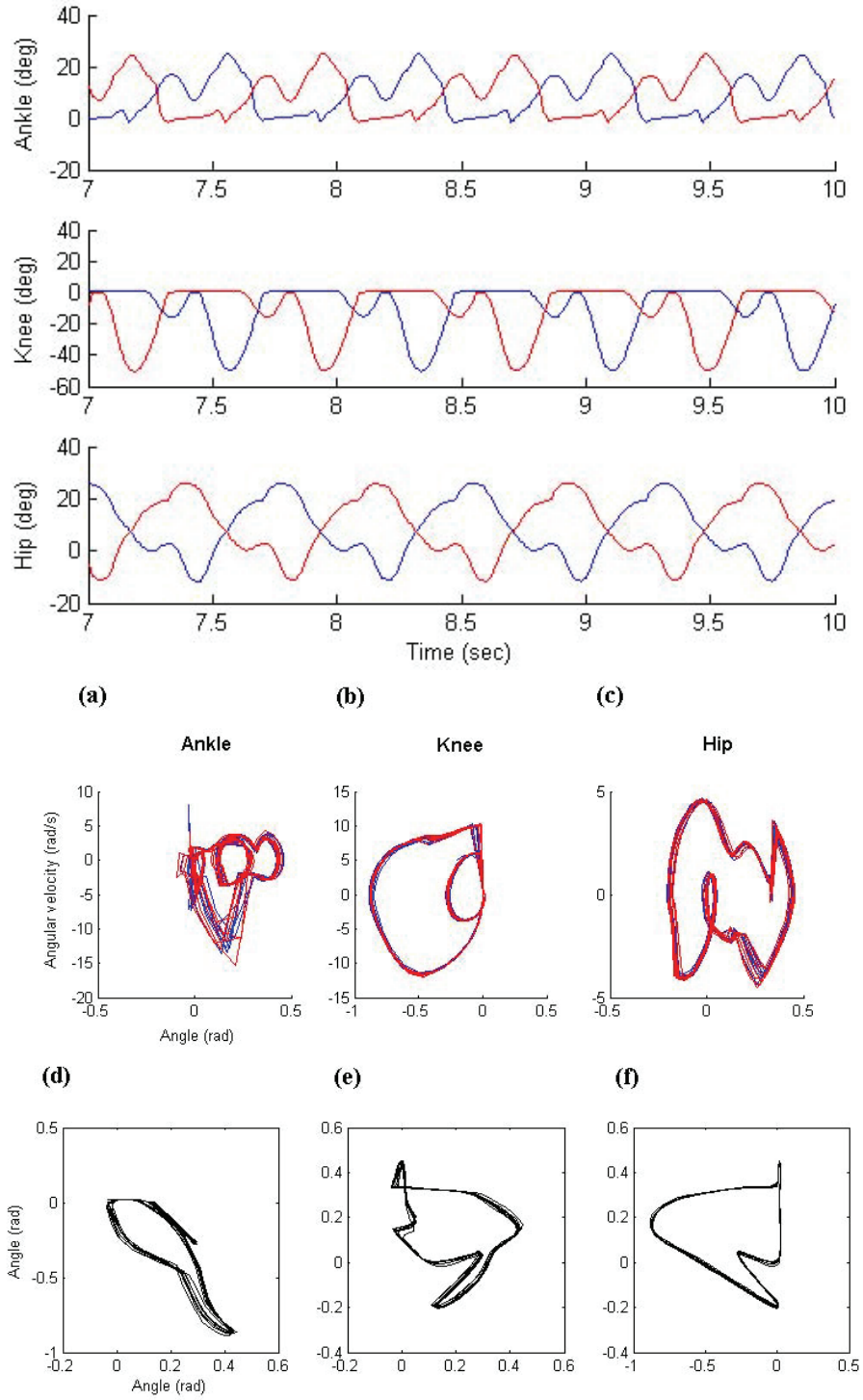

Figure 5-4: Steady state walking kinematics. Simulated time courses of hip, knee and ankle joints (top). Red line indicates joints in right leg, and blue in left leg. Joint phase-plane behavior: (a) ankle, (b) knee, and (c) hip (middle). Joint coordination plots: (d) ankle vs. knee, (e) ankle vs. hip, and (f) knee vs. hip (bottom).

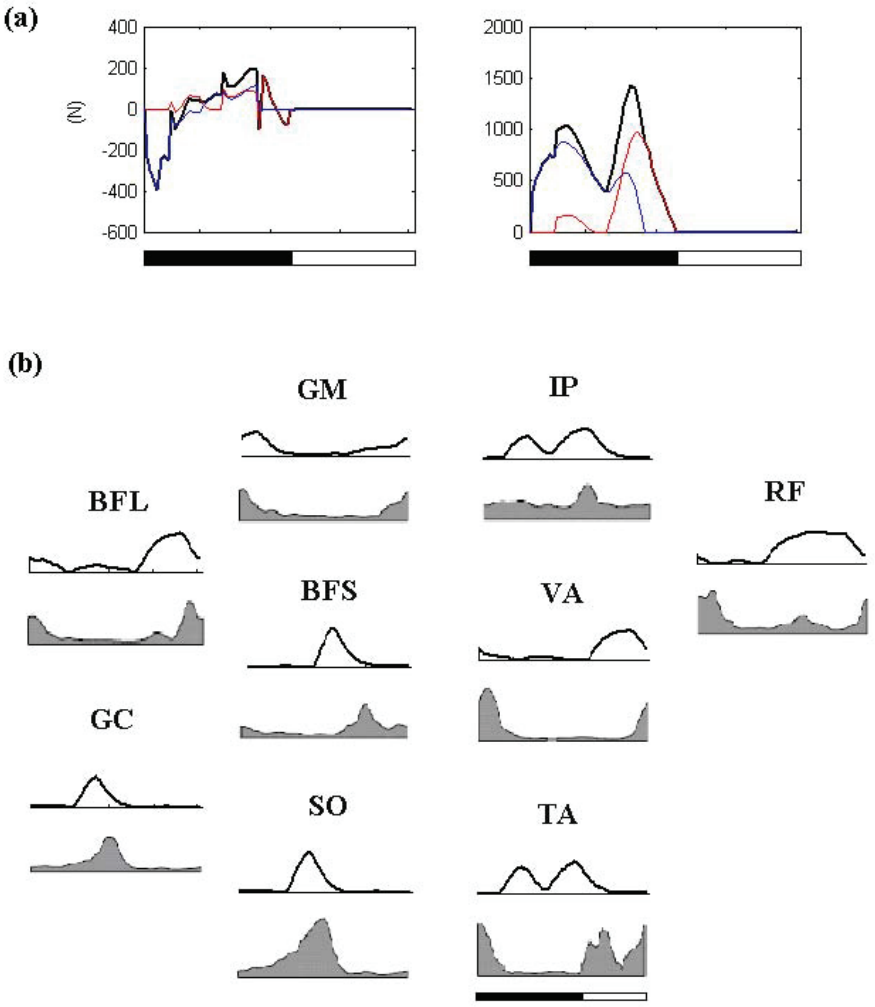

Figure 5-5: (a) Simulated reaction force profiles, (b) simulated (upper trace) and observed EMG patterns (bottom filled gray) during a gait cycle. Data is from Ivanenko et al 2005.

Reaction force and muscular activation

With specific optimization, the pulse epochs in spinal pattern generator are determined to achieve stable normal walking patterns. Then, the simulated EMG (muscle command act) is compared with real data from Ivanenko et al 2005 (Figure 5-5(b)). Activations of GM, GC, BFS, BFL and SO are reasonably close to real data, and activations of IP, TA, RF either include extra pulse or phase shift. Empirically the difference could not be avoided to simulate normal walking patterns. This may implicate some discrepancy between the model and real humans. Lateral pelvic tilt is strongly suspicious to be the reason. The model describes sagittal motion not lateral motion whose amplitude is actually about 5cm in real humans (Inman 1981). The side-to-side movement locates COM near the midline at heel strike and over the supporting leg during stance phase. This results in adduction of the leg during stance, and abduction of the leg during swing. Therefore, the model may require extra activation to have the same effect as lateral motion does. At transition from swing to stance, simulated activations of VA, RF trigger early to move an upper body forward to strike heel on time. During midstance, IP and TA have extra pulse to move the upper body forward to obtain a right posture for swing.

On the whole, the simulated EMG patterns have been more likely in comparison with those of SBBW model in chapter 4.

Factor analysis

Factor analysis is useful to evaluate the functional plausibility of the neuromuscular dynamics by comparison with real data. Many studies extracted principal pattern components that account for most of the variance of real EMG over all recorded muscles during walking (Davis and Vaughan 1993; Orlee and Vaughan 1995); Ivanenko et al 2004, 2005). They used Principal Component Analysis (PCA) with several steps of calculation of the correlation matrix, extraction of the initial principal components, application of the varimax rotation, calculation of factors scores, and factor coefficients (Ivanenko et al 2004; Ivanenko et al 2005). The same statistical method is

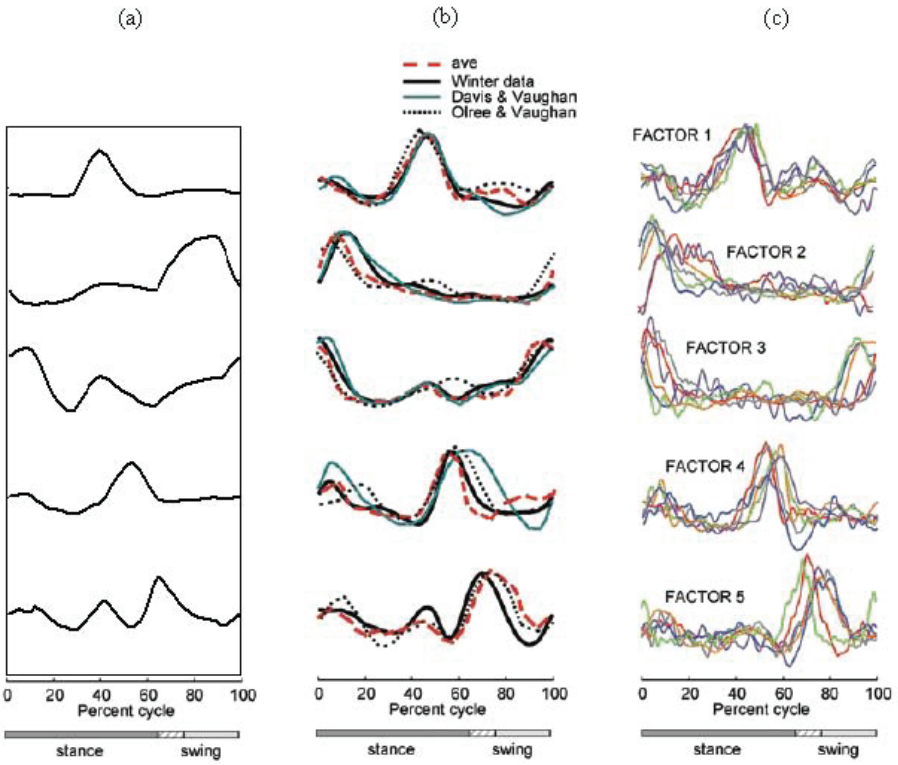

Figure 5-6: (a) Principal components of simulated EMG patterns in a gait cycle. Factors extracted from human EMG data: (b) comparison of principal factors from various published data (Winter 1991; Davis and Vaughan 1993; Orlee and Vaughan 1995), (c) principal factors form several individual subjects from Ivanenko et al 2004. (b) and (c) are adapted from Ivanenko et al 2004.

applied to the simulated EMGs, and finds the five principal patterns as in Figure R4(a). The result is compared with other published real data. It is shown that 4 factors among overall 5 are very consistent with those from real data. FACTOR 2 in Figure R4 is most different. Phase of FACTOR 2 in simulation is shifted even though its waveform is similar. The pulse peaks rather during swing not after heel-strike. The phase difference would be explained by the same reason as discussed in EMG pattern analysis. Even though there is somewhat discrepancy, overall principal factors seem to capture fairly well realistic functional dynamics. This may indirectly verify the neural systematic scheme of pattern generation.

5.3.2 Generation of walking patterns with voluntary modulation

An additional pulse activation $u_p(t)$ passes through neural network W_v to be $\mathrm{u}_v(t) = \mathrm{W}_V u_p(t)$. Then it is superposed to neural pattern generator network to implement behavior response to voluntary perturbation as follows.

$$\mathrm{u'}_\alpha(t) = \mathrm{u}_\alpha(t) + \mathrm{u}_v(\mathrm{t}-\mathrm{T}_{pr}) = \mathrm{u}_{desc}(\mathrm{t}-\mathrm{T}_{pr}) + \mathrm{u}_{reflex}(\mathrm{t}-\mathrm{T}_{pr}) + \mathrm{u}_{sp}(\mathrm{t}-\mathrm{T}_{pr}) + \mathrm{u}_v(\mathrm{t}-\mathrm{T}_{pr}) \tag{5.3}$$

It is notified that the overall activation from NPG and the additional pulse is still under the effect of the segmental spinal reflex (Equation 4.19). If a joint angle is over its threshold value, the activation is suppressed.

Kicking motion during walking

The eSBBW model is used to simulate a kicking task. A human walks at natural speed and kick with the right leg a stationary ball in the locomotion path. The force of the kick is fixed to be 90N according to experimental data (Ivanenko et al 2005), and the force is decomposed into horizontal and vertical as follows.

$F_x = -90\cos(30°), F_y = -90\sin(30°)$.

For simulation, the force is applied on the right foot at instant of kicking for 0.4msecs. An additional pulse of the voluntary activation for kicking is applied before the ball during swing phase (Figure 5-7(a)). To compensate for the impact of the kick and maintain stable posture, the pulse is distributed over the muscles in both legs.

For the right (swing) leg, $\mathrm{W}_V = \begin{bmatrix} 0.2 & 0 & 0 & 0 & 0.2 & 0 & 0 & 0 & 0 \end{bmatrix}^T$,

For the left (stance) leg, $\mathrm{W}_V = \begin{bmatrix} 0 & 0 & 0.4 & 0 & 0 & 0 & 0 & 0 & 0 \end{bmatrix}^T$.

Stepping over an obstacle during walking

As in Ivanenko et al 2005, the simulation describes that a human walks at natural speed and steps over an obstacle with the right leg. A new pulse of the voluntary activation for stepping is applied at the timing of swing just in front of an obstacle (Figure 5-7(b)). The pulse activation is transferred to each muscle via weight distribution. Joint angles of swing leg should have large excursions to lift up the foot over the obstacle while stance leg supports the whole body robustly and moves the swing leg quickly to the ground. Therefore, it is designed that the pulse activation affects on muscles in both legs.

For the right (swing) leg, $\mathrm{W}_V = \begin{bmatrix} 0.7 & 0 & 0.55 & 0 & 0.3 & 0 & 0 & 0 & 0 \end{bmatrix}^T$.

For the left (stance) leg, $\mathrm{W}_V = \begin{bmatrix} 0.2 & 0 & 0 & 0 & 0.3 & 0 & 0 & 0 & 0 \end{bmatrix}^T$.

In addition, the value of $\theta_{th,jo}$ in Equation 4.19 is temporally adjusted to allow large excursion of joint angles in swing leg. $\theta_{th,jo}$ is the descending tonic excitation which includes the command from supraspinal control. The cerebrum presumably regulates joint excursion by the descending signal. Therefore, $\theta_{th,jo}$ conveys a new value only for joints in swing leg during the voluntary behavior and recovers the old for normal walking.

$$\theta_{th,jo} = \begin{cases} 0.35 : jo = a, \\ -0.35 : jo = k, \\ 0.55 : jo = h \end{cases} \text{ for normal walking,}$$

$$\theta_{th,jo} = \begin{cases} 0.35{:}jo = a, \\ -0.65{:}jo = k, \\ 0.55{:}jo = h \end{cases} \quad \text{only while the voluntary pulse } u_p(t) \text{ activates.}$$

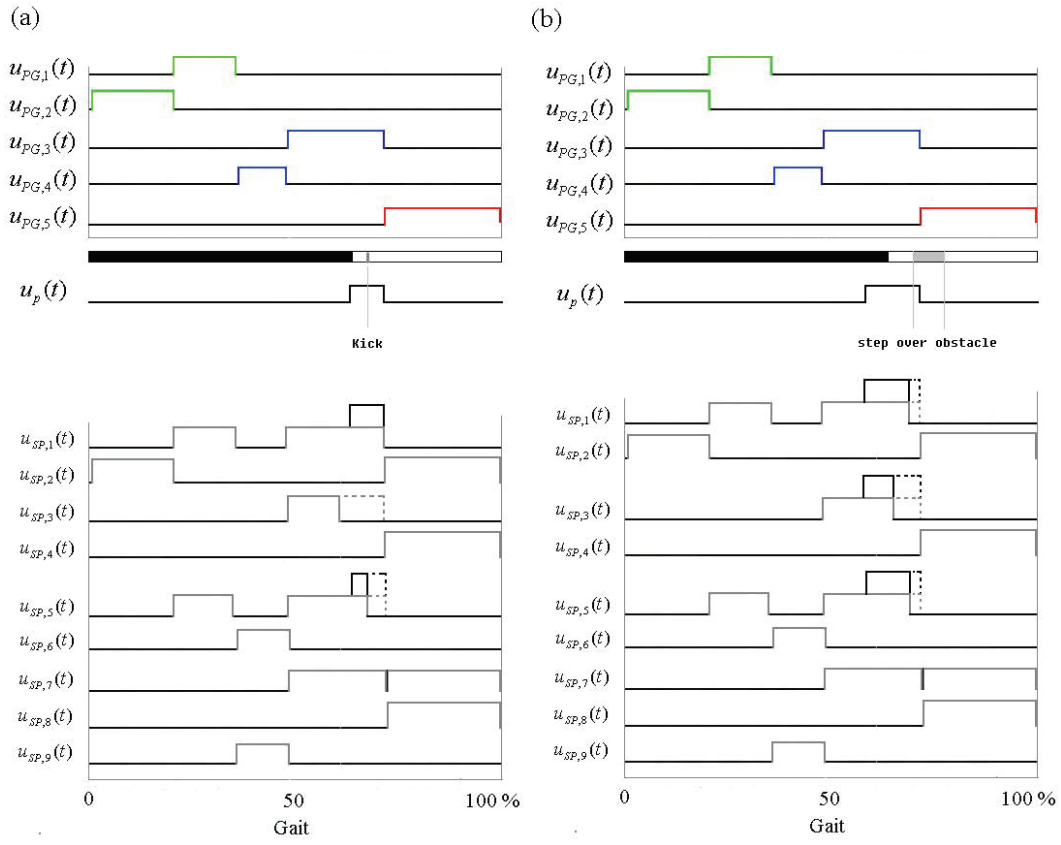

Figure 5-7: Decomposed synergetic signals: neural signals from the pattern generator plus an additional voluntary signal (top), spinally generated commands to muscles in right leg (bottom) for kicking a ball (a), and stepping over an obstacle (b).

Voluntary perturbations are applied after the model achieves closely steady walking patterns. The extra force reaction of the kick can affect on kinematic pattern. However, it experimentally turns out that the kinematic patterns of the kick are nearly identical to those of normal walking in the given situation (Ivanenko et al 2005). Figure 5-8 demonstrates that simulation abides it. Phase plane shows clearly deviation during kick motion from normal walking patterns. The deviation is not much. Instead, kinetic patterns are different to compensate for the impact of the kick. When a human steps over an obstacle in pathway, the kinematics are obviously

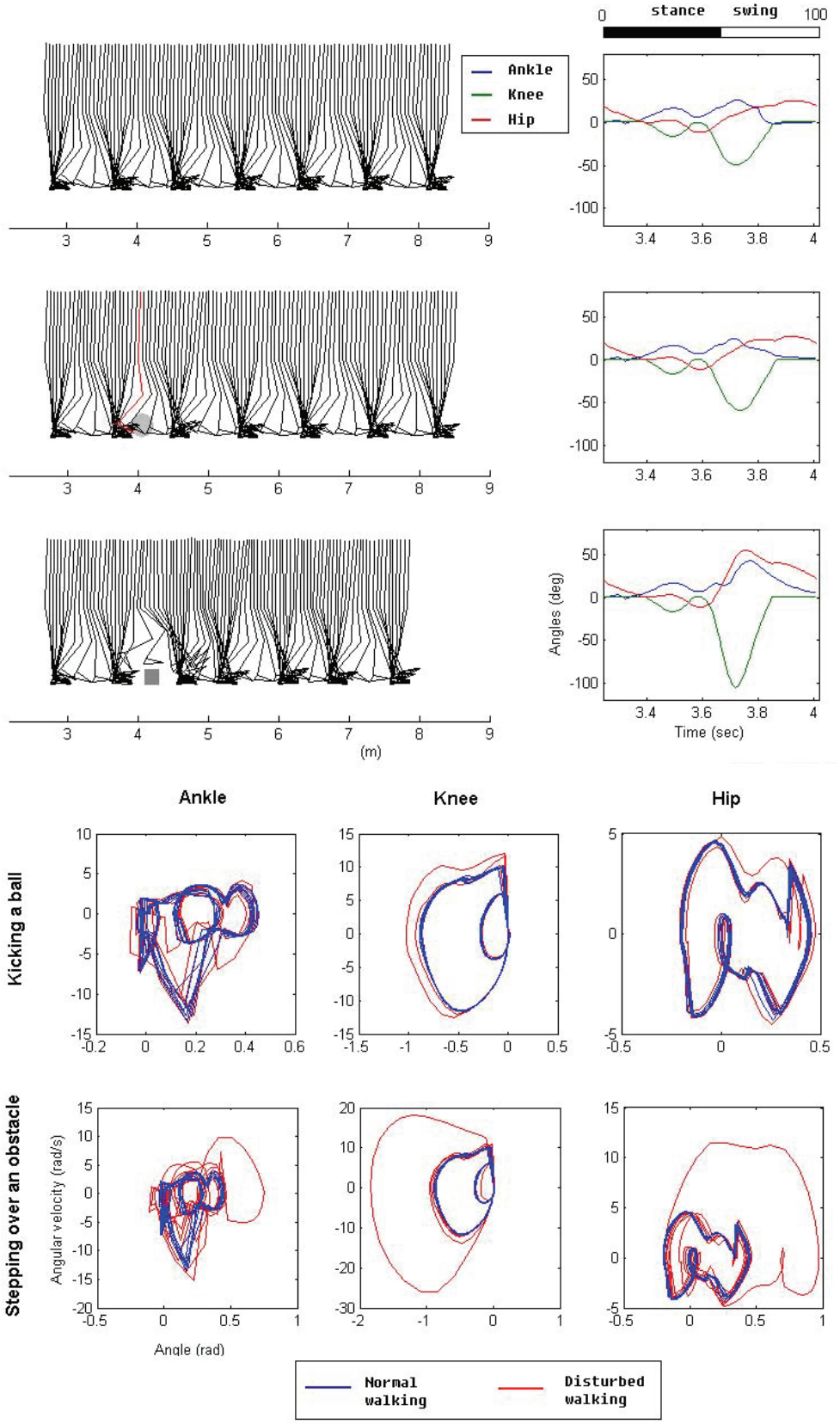

Figure 5-8: Stick plots of kinematics (right leg only for clarity)(top: left): the motion is sampled every 50msec. Joint trajectories during voluntary perturbation (top: right). Blue: ankle, green: knee, and red: hip. Bar indicates gait phase (black: stance, white: swing). Phase planes in comparison with normal walking pattern (bottom).

quite modified from those of normal walking. The knee and hip angles excurse largely to shorten the length of lower limb in swing phase (Figure 5-8).

5.3.3 Walking with trunk bent forward

Kinematic pattern

To implement simulation of the forward bent locomotion, The values of two components in model are changed: $\theta_{tr,ref}$ and some elements in W_{PG} . The change of the value of $\theta_{tr,ref}$ is intuitively fine because the parameter presents the desired position of trunk. To walk with bent trunk, cerebral cortex has presumably to command a bent desired position of trunk. The change of some element values in W_{PG} is controvertible. One potential explanation is that there exits a set of spinal pattern generation network for the bent locomotion. The other possible one is a limited set of pulse activations is superimposed on the spinal pattern generation network for the normal locomotion. The second scheme seems more interesting because it can be thought as an extension version of tasks in previous section: a set (network) of voluntary pulse-like commands activates instead of only an additional command. Further investigation will be required to find whether the hypothesis is correct or any other neural process takes place. The parameter values and rough initial positional conditions are summarized in Appendix A.3.3.

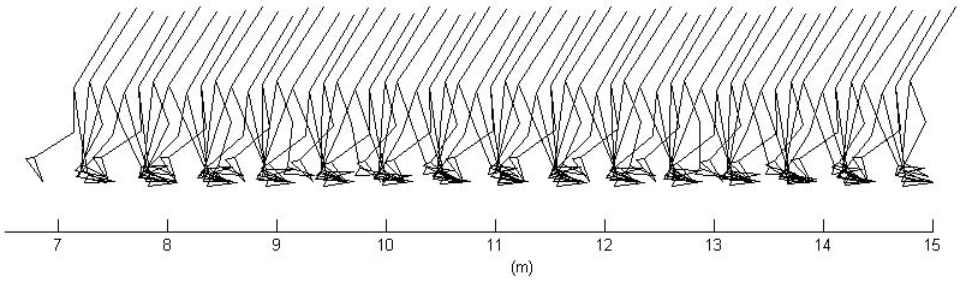

Figure 5-9: Stick plot of bent locomotion.

After some steps, walking converges to a steady motion as in Figure 5-9 and Figure 5-10. When human walks with trunk bent forward, body's COM locates at front in comparison with that of normal walking. Therefore, its location is closer to the front boundary of feasible stable support area, which means that a body would fall forward when stable posture is lost. To prevent the forward falling, hip tends to locates backward compared with its position in normal walking. The hip location helps keep COM within stable support area. The bent locomotion requires much more energy consumption (Grasso et al 2000).

With W_{PG} fixed as in equation, the different values of $\theta_{tr,ref}$ are used for simulation. This test is to see how robust the spinal pattern generation network is corresponding to the context of bent posture in cerebral cortex according to eSBBW model. Stable steady state walking is enabled with $\theta_{tr,ref}$ between 0.6 and 0.8. Figure 5-11 shows trunk pitch angle trajectories, and demonstrates there is about 10 degrees between maximum and minimum.

Reaction force and muscular activation

As mentioned earlier, no optimization is performed to achieve performance. Therefore, the best match with real data is not expected, but the comparison with real data helps understand the performance of the mechanism. The reaction force and EMG profiles provides useful information. Roughly speaking, planarflexor and dorsiflexor around the ankle are not quite consistent with real data . However, several close EMG profiles demonstrate the plausibility (Figure 5-12). In comparison with normal walking, bent walking simulation is less realistic in terms of EMG. It may imply that bent walking is more complicated dynamically. With no intention of optimization, it is impressive that the eSBBW model can implement the bent walking from the normal walking by a simple tuning of two parameters.

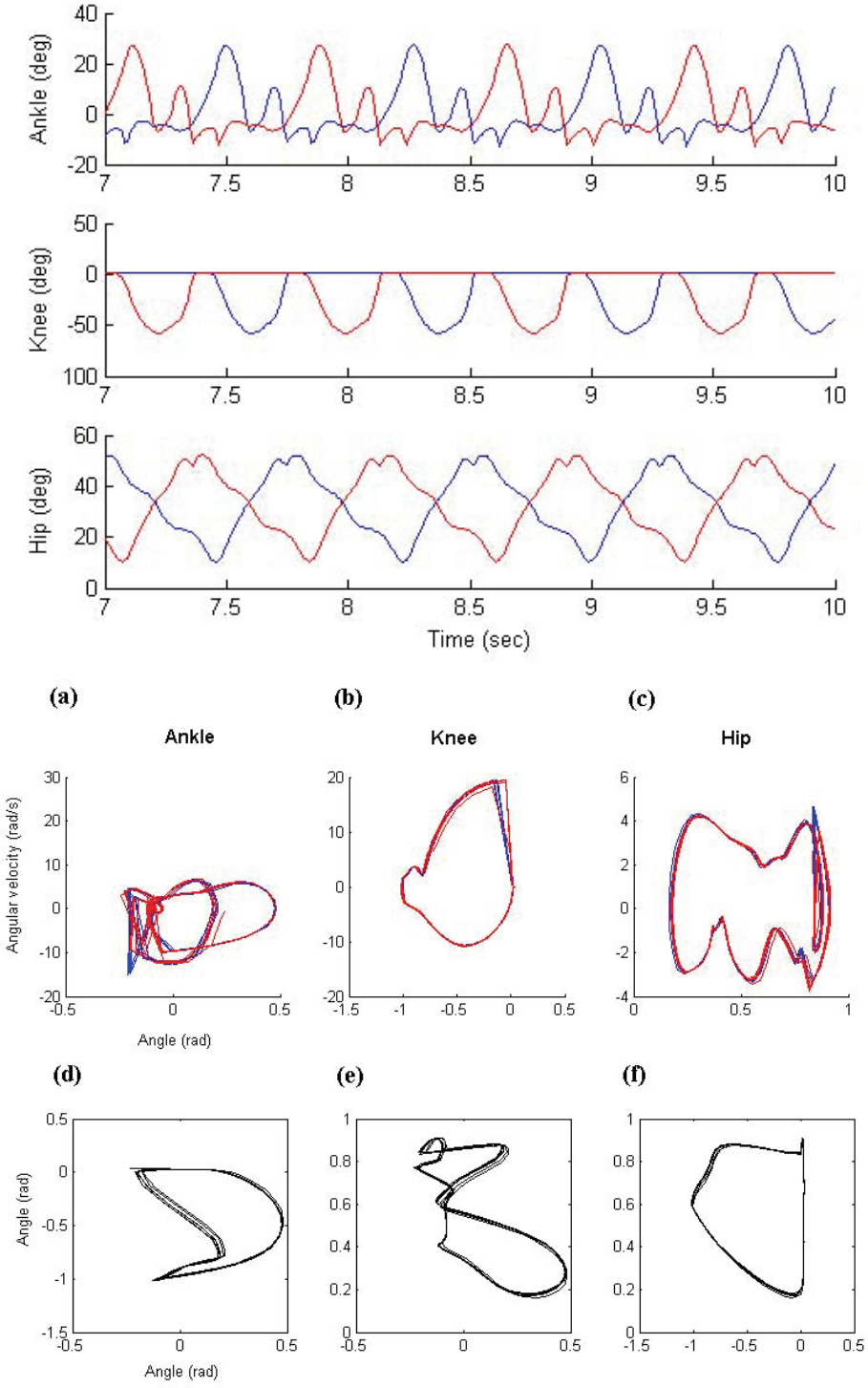

Figure 5-10: Steady state kinematics of the bent walking: simulated time courses of hip, knee and ankle joints (top). Red line indicates joints in right leg, and blue in left leg. Joint phase-plane behavior: (a) ankle, (b) knee, (c) hip (middle). Joint coordination plots: (d) ankle vs. knee, (e) ankle vs. hip, (f) knee vs. hip (bottom).

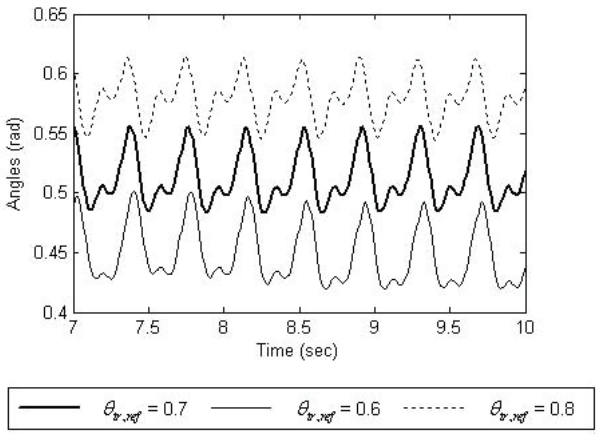

Figure 5-11: Simulated trajectories of trunk pitch angle (θ_{tr}) depending on $\theta_{tr,ref}$.

5.4 Preliminary conclusion

A simple computational scheme presumably consistent with neurophysiology could generate responses to voluntary modulations, i.e., kicking a ball and stepping over an obstacle during walking. In addition, forward bent walking is simulated. The perturbation caused modification of kinematic trajectories and extra force. The investigation proposes that such voluntary behaviors can be implemented without the internal models of dynamics. It was demonstrated here that the substantial decoupling of control may allow to add behaviors by simple superposition scheme. However, the effect of the residual coupling may be such that the action of different channels appear as disturbances to each other when weakly interconnected systems are driven independently. To prevent it, the feedback system (the cerebrocerebellar long-loop feedback control) helps each channel resists the effects of 'cross talk' thereby enhancing the degree of functional decoupling. Further research is required to verify whether it is physiologically supported.

This chapter did not discover a new way to control behaviors. Rather, it has identified arguably the potentially efficient way in which human balance and locomotor behaviors naturally decouple, which could be a motor behavioral basis. And this chapter has proposed that if simple control engages these natural dimensions with

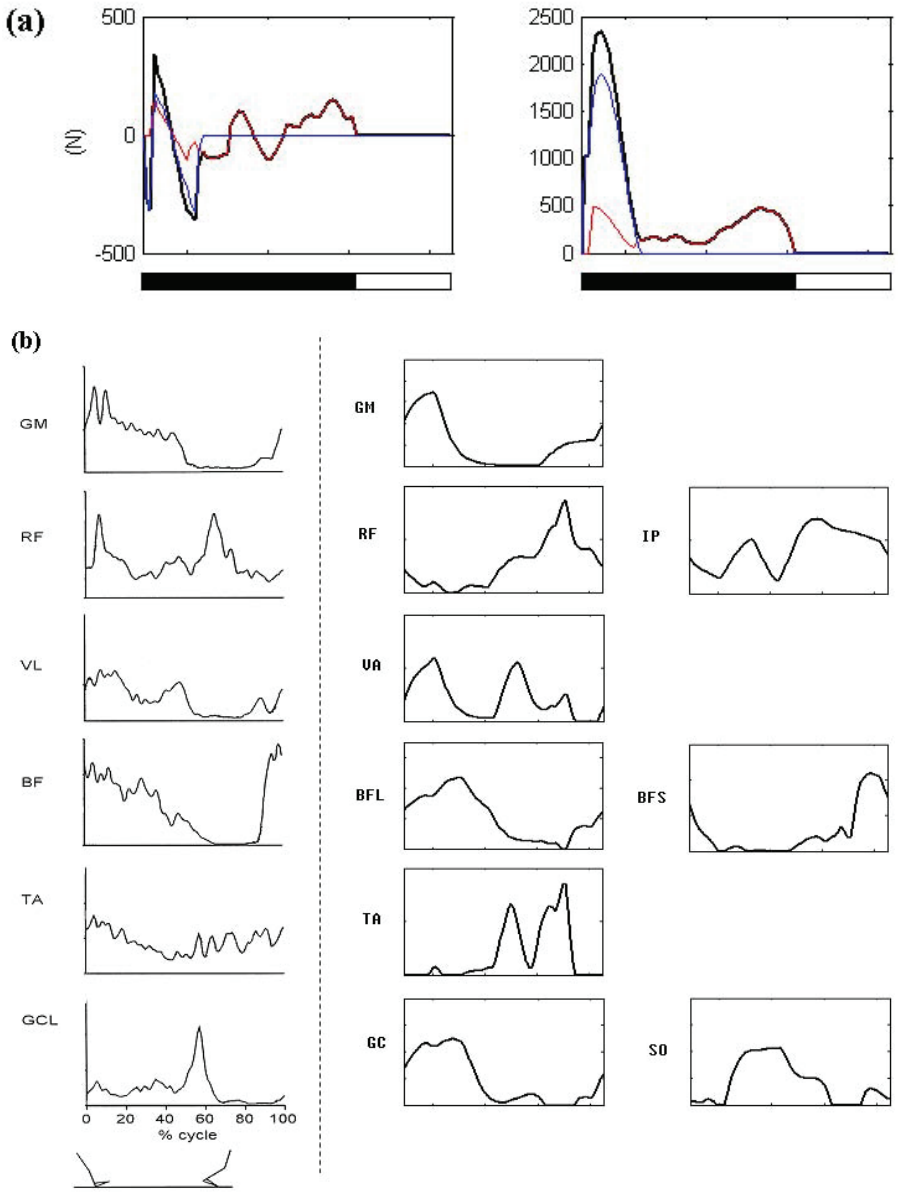

Figure 5-12: (a) Simulated reaction force profiles: force component at toe (red), at heel (blue), total force (black), and (b) real (left) and simulated (right) EMG patterns. Real data is adapted from Grasso et al 2000. Some of muscles have no real data.

simple, efficient, low-dimensional feedforward and feedback processing, that sturdy building blocks become available for a wealth of behaviors that can continue to be possibly controlled by simple commands with superposition. Most likely, this will help the adaptive scheme of behaviors.

Chapter 6

Conclusion and discussion

Both the postural balance (FRIPID) and walking (SBBW) models sought to achieve control using a minimal amount of sensed information. Approximately estimated COM position, and truncal verticality were chosen to be the most critical variables in both cases. In postural balance, ankle and hip angles are the principal determinants of the actual COM position and trunk angle assuming minimal motion of knee joint. Together with information about the disturbance intensity (reflected to ankle angular velocity), the COM position and trunk verticality are thus used implicitly to decide the hyper-plane of the gain switching. In addition, both desired COM position and trunk angle are defined to be zero because the desired position in the postural balance model is completely upright. The use of the two sensed variables for balance control is consistent with a recent human study (Freitas et al 2006). In the SBBW model, the same two variables were explicitly used for postural control during walking. The two models suggest that the information of COM and truncal position is processed simply by the supraspinal system in both cases of balance and walking. This means that kinematic control with no explicit internal model of body dynamics may be sufficient for those tasks.

6.1 Postural balance model

6.1.1 Kinematic feedback control of postural balance

The present study demonstrates that the combination of stabilized, scheduled long-loop proprioceptive and force feedback could provide flexible and powerful control to facilitate postural defense despite the presence of significant signal transmission delays and phase lags. Negative force feedback attenuates the otherwise large, and potentially injurious or destabilizing force transients that could be engendered more often by PID control alone. The findings also suggest that the body's control could be substantially linear within regions of the kinematic state-space with switching driven by a small number of sensed variables. The control segmentation need not be fine-grained and there is apparently no requirement for precise prediction of body state that would necessitate an internal forward dynamics model. Finally, the ability to reproduce at least qualitatively the balance dysfunction in cerebellar disease supports the model's attribution of long-loop scaling and stabilization to cerebellar circuitry.

It has already been shown (Kuo 1995) that for disturbances of the magnitude that occur within these experiments, human body dynamics can be effectively linearized. Therefore, in the context of effective full body state estimation/prediction by a linear internal dynamics model, it is possible to reasonably describe human responses to platform translation in terms of optimal linear (Linear Quadratic Gaussian) control (Kuo 1995). In this and other models (Hemami and Katbab 1982; Miall et al 1993) the control portion as opposed to estimation component is designed as if there were no delays. Studies (Miall et al 1993) have argued that the experimental disruption of visuomotor tracking produced by delays is consistent with the presence of an internal dynamics model used for prediction of target motion and internal feedback signals. And more generally, the potential advantages of physiological model-based state estimation have been well summarized (Wolpert et al 1995). However, it has not been established that such internal models exist, and even if so, it is also not necessary that low-level (pre- or subconscious) proprioception-dependent motor control depend

upon the same mechanism as visuomotor tracking.

The distinction between high-level tracking and low-level body stabilization is potentially important for any animal in an open environment where body motion in the context of novel loads may not be well predicted by existing internal dynamics models. If control system stability depended sensitively on state estimation/prediction, then the estimator would have to be accurately updated during the motion itself. This would be especially challenging in high-speed multijoint, environmentally interactive behaviors such as predation. It is not clear where or how such learning would likely occur in the CNS. Effective adaptation in cerebellum, basal ganglia and motor cortex seems to require at least several repetitions of movement even under constantly maintained novel conditions (Martin et al 1996; Tremblay et al 1998; Li et al 2001). Continuous reorganization of cerebral sensory cortical activity does not seem to be a likely candidate for improving low-level control on the scale of fractions of a second. And spinal circuitry does not appear to have the requisite complexity for such flexible general-purpose internal modeling. On the other hand, if the control scheme does not require accurate estimation/prediction of body state or environmental forces, then internal forward dynamics and/or delay models may not be needed. In this case, the computational circuitry may be simpler, the stability and performance more robust, and the adaptation allowed to proceed at a more moderate rate.

PID-type control formulas have been used to describe frequency domain characteristics of human body sway involving primarily ankle motion (Johansson 1988; Peterka 2001). However, balance maintenance in reaction to rapid external disturbances necessitates multijoint, e.g. mixed hip and ankle, responses. And, rapid disturbances may excite high frequency dynamics that give rise to undesirable oscillations, or destabilize a nonlinear system with delays or other phase lags. Therefore, it must be explicitly verified that PID control can be extended to explain the kinematics of both gentle and more violent disturbance recoveries. Moreover, it is desirable to determine how such control may be implemented physiologically.

6.1.2 Usefulness of cerebellar gainscheduling and force feedback

The inclusion of negative force feedback significantly improved the realism of the RIPID model responses. To investigate the most challenging possibility with regard to delay-engendered instabilities, a transcortical path was simulated. However, the long-loop processing of force information is not well understood. It is conceivable that shorter paths involving cerebellum but not the cerebral cortex might be important. In any case, it was still found to be necessary to posit that a different gainset became active as disturbances became more violent. Relatively simple interpolation between the gainsets on the basis of sensed kinematic state, was found to be sufficient even with sensing time lags. The proposed gainset selection mechanism based on sensed state is simple, and flexible. Though clearly speculative, it appears to be consistent with an implementation by spinocerebellar pathways that apparently carry a mixture of signals from the periphery (Osborn and Poppele 1992), and previous proposals for operation of cerebellar corticonuclear circuitry (Eccles et al 1967; Ito 1997). It has a flavor similar to the expansive recoding of kinematic state used by Kettner et al (1997). However, the function of this input is purely one of gainset selection, not in direct generation of a control output. With force feedback incorporated, only two cerebellar gainsets were needed to achieve realistic kinematics with appropriate limitation of COM excursion and peak ankle torque. This represents a significant improvement in efficiency and robustness of stability with respect to prior efforts (Jo 2002). Importantly, a 40 % increase in loop signal transmission time accentuated hip and ankle motions but resulted in only a trivial decrease in COM control. Still, the mechanism by which appropriate gainsets would be learned within the cerebellum is not clear. This remains an important issue for physiological credibility, and is therefore an important target for future investigations.

Managing the dynamics of upright posture presents a particular challenge for the purely proprioception-based RIPID models. First, the plant is inherently unstable due to an external force that varies nonlinearly with respect to body configuration,

potentially accentuating the destabilizing effects of control system delays. Second, in the presence of external forces, applied muscular torque cannot be deduced from kinematic state alone without an internal model of the kinematics-force relationship if such could be known. Third, the goal of upright balance is not necessarily the immediate return to vertical. Rather, it is first roughly to prevent excursion of the vertical projection of the center of mass beyond the base of support, and secondarily to return to vertical at a comfortable rate. In certain high performance situations, the latter phase may not even be required. Thus, early simulations indicated that the scheduled, purely proprioception-based RIPID model could not account well for natural postural recovery kinematics without resorting to multiple, precisely timed switches in controller gains. While not physiologically inconceivable, this lack of robustness was unattractive.

6.1.3 Feature and limitation of simulated EMG and pathological test

That the FRIPID model yielded simulated EMG patterns with several semi-quantitatively realistic features is not completely trivial because of the redundancy of musculature around joints and the possibility of muscular coactivation. Thus, EMG patterns are not fully determined by the kinematic behavior of the body model. On the other hand, the exploration of muscle activation patterns was very limited in this study. More sophisticated muscle models including continuously varying activation-dependent stiffness and segmental stretch responses would be essential for future efforts in this direction.

The finding that central features of the abnormal balance displayed by persons with cerebellar disease could be approximated at least qualitatively by reducing the gains of the cerebellar component of the model mirrors the similar finding in the modeling of arm control (Massaquoi 1999). The further improvement in realism by the addition of muscular coactivation appears reasonable, though it remains somewhat speculative. Enhancement of extracerebellar long-loop responses might have a similar

effect. Perhaps both changes occur. In any case, simulating the effects of cerebellar system lesions further supports the neuroanatomical specificity and architecture of the model.

6.2 Biped walking model

6.2.1 Kinematic qualities of simulated gait

The SBBW model accounts for a number of kinematic features of natural walking without requiring detailed programming of joint time-courses. The feedforward control signals consist of a steady intended forward displacement of the center of mass, a vertical reference for the trunk angle and a series of rectangular central NPG signals. Apparently, the neural feedback, the muscular synergy organization and muscle activation dynamic and viscoelastic properties are sufficient to add the coordination and modulation necessary to produce smooth, stable, natural appearing movements. The convergence to a consistent steady state cadence is not surprising given the regularity of the NPG. However, this was not a necessary outcome. The system dynamics include many significant nonlinearities and intermittent ground contact. Indeed, when there is reduced control at the ankle and speed is low, simulated walking can become significantly more chaotic.

Body kinematics are well summarized by joint angle, joint coordination, phase-plane and single/double support fraction data. Joint angle data shows slightly less knee flexion and ankle plantarflexion during the RET and FOW control epochs than seen in experimental data. This may relate to the failure to model swing leg hip drop as discussed below. However, the kinematic analysis indicates that body motion is generally quite realistic. Consistent with this, it was found (but not shown here) that the kinematics lie naturally close to a plane in three dimensional joint-space. This feature has been identified in human subjects (Lacquaniti et al 1999) in terms of *elevation angles*, the angles between body segments and a vertical reference. The transformation between joint angles as used in this study, and elevation angles is

affine. Therefore planarity in either system implies planarity in the other. Functionally, planarity corresponds to the fact that although the four segments defining body and leg orientation have in principle four degrees of freedom, during walking they exhibit two. The trunk is constrained to be always nearly vertical and the legs function primarily as swinging pistons that exhibit rotation of the leg at the hip and flexion and extension of the leg. For the most part, the upper and lower leg and foot move in unison. That the trajectory is substantially a single closed loop indicates that the two underlying degrees of freedom are coordinated in a consistent manner at the same frequency. The principal partial exception to this analysis is that the ankle motion during ground contact is slightly more complicated. During early stance phase, θ_1 increases somewhat while θ_2 declines slightly as the stance leg straightened. This is opposite to the overall coordination pattern between knee and ankle and results in a transient deviation from the plane. This can be seen in human data as well (Lacquaniti et al 1999). Planarity is recovered quickly with the rapid ankle plantar flexion flick at the end of ground and the corresponding rapid decline in θ_1. On average, the behavior remains that of a swinging piston.

As the SBBW addresses only sagittal plane performance and approximates the action of muscle groups without including, for example, variations in moment arm with joint angle, full Hill-type muscle dynamics (Winters and Stark 1985; Zajac 1989) and the action of toes. Therefore, no attempt was made to match the kinematics of a particular human subject. Nonetheless, the most characteristic features of natural walking appear to have been captured. This is also true in terms of clinically-oriented walking assessment scales.

Passive walkers (McGeer 1993) may exhibit very natural appearing gait patterns. However, this occurs characteristically for a narrow speed range dictated by the walker's geometry and mass distribution and by the slope of the decline. Gently actuated, near-passive walkers (Collins et al 2001; van der Linde 1999) can walk on a level surface, but still exhibit a fairly narrow speed range. It was therefore important

to show that without changing the physical characteristics of the model or surface, realistic walking could be produced at several speeds by varying only central neural control. The relationship between SBBW and current artificial walking devices is discussed further below.

6.2.2 Features of gait control and dynamics

The major features of gait kinematics were produced by the empirically-developed feedforward action of a spinal pulse generator and four muscle control synergies that it drives. A steady (tonic) reference command that specified a forward displaced COM enhanced walking speed as discussed below, but actually was not required for walking as long as COM and trunk pitch were under feedback control Other central neural pattern generator schemes have specified continuously varying intended motion at individual joints (two pattern generators) (Taga 1995; Ogihara and Yamazaki 2001). The present investigation proposes a simpler scheme. The five control epochs identified here: Loading, Regulation, Thrust, Retraction, and Forward swing were found empirically to be the minimal scheme that could account for a full range of walking speeds by scaling epoch durations proportionately. This resulted in the constancy of EMG pattern across speeds that has been noted experimentally (Ivanenko et al 2004). This is also consistent with the suggestion that the CNS may generate only a few basic patterns of muscular activity for locomotion (Patla et al 1985). The pulse generator command was selected to consist of rectangular pulses for simplicity. In fact, because of the significant low-pass filtering characteristics of muscle activation and impedance, net locomotor behavior is not especially sensitive to high-frequency details of muscle command signal morphology-any type of pulse-like waveform (see also Cajigas-Gonzales 2003) can have substantially similar effect. Overall, the control scheme is that of equilibrium trajectory-type control (Feldman 1986; Bizzi et al 1992), the performance of which is enhanced by more realistic activation level-dependent muscular viscoelasticity.

Initiation of movement required a small additional trigger pulse applied to hip flexors during the first step. This component essentially provides the initial swing leg elevation and forward momentum that would ordinarily be contributed by substantially passive dynamics in the middle of the gait cycle. That participation of a separate system is for the moment a conjecture. However, it is not inconsistent with the particular deficit in Parkinson's Disease wherein the initiation of walking may be disturbed preferentially. However, more analysis will be required to characterize such a system. Once started, walking speed could be varied from around 0.3 to 1.6 m/s by modulating only the frequency and amplitude of the central pattern generator pulses.

During double support, a biped is a closed kinematic linkage (Pandy and Berme 1988). As such, there exists no unique solution for the torques at each joint. Moreover, in single support correct kinematics implies only correct net torques. Given the agonist-antagonist organization of the muscles and the redundancy of actuation, the forces applied by individual muscle groups are not determined by the body motion. Therefore, it was important to verify that model forces and muscle activations are realistic. This can be done explicitly for ground contact for which there is considerable experimental data. The biphasic force profile with larger forces at heel-strike and toe-off is consistent with significant control at the ankle rather than the hip. This is quite realistic. The somewhat greater toe-off pulse in the simulation appears to result from the inability to reproduce in simulation the full stiffness of the typical floor. As a result, there is a mild bounce forward from rear foot to forefoot.

For approximation of joint torques, where less experimentally measured force data is available, the EMG pattern can serve as a crude surrogate assuming, as is here, that the muscle model is reasonably accurate under the conditions studied. Overall, the control system appeared to generate muscle activations that were similar to those observed in vivo. In particular, the finding of four principal independent waveforms in muscle activation corresponds closely with the four or five factors that have been found in human data. These appear to correspond approximately to the five prin-

cipal control epochs that have been proposed here. During each epoch, the muscle activation pattern tends to be quite different from the others which yields their independence, and near orthogonality. The epoch-specificity of the EMG is related to the significant differences in motor task during each period. Accordingly, analysis of phase-specific motor tasks may shed some light on the two features of predicted EMG that were potentially least realistic. These were: a) the more widespread inappropriately predicted muscular activity during the REG control epoch and b) the model's failure to predict TA activation throughout swing.

As pointed out above, EMG records from humans occasionally show activity during the REG control epoch. However, others clearly do not. Two effects may be important. Activation of VA and RF during REG was found to be important to keep the knee from buckling during stance. In principle, however, this is not a problem if the knee joint is substantially vertical or even locked in extension. This stabilizing requirement is very sensitive to small changes in knee angle. It is therefore quite possible that a model with more realistic muscle viscoelastic properties, and/or enhanced segmental or long-loop reflex action during LOA could obviate or reduce muscular action during REG.

In addition, during REG and THR that the ankle has its greatest efficacy in body control, especially during slow walking. This is because it is during late REG and early THR that the COM lies above the base of support. During LOA the landing leg is extended forward and gravity causes significant torque about the ankle. Because the foot itself is comparatively low mass with respect to the body, muscular ankle torque during LOA tends to cause ankle roll. Backward roll can contribute appreciably to COM deceleration, but forward roll provides little forward COM acceleration. Similarly, late in THR, the COM is forward, beyond the foot. Forward ankle roll can contribute significantly to forward COM acceleration, but not the reverse. During late REG and early THR (midstance), however, the ankle can accelerate or decelerate the body. Importantly, during RET the thigh adductors including the obturator

and adductor magnus (well developed in sprinters) function thigh flexors relative to the pelvis. These muscles may contribute to the forward swing of the leg and therefore to the forward movement of the COM. However, they were often not studied experimentally and were not included in the current simulations. Significant activity of these muscles during THR and RET may further reduce or obviate activation of ventral stance leg muscles during REG.

The failure of the SBBW to anticipate prolonged activation of TA may relate to the fact that the model only describes motions within the midline sagittal plane. Natural walking includes a small amount (about 6 degrees) of shifting pelvic tilt in the frontal plane that results in about 5cm of drop of the swing leg hip (Inman et al 1981). While subtle, this potentially interferes with foot ground clearance. Extended activation of the TA in vivo may be required to compensate for this tilt. Thus, the absence of direct swing leg control during the FOW epoch may account for the finding of four rather than five principal components in the muscle activation signals. Arguably, the 'missing synergy' includes activity of BFS, BFL and TA during swing that helps to maintain the leg in retraction. This would presumably correspond to the fifth FACTOR identified in experimental EMG data. In any case, it appears that EMG control during early to mid-stance and early to mid swing in the opposite leg is likely to be important, and sensitive to many factors. This suggests that more data will be required to determine the variety of possible muscle activation patterns that can be effective.

6.2.3 Stability of simulated gait

Steady state walking was shown to resist modest impulsive disturbances and mass increases without changes in parameters or changes in feedforward control signals. These alterations stressed the limit cycle-like behavior described above and suggest that the mechanics and control scheme have good stabilizing characteristics. The SBBW feedback control system is particularly simple and corresponds well with the two channel control of posture posited on the basis of human studies (Freitas et

al 2006). To some extent, this is quite expected based on first principles. Minimal necessary conditions for upright walking are a) maintenance of the COM near the base of support, b) maintenance of the trunk verticality. During single leg support, this means that the COM should be roughly over the foot, and during double support phase, the COM should be roughly within the convex hull of the two feet. These conditions are evidently fairly easy to achieve using long-loop feedback, especially when control is applied grossly to whole limbs. This is facilitated by the use of multiarticular synergies. As discussed further below, this approach has potentially important implications for cerebellar functional architecture and to our knowledge has not been used previously in simulations of natural locomotion and in robot locomotion control.

Limited exploration of the sensitivity of walking to simulated system lesions indicates that it is likely that all system components must be reasonably intact for successful walking. This suggests that the model has a generally parsimonious structure. In principle, there are a limited number of failure modes. The COM can fall forward, backward or directly downward. For the latter to occur, the knees must buckle. Given adequate activation of the knee extensors VA and RF, or extension of the knee by other means during the REG epoch, this is unlikely. If the body falls forward or backward, either the legs spread in a "split", or the swing leg encounters the ground causing a trip. In all simulated system lesions, the body tripped forward. This is most likely when there is appreciable forward momentum. It may be characteristic of cerebellar disease and peripheral neuropathy when vision is removed. The great propensity to trip is also reminiscent of the falling that toddlers typically exhibit and indicates the key point of vulnerability during walking. It suggests that stronger management toe clearance, as would be a responsibility of a fifth control synergy during swing involving BFS, BFL and TA as described above, is very likely to be critical to improved locomotor control.

6.2.4 Limitations in performance and stability

The model displays the ability to begin walking from a standstill, and some capacity to adjust its walking speed in response to changes in the feedforward commands. However, control of deceleration and walking at speeds slower than 0.3m/s was limited. In particular, slowing and stopping to a standing balance was not achieved by the SBBW. Slow walking evidently requires prolonged time in single leg stance phase. This places particular demand on the balance system. While it is expected that a more complete balance mechanism such as that possessed by the FRIPID model would be stable under these conditions, the more rudimentary SBBW model has difficulty. This finding is grossly consistent with the difficulties that toddlers have in stopping without falling down. Quickly slowing to a stand apparently requires more precise control to cancel forward linear and angular momentum simultaneously using the legs, and/or strong standing balance mechanisms to dissipate residual energy, without moving the feet. Thus, it appears that some type of 'clutch' is needed to properly coordinate the walking and standing balance systems during slow walking and stopping. As suggested above, another important factor is likely to be control of the swing leg. This could include long-loop feedback as well as feedforward spinal input. Moreover, the current model balances upright only with enhanced ankle stiffness. While this level of stiffness is within physiological range, more complete feedback control as used in the FRIPID balance model has the potential to afford superior balance control with more modest ankle stiffness. It seems that an important remaining challenge is to integrate additional feedback mechanisms with the locomotion control investigated here.

6.2.5 Implications for neural architecture

It has been shown experimentally that electrical stimulation of the posterior structures of the lumbar spinal cord can induce patterned, locomotor-like activity (Dimitrijevic et al 1998). Importantly, focal stimulation elicits simultaneous rhythmic EMG activities in muscles at different joints in the lower limb. This suggests that neural os-

cillators are not joint specific and is highly consistent with the synergies used here. A synergy is in principle a consistent pattern of activity among a set of muscles activated stereotypically, that may be modulated or shifted by the same extent, but is otherwise kept intact. Synergies have been defined in terms of EMG, both time-dependent and time-independent formulations (d'Avella and Bizzi 2005; Cheung et al 2005) and in terms of function (Cajigas -Gonzalez 2003). These views are compatible but with different emphases. The current investigation adopts an approach that is similar to Cajigas-Gonzalez (2003) who showed that the 12 EMG synergies in frog leg control identified by d'Avella could be collapsed into four time-invariant Kinematic Control Synergies (KCS). The latter could be shown to account for the swinging piston-like behavior of a frog's leg during walking, swimming and wiping behaviors. In fact, a significant range of frog leg behaviors could be accounted for by the four control synergies. Moreover, the driving temporal waveforms both here and with KCS are taken to be simple pulses that have scalable intensity and duration. While a rich variety of time-varying activations can be afforded, the control is ultimately constrained significantly by these assumptions. In any case, the SBBW supports the possibility of time-invariant control synergies mediated by effectively fixed, linear connections between spinal pulse generator circuitry and motor neuron pools, thereby decoupling and simplifying the temporal and distributional components of limb control.

Recent work in the frog indicates that as previously suspected, peripheral sensory feedback may modulate the expression of motor synergies (Cheung et al 2005). However, in general, this is found to be relatively minor in that basic behaviors are retained following peripheral deafferentation. On the other hand, upright bipedal locomotion places particularly strong demands on the control of leg trajectory. The SBBW found it extremely useful to have some modulation of especially the retraction control phase according to sensed leg position. Presynaptic inhibition in spinal cord as assumed by the model has been identified (Rudomin and Schmidt 1999; Baxendale and Ferrell 1981; Duysens et al 2000; Rossignol et al 2006). Simulated compromise of this mechanism resulted in excessive leg retraction that bears significant resem-

blance to clinical high-stepping gait abnormality seen in tabes dorsalis a compromise of spinal level sensory input due to syphilis (Ropper and Brown 2005). This suggests the basic plausibility of the mechanism. However, more extensive analysis will be required for validation.

While many studies show the existence of muscle synergy organization at the spinal cord level, and spinalized cats display fairly normal locomotor patterns when suspended and placed on treadmills (Lam and Pearson 2001; Hiebert and Pearson 1999; Kandel et al 2000), it is also clear that supraspinal control is extremely important to fully normal locomotor function (Morton and Bastian 2004; Dietz 1992; Shik and Orlovsky 1976; Brooke et al 1997; Nielsen 2003). The SBBW model does not attempt to provide a strong argument for a particular neural implementation because several could be conceived. However, it was important to demonstrate that feedback control could be implemented stably by trans-cerebellar long-loop mechanisms. As argued elsewhere, the cerebellum is very likely to provide important scaling and dynamic processing for many centers within the central nervous system. Therefore, the SBBW represented control system tuning as simple changes in scalar gains. In particular, it is considered explicitly that the gain in the COM and trunk pitch feedback loops could be adjusted through cerebellar adaptation. While not explicitly attributed to cerebellar circuits, the scheduled scaling of especially the amplitude of central neural pattern generator signaling with movement speed could also be implemented or at least refined by cerebellar circuits. More detailed study of control derangements in cerebellar disease would be needed to determine the validity of this conjecture.

The particular architecture adopted by SBBW shows further that the ability of synergies to provide efficient, reduced dimensional control over the trunk and legs, thereby enables cerebellar control to be particularly simple. In contrast to the FRIPID cerebro-cerebellar balance control model wherein cerebellar action over ankle, knee and hip was represented as full 3 x 3 matrices with in principle independently specifiable elements, the SBBW model demonstrates that multi-joint control of walking can

be managed by a collection of control matrices each having more restricted structure. Specifically, it implies that the cerebellar contribution to body control is decoupled and can be represented by a diagonal matrix with elements of form $(gk + gbd(\cdot)/dt)$. This is contrary to the older notion of the cerebellum as a large switchboard that provides explicit coordination between different joints. Instead, it suggests that the cerebellum connects and scales appropriate multijoint synergies that in turn implement the interjoint coordination. While the views are not mutually exclusive, latter is particularly compatible with recent anatomical studies (Kelly and Strick 2003) that emphasize very narrow point-to-point modular processing by cerebellum, rather than broad fan-in and fan-out. The only gainscheduling needed by the SBBW was that based on detection of foot-ground contact. COM and trunk pitch feedback gains were applied to signals obtained from the stance leg only.

Finally, while walking and running at a regular cadence represent central functions of the legs, there clearly must be much greater flexibility of function. First of all, when footing is potentially treacherous, it is important to be able to perform some level of targeting of foot placement during locomotion. Therefore, presumably suprasegmental circuits must be able to intervene and modify leg and foot trajectory as needed. This was beyond the present modeling effort. Still, it is noteworthy that here the legs were controlled effectively with simple pulse-like waveform. Such output is arguably generated by fronto-basal ganglionic circuits (Massaquoi and Mao, unpublished) that could assist in the specification of more complex bipedal behavior.

6.3 Implication for design of humanoid robotic balance and locomotion

The FRIPID postural balance model demonstrates that balance control without internal model-based dynamic computation is possible and is greatly enhanced by a simple gainscheduling mechanism that is useful to maintain stable posture against disturbances. The SBBW shows that kinematic information without internal model-based

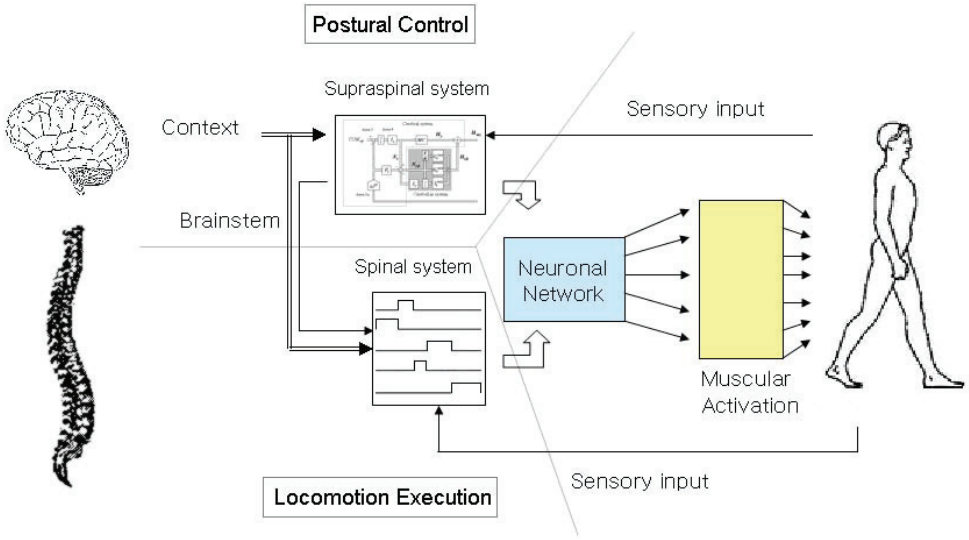

Figure 6-1: Hierarchical neural control of walking.

control is sufficient for gait generation. Therefore, this work suggests that explicit compensation of body dynamics may not be required for control of natural balancing and walking that is reasonably robust to disturbances. This work also demonstrates simple strategies to execute various tasks even though it does not fully guarantee its success yet. Further investigation will be required to establish whether the model's physio-anatomical interpretations are correct. In any case, the computational investigation already teaches us a simple scheme that may be useful for the design of bipedal robot locomotion controllers and potentially neurally driven prosthetic devices. The ability of this scheme to avoid complex (probably dynamic) computation is potentially powerful.

Three features of the SBBW model appear to underlie its natural behavior and simplicity of control. First, its feedback systems provide basic upright stability in terms of posture and COM location. Second, its feedforward pattern generator activates synergies each of which performs a separate fundamental dynamic function that are required within every gait cycle irrespective of speed. In both the feedforward and feedback control components, there is substantial decoupling of the various con-

trol circuits while functionally compatible joint actuations are packaged together as synergies. The control architecture therefore reflects the degrees of freedom that are specifically important for bipedal locomotion. This enables components of the gait control and postural regulation to be tuned with considerable independence. The decoupling scheme fosters computational efficiency and eases the implementation of new behaviors. Therefore, simple local adjustments in the neural system were able to elicit several different behaviors, e.g., different walking speeds by tuning parameters in spinal pattern generator only (Chapter 4), ball-kicking or stepping over an obstacle during walking by superposition of additional pulse commands (Chapter 5). On the other hand, because of the synergy structure, control of the body into arbitrary configurations is not possible using this system. Third, the viscoelasticity of the muscles smoothes the effect of command inputs and enables stable contact with the ground without explicit computation of joint torques or foot forces (Hogan 1985). Many of these features could be applied to the control of artificial humanoid robots if driven by series elastic actuators (Blaya and Herr 2004) that behave much more as muscles than do typical torque motors.

The control features of the SBBW model lie in the middle of the range of those used for artificial bipedal walkers. Passive walkers (McGeer 1993) may exhibit very natural appearing gait patterns. However, these occur characteristically for only a narrow speed range that is dictated by the walker's geometry and mass distribution and by the slope of the decline. Gently actuated, near passive walkers can traverse horizontal ground by injecting energy via foot plantar (Collins et al 2001) and rearward rotation at the hip as well (van der Linde 1999). However, because of the lack of active stabilizing feedback, these walkers also exhibit a fairly narrow speed range and also do not resist external disturbances well. At the other end of the spectrum, fully actuated humanoid robots such as ASIMO developed by Honda motor corporation (Hirai et al 1998) demonstrate highly flexible position control of all body segments. However, they are comparatively heavy, energy inefficient and have control that relies on much more complete limb trajectory specification based on relative relation between ZMP

(Vukobratovic et al 1990) and COM.

Although not investigated extensively here, the energetics of the SBBW model are likely to be favorable. First, all synergies are organized to minimize muscular coactivation. Each synergy activates only muscles that do not do compete with each other at any joint. Furthermore, synergies are driven by any single source to not overlap in time. The current implementation uses substantially passive leg swing that likely contributes to energetic efficiency. Preliminary analysis shows that C_{mt}, an index used to estimate mechanical energetic efficiency, is defined (Collin et al 2005) as:

$$C_{mt} = \frac{\text{mechanical energy used}}{(\text{weight})(\text{distance traveled})}. \tag{6.1}$$

The index for the SBBW is about 0.09 without any attempt to optimize this value. Passive and near passive walkers have generally shown C_{mt} less than 0.1, and humans C_{mt} of about 0.05, while ASIMO has a C_{mt} of 1.6 (Collin et al 2005). This supports the impression that SBBW already provides a fairly realistic description of human locomotion and suggests that human-type actuation and control may afford considerable locomotor performance and stability without incurring great loss of energetic efficiency. However, further investigation including estimation of metabolic costs of muscle activation will be required for a full energetic characterization.

In summary, the hierarchical combination of the postural feedback controller, the state activation pattern generator, the segmental interlimb relation, and the viscoelastic muscle contains such features as simplicity of feedforward waveform, linearity of most modulation and signal distribution, efficient use of feedback, minimization of coactivation and efficient use of passive limb dynamics. The hierarchical neural systems are functionally decoupled in performance perspective. For example, the feature empowers the muscle to regulate different motion speeds even for motions in a same path. Also, the gain control is related to energy efficiency as well as fast motion control. These aspects may be of significance in the development of human-sized robots.

Therefore, the investigation of the neural control of human balance and walking in this thesis may provide a framework for designing a humanoid robotic locomotion.

Appendix A

Model parameters

A.1 Postural balance model

A.1.1 Dynamic equation

A three link inverted pendulum model represents the model of human body with three segments, e.g. the lower leg, the upper leg, and the trunk. The segments are connected by frictionless hinge joints, and the feet remain flat on the ground. m_i is the mass of a segment i , l_i is the length of a segment i , and h_i is the moment of inertial of a segment i at center. Segment 1 is the lower leg, 2 is the upper leg, and 3 is the trunk. Body model parameter values are: m_1=4 kg, m_2=7 kg, and m_3=49 kg ; l_1 =0.4 m , l_2=0.5 m, and l_3=0.8m ; h_1=0.12 kgm^2 , h_2=0.14 kgm^2, and h_3=2.3 kgm^2; and g=9.81 m/s^2 (adapted from van der Kooij et al 1999).

$$H(\Theta)\ddot{\Theta} + C(\Theta,\dot{\Theta}) = \tau_M(\Theta,\dot{\Theta},u_\theta) + \tau_D(\ddot{D},,\Theta) + G(\Theta)$$

$$H(\Theta) = \begin{bmatrix} H(1,1) & H(1,2) & H(1,3) \\ H(2,1) & H(2,2) & H(2,3) \\ H(3,1) & H(3,2) & H(3,3) \end{bmatrix}, C(\Theta,\dot{\Theta}) = \begin{bmatrix} C(1) \\ C(2) \\ C(3) \end{bmatrix}, G(\Theta) = \begin{bmatrix} G(1) \\ G(2) \\ G(3) \end{bmatrix},$$

$$\tau_D(\ddot{D},,\Theta) = \begin{bmatrix} W(1) \\ W(2) \\ W(3) \end{bmatrix}.$$

$$H(1,1) = h_1 + h_2 + h_3 + m_1 r_1^2 + m_2(l_1^2 + r_2^2) + m_3(l_1^2 + l_2^2 + r_3^2)$$
$$+ 2(m_2 l_1 r_2 + m_3 l_1 l_2) + 2m_3 l_2 r_3 \cos\theta_3 + 2m_3 l_1 r_3 \cos(\theta_2 + \theta_3)$$
$$H(1,2) = h_1 + h_2 + m_2 r_2^2 + m_3(l_2^2 + r_3^2) + m_2 l_1 r_2 \cos\theta_2$$
$$+ (m_2 l_1 + 2m_3 r_3) l_2 \cos\theta_3 + m_3 l_1 r_3 \cos(\theta_2 + \theta_3)$$
$$H(1,3) = h_3 + m_3 r_3^2 + m_3 l_2 r_3 \cos\theta_3 + m_3 l_1 r_3 \cos(\theta_2 + \theta_3)$$
$$H(2,1) = H(1,2)$$
$$H(2,2) = h_1 + h_2 + m_2 r_2^2 + m_3(l_2^2 + r_3^2) + 2m_3 l_2 r_3 \cos\theta_3$$
$$H(2,3) = m_3 l_2 r_3 \cos(\theta_1 + \theta_2)$$
$$H(3,1) = H(1,3)$$
$$H(3,2) = H(2,3)$$
$$H(3,3) = h_3 + m_3 r_3^2$$

$$C(1) = (m_2 r_2 + m_3 l_2) l_1 (2\dot{\theta}_1 + \dot{\theta}_2)\dot{\theta}_2 \sin\theta_2 + m_3 l_2 r_3 (2\dot{\theta}_1 + 2\dot{\theta}_2 + \dot{\theta}_3)\dot{\theta}_3 \sin\theta_3$$
$$+ m_3 l_1 r_3 (2\dot{\theta}_1 + \dot{\theta}_2 + \dot{\theta}_3)(\dot{\theta}_2 + \dot{\theta}_3) \sin(\theta_2 + \theta_3)$$
$$C(2) = (m_2 r_2 + m_3 l_2) l_1 \dot{\theta}_1^2 \sin\theta_2 + m_3 l_1 r_3 \dot{\theta}_1^2 \sin(\theta_2 + \theta_3)$$
$$+ m_3 l_1 r_3 (2\dot{\theta}_1 + 2\dot{\theta}_2 + \dot{\theta}_3)\dot{\theta}_3 \sin\theta_3$$
$$C(3) = m_3 l_1 r_3 \dot{\theta}_1^2 \sin(\theta_2 + \theta_3) + m_3 l_2 r_3 (\dot{\theta}_1 + \dot{\theta}_2)^2 \sin\theta_3$$

$$G(1) = (m_1 r_1 + (m_2 + m_3) l_1) g \sin\theta_1$$
$$G(2) = (m_2 r_2 + m_3 l_2) g \sin\theta_2$$
$$G(3) = m_3 r_3 g \sin\theta_3$$

$$W(1) = (m_1 r_1 + (m_2 + m_3) l_1) \ddot{D} \cos\theta_1$$
$$W(2) = (m_2 r_2 + m_3 l_2) \ddot{D} \cos\theta_2$$
$$W(3) = m_3 r_3 \ddot{D} \cos\theta_3$$

A.1.2 Parameters used in the base FRIPID control simulation

$$G_k^{(1)} = \begin{bmatrix} 91 & -60 & 26 \\ -24 & 25 & -8 \\ 20 & -12 & 10 \end{bmatrix}, G_k^{(2)} = \begin{bmatrix} 60 & -90 & 32 \\ -7 & 25 & -4 \\ -7 & -55 & 8 \end{bmatrix}, I_1^{(1)} = \begin{bmatrix} 470 & -220 & 164 \\ -46 & 200 & -17 \\ 200 & -113 & 125 \end{bmatrix},$$

$$I_1^{(2)} = \begin{bmatrix} 503 & -286 & 176 \\ -60 & 170 & 0 \\ 212 & -113 & 125 \end{bmatrix}, I_2 = \begin{bmatrix} 60 & 0 & 0 \\ 0 & 60 & 0 \\ 0 & 0 & 60 \end{bmatrix}, I_a = \begin{bmatrix} 0.1 & 0 & 0 \\ 0 & 0.1 & 0 \\ 0 & 0 & 0.1 \end{bmatrix}, I_\tau =$$

$$\begin{bmatrix} 0.07 & 0 & 0 \\ 0 & 0.01 & 0 \\ 0 & 0 & 0.16 \end{bmatrix}, F_2 = \begin{bmatrix} 0.65 & 0 & 0 \\ 0 & 0.65 & 0 \\ 0 & 0 & 0.65 \end{bmatrix}, MC = \begin{bmatrix} 0.1 & 0 & 0 \\ 0 & 0.1 & 0 \\ 0 & 0 & 0.1 \end{bmatrix}, CA =$$

$$\begin{bmatrix} 0.32 & 0 & 0 \\ 0 & 0.04 & 0 \\ 0 & 0 & 0 \end{bmatrix}$$

A.2 SBBW model

A.2.1 Parameters for SBBW model

1. Muscle parameters

   α , β , and γ are set to be 0.11, 0.4, and 0.6 respectively.

   $$A = \begin{bmatrix} 0 & 0 & 0 & 0 & 0.023 & -0.036 & 0 & 0 & -0.040 \\ 0 & 0 & -0.040 & 0.049 & 0 & 0 & -0.025 & 0.049 & 0.050 \\ 0.132 & -0.092 & 0 & 0 & 0 & 0 & 0.049 & -0.054 & 0 \end{bmatrix}^T$$

2. Foot interaction to the ground

   $K_{gy} = 30000$, $B_{gy} = 500$, $K_{gx} = 10000$, $B_{gx} = 1000$; $\mu_k = 0.6$, $\mu_s = 1.2$.

   $y_{gy}(x) = 0$ to represent the flat ground.

3. Neuronal network of spinal pattern generation

   $m_{PG} = 1.2$, $f_{PG} = 1.3$.

$$\mathrm{W}_{PG} = \begin{bmatrix} 0.3 & 0 & 0 & 0.8 & 0.76 & 0 & 0 & 0 & 0 \\ 0 & 0.38 & 0 & 0 & 0 & 0 & 0 & 0 & 0 \\ 0.4 & 0 & 0.64 & 0 & 0 & 0 & 0 & 0 & 0 \\ 0 & 0 & 0 & 0.8 & 0.9 & 0.4 & 0 & 0 & 0 \end{bmatrix}^T .$$

4. Tactile receptor on the foot

   $\delta_F = 20.$

5. Spinal segmental reflex

   $\theta_{th,a} = 0.35$; $\theta_{th,k} = -0.35$; $\theta_{th,h} = 0.55$;

   $$\mathrm{W}_{reflex} = \rho \begin{bmatrix} 0 & 0 & 0 & 0 & 1 & 0 & 0 & 0 & 0 \\ 0 & 0 & 1 & 0 & 0 & 0 & 0 & 0 & 0 \\ 1 & 0 & 0 & 0 & 0 & 0 & 0 & 0 & 0 \end{bmatrix}^T$$

   where ρ is a sufficient large number ($\rho > m_{PG}$).

6. Suprasegmental control

   Reference signals: $COM_{ref} = 0.25$; $\theta_{tr,ref} = 0.$

   Approximated horizontal position of COM ($\hat{x}_{com}$):

   $p_{11} = 0.9663$, $p_{21} = 0.5343$, $p_{31} = 0.1414$;$p_{12} = 1$, $p_{22} = -1$, $p_{32} = 1$;

   $gb_1 = 0$, $gk_1 = 3$; $gb_2 = 0$, $gk_2 = 30$;

   $$\mathrm{I}_a = \begin{bmatrix} 0.2 & 0 \\ 0 & 1 \end{bmatrix}; \ \mathrm{F}_2 = \begin{bmatrix} 0.6 & 0 \\ 0 & 0.3 \end{bmatrix}; \ \mathrm{I}_2 = \begin{bmatrix} 100 & 0 \\ 0 & 100 \end{bmatrix}; \ \mathrm{I}_1 = \begin{bmatrix} 0 & 0 \\ 0 & 0 \end{bmatrix};$$

   $$MC = \begin{bmatrix} 0 & 0 \\ 0 & 0 \end{bmatrix}.$$

   $$\mathrm{W}_C = \begin{bmatrix} 0 & 0 & 2 & -5 & 6 & -1 & 3 & -1 & -3 \\ 4 & -2.8 & 0 & 0 & 0 & 0 & 1.5 & -1.6 & 0 \end{bmatrix}^T$$

7. Initial conditions

   Initial positions: $\theta_1 = 0.2$, $\theta_3 = 0$, $\theta_5 = -0.2$ for right leg; $\theta_2 = 0$,$\theta_4 = -0.1$,$\theta_6 = 0.4$ for left leg.

Initial velocities: $\dot{\theta}_1 = (f_{PG}+1)/2$, $\dot{\theta}_3 = -(f_{PG}+1)/2$, $\dot{\theta}_5 = (f_{PG}+1)/2$ for right leg; $\dot{\theta}_2 = -(f_{PG}+1)/2$, $\dot{\theta}_4 = (f_{PG}+1)/2$, $\dot{\theta}_6 = -(f_{PG}+1)/2$ for left leg.

A.3 eSBBW model

A.3.1 Parameters for normal walking

Most of parameter values are the same as in A.2 except the following:

Neuronal network of spinal pattern generation:

$$\mathrm{W}_{PG} = \begin{bmatrix} 0.3 & 0 & 0 & 0 & 0.8 & 0 & 0 & 0 & 0 \\ 0 & 0.29 & 0 & 0 & 0 & 0 & 0 & 0 & 0 \\ 0.4 & 0 & 0.64 & 0 & 0.9 & 0 & 0.35 & 0 & 0 \\ 0 & 0 & 0 & 0 & 0 & 0.4 & 0 & 0 & 0.3 \\ 0 & 0.1 & 0 & 0.8 & 0 & 0 & 0.4 & 0.1 & 0 \end{bmatrix}^T .$$

A.3.2 Parameters for voluntary behaviors during walking

Most parameters are the same as in A.3.1 and modifications are mentioned in the text (see section 5.3.2).

A.3.3 Parameters for forward bent walking

Most parameters are the same as in A.3.1 except the followings:

Initial positions: $\theta_1 = 0.2$, $\theta_3 = 0$, $\theta_5 = 0.7$ for right leg; $\theta_2 = 0$, $\theta_4 = -0.1$,$\theta_6 = 1.3$ for left leg.

Reference signals: $\theta_{tr,ref} = 0.7$.

Neuronal network of spinal pattern generation:

$$\mathrm{W}_{PG} = \begin{bmatrix} 0.4 & 0 & 0 & 0 & 0 & 0.1 & 0 & 0.4 & 0.2 \\ 0 & 0.3 & 0.5 & 0 & 0 & 0 & 0 & 0.3 & 0.2 \\ 0.5 & 0 & 0.64 & 0 & 1.0 & 0 & 0.35 & 0 & 0 \\ 0 & 0 & 0 & 0 & 0 & 0.1 & 0 & 0.2 & 0 \\ 0.4 & 0.1 & 0 & 0.8 & 0 & 0 & 0.4 & 0.1 & 0 \end{bmatrix}^T .$$

Bibliography

Allen, G.I. and N. Tsukahara (1974) Cerebrocerebellar communication systems. Physiol Rev 54: 957-1006.

Allum, J.H. and F. Honegger (1992) A postural model of balance-correcting movement strategies, J Vestib Res 2(4): 323-47.

Amstrong, D.M. and S.A. Edgley (1988) Discharges of interpositus and Purkinje cells of the cat cerebellum during locomotion under different conditions. J Physiol 400: 425-445.

Anderson,F.C. and M.G. Pandy (2001) Dynamic optimization of human walking, J Biomech Eng, 123: 381-390.

Ayaso, O. et al (2002). Coarse gain recurrent integrator model for sensorimotor cortical command generation. Proceedings of the American Control Conference, Anchorage, Alaska.

Baxendale, R.H., and W.R. Ferrell (1981) The effect of knee joint afferent discharge on transmission in flexion reflex pathways in decerebrate cats. J Physiol (Lond) 315: 231-242.

Bizzi, E. et al (2000) New perspectives on spinal motor systems, Nat Neurosci 101-108.

Bizzi, E. et al (1992) Does the nervous system use equilibrium-point control to guide single and multiple joint movements? Behav & Brain Sci 15: 603-613.

Blaya, J. and H. Herr (2004) Adaptive control of a variable-impedance ankle-foot orthosis to assist drop-foot gait. IEEE Trans Neural Sys & Rehabil Eng 12(1): 24-31.

Bloedel, J. R. and J. Courville (1981). Cerebellar afferent systems. Handbook of physiology: the nervous system II. J. M. Bookhart, V. B. Mountcastle, V. B. Brooks and S. R. Geiger. Bethesda, MD, American Physiological Society. Section I, Volume II: Motor Control, Part 2: 735-829.

Bosco, G. and R.E. Poppele (2001) Proprioception from a spinocerebellar perspective, Physiol Rev 81.

Bower, J.M. (2002) The organization of cerebellar cortical circuitry revisited: implications for function, Ann N Y Acad Sci 978: 135-155.

Brand, R.A. et al. (1986). The sensitivity of muscle force predictions to changes in physiological cross-sectional area. J Biomech 8: 589-596.

Braitenberg, V. (1961) Functional interpretation of cerebellar histology. Nature 190: 539-540.

Bretzner, F. and T. Drew (2005) Contribution of the motor cortex to the structure and the timing of hindlimb locomotion in the cat. J Neurophysiol 94(1): 657-672.

Brodal, A. (1981). Neurological Anatomy in Relation to Clinical Medicine. New York, NY, Oxford University Press.

Brooke, J.D. et al (1997) Sensori-sensory afferent conditioning with leg movement: gain control in spinal reflex and ascending paths. Prog Neurbiol 51: 393-421.

Brooks, V.B. (1986) The neural basis of motor control, Ch.10, Oxford.

Cajigas-Gonzalez I. (2003) Linear control model of the spinal processing of descending neural signals, Master's thesis, Elect Eng & Comp Sci, Massachusetts Institute of Technology

Calancie, B. et al (1994) Involuntary stepping after chronic spinal cord injury: Evidence for a central rhythm generator for locomotion in man. Rain 117: 1143-1159.

Capaday, C. et al (1999) Studies on the corticospinal control of human walking: I. Response to focal transcranial magnetic stimulation of the motor cortex. J Neurophysiol 81(1): 129-139.

Cheung, V.C. et al (2005) Central and sensory contributions to the activation and organization of muscle synergies during natural motor behaviors. J Neursci 25(27): 6419-34.

Christensen, L.O. et al (2000) Cerebral activation during bicycle movements in man. Exp Brain Res 135(1): 59-68.

Cisek, P. et al (2003) Neural activity in primary motor and dorsal premotor cortex in reaching tasks with the contralateral versus ipsilateral arm, J Neurophysiol 89: 922-942.

Cohen, D. and Y. Yarom (1998) Patches of synchronized activity in the cerebellar cortex evoked by mossy-fiber stimulation: questioning the role of parallel fibers, Proc Natl Acad Sci 95: 15032-15036, Neurobiology.

Collins, S.H. et al (2001) A three-dimensional passive-dynamic walking robot with two legs and knees. Int J Robotics Res 20(7): 617-615.

Collins, S.H. et al (2005) Efficient bipedal robots based on passive-dynamic walkers, Science 307: 1082-1085.

Coltz, J. et al (2000) Population code for tracking velocity based on cerebellar Purkinje cell simple spike firing in monkeys, Neurosci Lett 296: 1-4.

d'Avella, A. and E. Bizzi (2005) Shared and specific muscle synergies in natural motor behaviors, Neuroscience 102: 3076-3081.

d'Avella, A. et al (2003) Combinations of muscle synergies in the contruction of a natural motor behavior, Nat Neurosci 6(3): 300-308.

Davis, B.L. and C.L.Vaughan (1993) Phasive behavior of EMG signals during gait: Use of multivariate statistics. J EMG Kinesiol 3: 51-60.

Della Croce, U. et al (2001) A refined view of the determinants of gait, Gait & Posture 14(2): 79-84.

Delp, S.L. et al. (1999) Variation of rotation moment arms with hip flexion. J Biomech 32: 493-501.

Diener, H.C. and J. Dichgans (1992) Pathophysiology of cerebellar ataxia. Mov Disord 7(2): 95-109.

Dimitrijevic, M.R. et al (1998) Evidence for a spinal central pattern generator in humans. Ann NY Acad Sci 860: 360-376.

Dietz, V. (1992) Human neuronal control of automatic functional movements: interaction between central programs and afferent input. Physiol Rev 72(1): 33-69.

Dietz, V. and J. Harkema (2004) Locomotor activity in spinal cord-injured persons. J Appl Physiol 96: 1954-1960.

Drew, T.(1993) Motor cortical activity during voluntary gait modifications in the cat. J Neurophysiol 70(1): 179-199.

Dutra, M.S. (2003) Modeling of a pidedal locomotor using coupled nonlinear oscillators of Van der Pol, Biol Cybern 88: 286-292.

Duysens, J. et al (2000)Loading-regulating mechanisms in gait and posture: comparative aspects Phyisol Rev 80(1): 83-133.

Ebner, T.J. and J.R. Bloedel (1981) Temporal patterning in simple spike discharge of Purkinje cells and its relationship to climbing fiber activity, J neurophysiol, 45(5).

Eccles, J.C. et al (1967) The cerebellum as a neuronal machine. New York, Springer-Verlag.

Eccles, J.C. et al (1974) Temporal patterns of responses of interpositus neurons to peripheral afferent stimulation. J. Neurophysiol 37: 1427-1437.

Endo, K. et al (2002) Co-evolution of morphology and walking pattern of biped humanoid robot using evolutionary computation-consideration of characteristic of the servomotors, Proc of IEEE/RSJ Intl conf on intelligent robots and systems, EPFL, Lausanne, Switzerland.

Feldman, A.G. (1986). Once more on the equilibrium-point hypothesis (lambda model) for motor control. J Mot Behav 18(1): 17-54.

Flash, T. (1987). The control of hand equilibrium trajectories in multi-joint arm movements. Biol Cybern 57: 257-274.

Fortier, P.A. et al (1989) Cerebellar neuronal activity related to whole-arm reaching movements in the monkey, J Neurophysiol 62(1): 198-211.

Franklin, G.F. et al. (1994) Feedback control of dynamic systems. 3rd ed. Addison-Wesley.

Freitas, S. et al (2006) Two kinematic synergies in voluntary whole-body movements during standing. J Neurophysiol 95:636-645.

Frysinger, R.C. et al (1984) Cerebellar cortical activity during antagonist cocontraction and reciprocal inhibition of forearm muscles, J Neurophysiol 51: 32-49.

Fuglevand, A.J. and D.A. Winter (1993). Models of recruitment and rate coding organization in motor-unit pools. J Neurophysiol 70(6): 2470-2488.

Fujimoto, Y. and A. Kawamura (1998) Control and Simulation of an Autonomous Biped Walking Robot Including Environmental Force Interaction, IEEE Robotics and Automation Magazine, 5(2): 33-42.

Fujita, K. and H. Sato (1998) Intrinsic viscoelasticity of ankle joint during standing. Proceedings1 of the 20th annual international conference of the IEEE engineering in medicine and biology society, 20(5): 2343-2345.

Fukuoka, Y. et al (2003) Adaptive dynamic walking of a quadruped robot on irregular terrain based on biological concepts, Int J of Robotics Research, 22(3-4): 187-202.

Gao, W. et al (2003) Optical imaging of long-term depression in the mouse cerebellar cortex in vivo, J Neurosci, 23(5):1859-1866.

Gatev, P. et al (1999) Feedforward ankle strategy of balance during quiet stance in adults, J Physiol 514.3, 915-928.

Georgopoulos, A. P. (1988) Neural integration of movement: role of motor cortex in reaching, FASEB J, 2: 2849-2857.

Georgopoulos, A. et al (1983) On the relations between the direction of two- dimensional arm movements and cell discharge in primate motor cortex, J Neurosci 2: 1527-1537.

Gilchrist, L.A. and D.A. Winter (1997) A mutlsegment computer simulation of normal human gait, IEEE trans on Rehabil Eng.

Goodwin, G.C. and K.S. Sin (1984) Adaptive filtering prediction and control. Prentice-Hall, Englewood Cliffs, NJ.

Gordon, W. et al (1999) Contribution of sensory feedback to the generation of extensor activity during walking in the decerebrate cat, J Neurophysiol 81: 758-770.

Goswami, A. (1999) Postural stability of biped robots and the foot-rotation indicator (FRI) point. Int J Robotics Res 18(6): 523-533.

Grasso, R. et al (2000) Interaction between posture and locomotion: motor patterns in humans walking with bent posture versus erect posture, J Neurophysiol 83: 288-300.

Grasso, R. et al (2004) Distributed plasticity of locomotor pattern generators in spinal cord injured patients. Brain 127(5): 1019-1034.

Grillner, S. (1975) Locomotion in vertebrates: central mechanisms and reflex interaction. Physiol Rev 55(2): 247-304.

Grillner, S. and P. Wallen (1985) Central pattern generators for locomotion, with special reference to vertebrates, Ann Rev Neurosci 8: 233-261.

Haruno, M. et al (2001) MOSAIC model for sensorimotor learning and control, Neural Computation 13: 2201-2220.

Hemami, H. and A. Katbab (1982) Constrained inverted pendulum model of evaluating upright stability. J Dyn Meas Syst Control 104: 343-349.

Hemami, H. and R. Farnsworth (1977) Postural and gait stability of a palnar five biped by simulation. IEEE Trans Automatic Control 22(3): 452-458.

Henry, S.M. et al (1998) Control of stance during lateral and anterior/posterior surface translations. IEEE Trans Rehabil Eng 6(1): 32-42.

Hiebert, G.W. and K.G. Pearson (1999) Contribution of sensory feedback to the generation of extensor activity during walking in the decerebrate cat. J Neurophysiol 81: 758-770.

Hirai, K. et al (1998) The development of Honda humanoid robot, Proc of the IEEE Int conf on robotics & automation, Leuven, Belgium.

Hof, A.L. et al (2002) Speed dependence of averaged EMG profiles in walking. Gait & Posture 16: 78-86.

Hofmann, A. (2006) Control rules for biomimetic human bipedal locomotion based on biomechanical principles. PhD thesis, Electrical Engineering and Computer Science, Massachusetts Institute of Technology.

Hogan, N. (1985) The mechanics of multi-joint posture and movement control. Biol Cybern 52(5): 315-331.

Hogan, N. et al (1999) Arm movement control is both continuous and discrete, Cognitive Studies 6(3): 254-273.

Horak, F.B. and H.C. Diener (1994) Cerebellar control of postural scaling and central set in stance, J Neurophysiol 72: 479-493.

Horak, F.B. and L.M. Nashner (1986) Central programming of postural movements: adaptation to altered support-surface configurations. J Neurophysiol 55(6): 1369-1381.

Hore, J. and T. Vilis (1984) A cerebellar-dependent efference copy mechanism for generating appropriate muscle response to limb perturbations. In: Bloedel, J.R. J. Dichgans, W. Precht (eds) Cerebellar functions. Springer, Berlin Heidelberg New York, pp 24-35.

Huffman, K.J. and L. Krubitzer (2001) Thalamo-cortical connections of areas 3a and M1 in marmoset monkeys. J Comp Neurol 435(3): 291-310.

Inman, V.T. et al (1981) Human walking. J.C. Lieberman, editor. Balitimore: Williams & Wilkins 41-55.

Ito, M. (1984). The Cerebellum and Neural Control. New York, Raven Press.

Ivanenko, Y.P. et al (2004) Five basic muscle activation patterns account for muscle activity during human locomotion, J Physiol 556.1: 267-282.

Ivanenko, Y.P. et al (2005) Coordination of locomotion with voluntary movements in humans. J Neurosci 25(31): 7238-7253.

Ivanenko, Y.P. et al (2006) Spinal cord maps of spatiotemporal alpha-motoneuron activation in humans walking at different speeds. J Neurophysiol 95: 602-618.

Jeka, J. et al (2004) Controlling human upright posture: velocity information is more accurate than position or acceleration, J Neurophyiol 92: 2368-2379.

Jo, S. (2002) A model of cerebellum-mediated long-loop control of upright balance. Society for Neuroscience 32nd annual meeting, Orlando FL.

Johansson, R. et al (1988) Identification of human postural dynamics. IEEE Trans Biomed Eng 35(10): 858-869.

Johnson, M.T.V. and T.J. Ebner (2000) Processing of multiple kinematic signals in the cerebellum and motor cortices, Brain Res Rev 33(2-3): 155-168.

Jonathon, D. et al (2000) Population code for tracking velocity based on cerebellar Purkinje cell simple spike firing in monkeys, Neurosci Lett 296(1): 1-4.

Kalaska, J.F. et al (1983) Cortical mechanisms related to the direction of two-dimensional arm movements: relations in parietal area 5 and comparison with motor cortex, Exp Brain Res 51: 247-260.

Kandel, E.R. et al (2000) Principles of neural science, 4th ed. McGraw-Hill.

Karameh, F. (2002) A model for cerebral cortical neuronal group electric activity and its implications for cerebral function, PhD thesis, Electrical Engineering and Computer Science, Cambridge, MA, Massachusetts Institute of Technology.

Katayama, M. and M. Kawato (1993). Virtual trajectory and stiffness ellipse during multijoint arm movement predicted by neural inverse models, Biol Cybern 69: 353-362.

Kelly, R.M. and P.L. Strick (2003) Cerebellar loops with motor cortex and prefrontal cortex of a nonhuman primate. J Neurosci 23: 8432-8444.

Kettner, R.E. et al (1997) Prediction of complex two-dimensional trajectories by a cerebellar model of smooth pursuit eye movement. J Neurophysiol 77: 2115-2130.

Kim, J.H. et al (1987) Climbing fiber afferent modulation during treadmill locomotion in the cat. J Neurophysiol 57(3).

Kimura, H. et al (2001) Adaptive dynamic walking of a quadruped robot by using neural system model, Advanced robots 15(8): 859-876.

King, W.T. (1927) Observations on the role of the cerebral cortex in the control of the postural reflex. An J Physiol 80: 311-326.

Knikou, M. et al (2005) Modulation of flexion reflex induced by hip angle changes in human spinal cord injury. Exp Brain Res 164(4):577-586.

Kriellaars, D.J. et al (1994) Mechanical entrainment of fictive locomotion in the decerebrate cat. J Neurophysiol 71(6):2074-2086.

Kuo, A. (1995) An optimal control model for analyzing human postural balance, IEEE Trans on Biomed Eng 42: 87-101.

Lacquaniti, F. and J. F. Soechting (1986) Simulation studies on the control of posture and movement in a multi-jointed limb. Biol Cybern 54: 367-378.

Lacquaniti, F. et al (1997) Posture and movement: coordination and control, Arch Ital Biol 135: 353-367.

Lacquaniti, F. et al (1999) Motor patterns I in walking, News Physiol Sci., 14.

Lam, T. and K.G. Pearson (2001) Proprioceptive modulation of hip flexor activity during the swing phase of locomotion in decerebrate cats. J Neurophysiol 86: 1321-1332.

Lee, D. et al (1997) Manual interception of moving targets II. On-line control of overlapping submovemnts, Exp Brain Res 116: 421-433.

Li, C.-S.R. et al (2001) Neuronal correlates of motor performance and motor learning in primary motor cortex of monkeys adapting to an external force field. Neuron 30: 593-607.

Loram, I.D. and M. Lakie (2002) Direct measurement of human ankle stiffness during quiet standing: the intrinsic mechanical stiffenss is insufficient for stability, J Physiol, 545.3: 1041-1053.

Loram, I.D. et al (2004) Paradoxical muscle movement in human standing. J Physiol 556.3: 683-689.

Mann, M. D. (1973) Clarke's column and the dorsal spinocerebellar tract: A review. Brain Behav Evol 7: 34-83.

Martin, T.A. et al (1996) Throwing while looking through prisms: I. Focal olivocerebellar lesions impair adaptation. Brain 119: 1183-1198.

Masani, K. et al (2003) Importance of body sway velocity information in controlling ankle extensor activities during quiet stance, J Neurophysiol 90(6), 3774-82.

Massaquoi, S.G. (1999) Modelling the function of the cerebellum in scheduled linear servo control of simple horizontal planar arm movements, PhD thesis, Electrical Engineering and Computer Science, Cambridge, MA, Massachusetts Institute of Technology.

Massaquoi, S.G. and M. Hallett (1997). Ataxia and other cerebellar syndromes. Parkinson's Disease and Movement Disorders -3. J. Jankovic and Tolosa. Baltimore, M.D., Williams & Wilkins.

Massaquoi, S. G. and Z.-H. Mao, A multi-input multi-output adaptive switching model of frontocortical and basal ganglionic interaction in supervised procedural learning and execution, (submitted).

Massaquoi, S.G., J.-J.E. Slotine (1996) The intermediate cerebellum may function as a wave-variable processor. Neurosci Lett 215: 60-64.

Massaquoi, S.G. and H. Topka (2002). Models of Cerebellar Function. The Cerebellum and its Disorders. M. Pandolfo and M. Manto. Cambridge, U.K., Cambridge University Press: 69-94.

Massion, J. et al (1997) Movement, posture and equilibrium: interaction and coordination, Prog Neurobiol 38: 35-56.

McGeer, T. (1993) Dynamics and control of bipedal locomotion. J Theor Biol 163(3): 277-314.

Miall, R.C. et al (1993) Is the cerebellum a Smith predictor? J Mot Behav 25(3): 203-216.

Miyakoshi, S. et al (1998) Three dimensional bipedal stepping motion using neural oscillators-towards humanoid motion in the real world, Proc of IEEE/RSJ Intl conf on intelligent robots and systems, Victoria, B.C., Canada.

Morasso, P.G. and V. Sanquineti (2001) Ankle muscle stiffness alone cannot stabilize balance during quiet standing, J Neurophysiol, 88: 2157-2162.

Mori, S. et al (2004) Integration of multiple motor segments for the elaboration of locomotion: role of the fastigial nucleus of the cerebellum. Prog Brain Res 143: 341-351.

Mori, S. et al (1999) Stimulation of a restricted region in the midline cerebellar white matter evokes coordinated quadrupedal locomotion in the decerebrate cat. J Neurophysiol 82(1): 290-300.

Mori, S. et al (1998) Cerebellar-induced locomotion: reticulospinal control of spinal rhythm generating mechanism in cats. Ann N Y Acad Sci 860: 94-105.

Morimoto, J. et al (2004) A simple reinforcement learning algorithm for biped walking, Proc of IEEE intl conf on Robotics Automation, New Orleans, LA.

Morton, S.M. and A.J. Bastian (2003) Relative contributions of balance and voluntary leg-coordination deficits to cerebellar gait ataxia, J Neurophysiol 89: 1844-1856.

Morton, S.M. and A.J. Bastian (2004) Cerebellar control of balance and locomotion, The Neuroscientist 10(3): 247-259.

Morton, S.M. et al (2004) Cerebellar damage produces context-dependent deficits in control of leg dynamics during obstacle avoidance, Exp Brain Res 156: 149-163.

Nakanishi J et al (2004) Learning from demonstration and adaptation of biped locomotion, Robotics & Auto Sys 47: 79-91.

Nashner, L.M. et al (1982) Adaptation to altered support and visual conditions during stance: patients with vestibular deficits. J Neurosci 2(5): 536-544

Nashner, L.M., and G. McCollum. (1985) The organization of human postural movements: A formal basis and experimental synthesis. Behav Brain Sci 8(1): 135-150.

Nathan, P.W. (1994) Effects on movement of surgical incisions into the human spinal cord. Brain 117(Pt2): 337-346.

Neptune, R.R. et al (2004) Muscle mechanical work requirements during normal walking: the energetic cost of raising the body's center-of-mass is significant. J Biomech 37: 817-825.

Nielsen, J.B. (2003) How we walk: central control of muscle activity during human walking. The Neuroscientist 9(3): 195-204.

Ogihara, N, and N. Yanazaki. (2001). Generation of human bipedal locomotion by a bio-mimetic neuro-musculo-skeletal model. Biol Cybern 84: 1-11.

Olree, K.S. and C.L. Vaughan (1995) Fundamental patterns of bilateral muscle activity in human locomotion, Biol Cybern 73(5): 409-414.

Osborn, C. E. and R. E. Poppele (1992). Parallel distributed network characteristics of the DSCT. J Neurophysiol 68(4): 1100-1112.

Oscarsson, O. (1965). Functional organization of the spino- and cuneocerebellar tracts. Phys Rev 45: 495-522.

Pandy, M.G. and M. Berme (1988) A numerical method for simulation the dynamics of human walking. J Biomech 21(12): 1043-1051.

Pardoe, J. et al (2004) Changes in excitability of ascending and descending inputs to cerebellar climbing fibers during locomotion, J Neursci 24(11): 2656-2666.

Park, S. et al (2004) Postural feedback responses scale with biomechanical constraints in human standing. Exp Brain Res 154: 417-427.

Patla, A.E. et al (1985) Model of a pattern generator for locomotion in mammals. Am J Physiol 248: R484-494.

Paulin, M.G. (1993) A model for the role of the cerebellum in motor control, Hum Mov Sci 12: 5-16.

Paulin, M.G. (1997) Neural representations of moving systems. In: Schmathmann, J.D. (ed) The cerebellum and cognition, vol 41, Academic, San Diego, pp 515-533.

Perry, J. (1992) Gait analysis: normal and pathological function, New York: McGraw-Hill, Inc.

Peterak, R. (2001) Sensorimotor integration in human postural control. J Neurophysiol 88: 1097-1118.

Peterka, R. (2003) Simplifying the complexities of maintaining balance. IEEE Eng Med Biol March/April: 63-68.

Peterson, N.T. et al (1998) The effect of transcranial magnetic stimulation on the soleus H reflex during human walking. J Physiol (Lond) 513(Pt 2):599-610.

Pina Fiho, A.C. et al (2005) Modeling of a bipedal robot using mutually coupled Rayleigh oscillators, Biol Cybern 92: 1-7.

Pinter, M.M. and M.R. Dimitrijevic (1999) Gait after spinal cord injury and the central pattern generator for locomotion, Spinal cord 37(8): 531-537.

Porter, R. and R. Lemon (1993) Corticospinal function and voluntary movement. New York: Oxford Univ Press.

Pratt, J. and G. Pratt (1998) Intuitive control of a planar bipedal walking robot, Proc of Int Conf on Robotics and Automation, Belgium.

Prentice, S.D. and T. Drew (2001) Contributions of the reticulospinal system to the postural adjustments occurring during voluntary gait modifications. J Neurophysiol 85(2): 679-698.

Rab, G.T., Muscle. In: Rose J, Gamble J.G., editors, Human walking, 2nd ed., Baltimore: Williams & Wilkins, 1994: 101-121.

Ropper, A. and R.H. Brown (2005) Adams & Victor's principles of neurology, eighth ed., McGraw Hill Professional.

Rossignol, S. et al (2006) Dynamic sensorimotor interaction in locomotion, Physiol Rev 86: 89-154.

Rudomin, P. and R.F. Schmidt (1999) Presynaptic inhibition in the vertebrate spinal cord revisited, Exp Brain Res 129(1): 1-37.

Runge, C.F. et al. (1999) Ankle and hip postural strategies defined by joint torques. Gait & Posture. 10: 161-170.

Santamaria, F. et al (2002) Modulatory effects of parallel fiber and molecular layer interneuron synaptic activity on Purkinje cell responses to ascending segment input: a modeling study, J Comp Neurosci 13: 217-235.

Saunders, J.B. et al (1953) The major determinants in normal and pathological gait, J Bone and Joint Surgery, 35A: 543-558.

Shik, M.L. and G.N. Orlovsky (1976) Neurophysiology of locomotor automatism. Phsyiol Rev 56(3): 465-501.

Sugihara, T. et al (2002) Realtime Humanoid Motion Generation through ZMP Manipulation based on Inverted Pendulum Control. Proc. of IEEE Int Conf on Robotics and Automation, 2: 1404-1409, Washington D.C., U.S.A.

Taga, G. (1995) A model of the neuro-musculo-skeletal system for human locomotion I. Emergence of basic gait, Biol Cybern 73: 97-111.

Taga, G. (1998) A model of the neuro-musculo-skeletal system for anticipatory adjustment of human locomotion during obstacle avoidance, Biol Cybern 78(1): 9-17.

Tanji, J. (2001) Sequential organization of multiple movements: involvement of cortical motor areas, Annu Rev Neurosci 24: 631-651.

Thach, W.T. et al (1992) the cerebellum and the adaptive control of movement, Annu Rev Neurosci, 15:403-442.

Ting, L.H. and J.M. Macpherson (2005) A limited set of muscle synergies for force control during a postural task, J Neurophysiol 93: 609-613.

Tremblay, L. et al (1998) Modifications of reward expectation-related neuronal activity during learning in primate striatum. J Neurophysiol 80: 964-977.

Tresch, M.C. et al (1999) The construction of movement by the spinal cord. Nat Neurosci 2: 162-167.

Tzafestas, S. et al (1997) Robust sliding-mode control of nine-link biped robot walking. J Intell & Robotic Sys 20(2-4): 375-402.

Uno, Y. et al (1989) Formation and control of optimal trajectory in human multijoint arm movement. Biol Cybern 61: 89-101.

Vaughan, C.L. (2003) Theories of bipedal walking: an odyssey. J Biomech 36(4): 513-523(11).

Vukobratovic, M. et al (1990) Scientific fundamentals of rotobics 7. Biped locomotion: dynamics, stability, control and application. Springer-Verlag, New York.

van der Kooij, H. et al (2003) An alternative approach to synthesizing bipedal waking, Biol Cybern, 88: 46-59.

van der Linde, R.Q. (1999) Passive bipedal walking with phasic muscle contraction. Biol Cybern 81:227-237.

Wadden, T. and Ö. Ekeberg (1998) A neuro-mechanical model of legged locomotion: single leg control, Biol Cybern 79: 161-173.

Winter, D.A. (1990) Biomechanics and motor control of human movement. 2nd ed. Wiley & Sons, Inc.

Winter, D.A. (1991) The biomechanics and motor control of human gait: normal, elderly and pathological. Waterloo Biomechanics Press, Waterloo, Ontario.

Winter, D.A. (1995) Human balance and posture control during standing and walking, Gait & Posture, 3: 193-214.

Winters, J.M. (1995) How detailed should muscle models be to understand multi-joint movement coordination? Hum Mov Sci 14: 401-442.

Winters, J.M. and L. Stark (1985) Analysis of fundamental human movement patterns through the use of in-depth antagonistic muscle models. IEEE Trans Biomed Eng 32(10): 820-839.

Wolpert, D.M. et al (1998) Internal models in the cerebellum. Trend Cog Sci 2(9): 338-347.

Yang, J-S. (1993) Adaptive inverse dynamics control for a biped locomotion system. 2rd IEEE conf Control Applications. Sept 13-16, Vancouver, B.C.

Yang, J.F. et al (2005) Split-belt treadmill stepping in infants suggests autonomous pattern generators for the left and right leg in humans. J Neurosci 25(29): 6869-6876.

Zajac, F.E. (1989) Muscle and tendon: properties, models, scaling, and application to biomechanics and motor control. Critical Rev Biomed Eng 17(4): 359-411.

Zajac, F.E. et al (2003) Biomechanics and muscle coordination of human walking Part II: Lessons from dynamical simulations and clinical implications, Gait & Posture 17: 1-17.

Zijlstra, W. et al (1998) Voluntary and involuntary adaptation of gait in Parkinson's disease. Gait & Posture 7(1): 53-63.